THESIS FOR THE DEGREE OF DOCTOR OF PHILOSOPHY

Optical Transmission Systems Based on Phase-Sensitive Amplifiers

SAMUEL L. I. OLSSON

Photonics Laboratory
Department of Microtechnology and Nanoscience - MC2
CHALMERS UNIVERSITY OF TECHNOLOGY
Göteborg, Sweden 2015

Front cover illustration: Measured constellation diagrams of 10 GBd 16-QAM
signal after 105 km transmission in linear and nonlinear transmission regime and
after phase-insensitive and phase-sensitive preamplification.

Optical Transmission Systems Based on Phase-Sensitive Amplifiers

SAMUEL L. I. OLSSON

Photonics Laboratory
Department of Microtechnology and Nanoscience - MC2
Chalmers University of Technology

Abstract

The capacity and reach of today's long-haul fiber optical communication systems is limited by amplifier noise and fiber nonlinearities. Conventional, phase-insensitive amplifiers (PIAs), have a quantum limited noise figure (NF) of 3 dB at high gain, meaning that with a shot-noise limited input signal the signal-to-noise ratio (SNR) is degraded by at least 3 dB. Phase-sensitive amplifiers (PSAs), have a quantum limited NF of 0 dB, meaning that a shot-noise limited input signal can be amplified without degrading the SNR. The capability of PSAs to provide noiseless amplification makes them interesting for transmission system applications.

The objective of this thesis has been to experimentally realize transmission systems based on two-mode PSAs and explore their properties, both experimentally and numerically. We present the first demonstrations of multi-channel compatible and modulation format independent single-span and multi-span PSA-amplified transmission systems. In addition to demonstrating a performance benefit due to reduced amplifier noise we also show that two-mode PSA-amplified transmission systems can mitigate distortions originating from fiber nonlinearities, such as self-phase modulation (SPM) and nonlinear phase noise (NLPN).

In particular, we demonstrate PSA-amplified transmission of 10 GBd quadrature phase-shift keying (QPSK) and 16-ary quadrature amplitude modulation (16QAM) signals over 105 km single-span transmission systems showing significant performance improvements, in terms of sensitivity, compared to conventional PIA-amplified transmission systems. In the case of 16QAM transmission the improved sensitivity allows for 12 dB larger span loss. We also demonstrate PSA-amplified multi-span transmission of a 10 GBd QPSK signal achieving a maximum reach of 3465 km, a threefold reach improvement compared to the maximum reach of 1050 km that was obtained using in-line PIAs at optimal launch power.

Keywords:fiber nonlinearities, four-wave mixing, fiber optic parametric amplification, phase-sensitive amplification, fibre optics, optical fiber communication, low-noise amplification, fiber nonlinearity mitigation, optical injection locking.

iv

List of papers

Appended papers

This thesis is based on work contained in the following papers:

[A] **S.L.I. Olsson**, B. Corcoran, C. Lundström, E. Tipsuwannakul, S. Sygletos, A.D. Ellis, Z. Tong, M. Karlsson, and P.A. Andrekson, "Injection locking-based pump recovery for phase-sensitive amplified links," *Optics Express*, vol. 21, no. 12, pp. 14512–14529, June 2013.

[B] B. Corcoran, **S.L.I. Olsson**, C. Lundström, M. Karlsson, and P. Andrekson, "Phase-sensitive Optical Pre-Amplifier Implemented in an 80km DQPSK Link," in *Optical Fiber Communication Conference (OFC)*, Los Angeles, CA, March 2012, postdeadline paper PDP5A.4.

[C] R. Malik, **S.L.I. Olsson**, P. Andrekson, C. Lundström, and M. Karlsson, "Record-high sensitivity receiver using phase sensitive fiber optical parametric amplification," in *Optical Fiber Communication Conference (OFC)*, San Francisco, CA, March 2014, paper Th2A.54.

[D] **S.L.I. Olsson**, B. Corcoran, C. Lundström, M. Sjödin, M. Karlsson, and P.A. Andrekson, "Phase-Sensitive Amplified Optical Link Operating in the Nonlinear Transmission Regime," in *European Conference on Optical Communication (ECOC)*, Amsterdam, The Netherlands, September 2012, paper Th.2.F.1 (Best student paper award winner).

[E] B. Corcoran, **S.L.I. Olsson**, C. Lundström, M. Karlsson, and P.A. Andrekson, "Mitigation of Nonlinear Impairments on QPSK Data in Phase-Sensitive Amplified Links," in *European Conference on Optical Communication (ECOC)*, London, England, September 2013, paper We.3.A.1.

[F] **S.L.I. Olsson**, B. Corcoran, C. Lundström, T.A. Eriksson, M. Karlsson, and P.A. Andrekson, "Phase-Sensitive Amplified Transmission Links for Improved Sensitivity and Nonlinearity Tolerance," *Journal of Lightwave Technology*, vol. 33, no. 3, pp. 710–721, February 2015 (Invited paper).

[G] B. Corcoran, R. Malik, **S.L.I. Olsson**, C. Lundström, M. Karlsson, and P.A. Andrekson, "Noise beating in hybrid phase-sensitive amplifier systems," *Optics Express*, vol. 22, no. 5, pp. 5762–5771, March 2014.

[H] **S.L.I. Olsson**, M. Karlsson, and P.A. Andrekson, "Nonlinear phase noise mitigation in phase-sensitive amplified transmission systems," *Optics Express*, vol. 23, no. 9, pp. 11724–11740, May 2015.

[I] **S.L.I. Olsson**, C. Lundström, M. Karlsson, and P.A. Andrekson, "Long-Haul (3465 km) Transmission of a 10 GBd QPSK Signal with Low Noise Phase-Sensitive In-Line Amplification," in *European Conference on Optical Communication (ECOC)*, Cannes, France, September 2014, postdeadline paper PD.2.2.

Other papers

The following papers have been published but are not included in the thesis. The content partially overlap with the appended papers or is outside the scope of this thesis.

[J] **S.L.I. Olsson**, B. Corcoran, C. Lundström, E. Tipsuwannakul, S. Sygletos, A.D. Ellis, Z. Tong, M. Karlsson, and P.A. Andrekson, "Optical Injection-Locking-Based Pump Recovery for Phase-Sensitively Amplified Links," in *Optical Fiber Communication Conference (OFC)*, Los Angeles, CA, March 2012, paper OW3C.3.

[K] C. Lundström, B. Corcoran, **S.L.I. Olsson**, Z. Tong, M. Karlsson, and P.A. Andrekson, "Short-Pulse Amplification in a Phase-Sensitive Amplifier," in *Optical Fiber Communication Conference (OFC)*, Los Angeles, CA, March 2012, paper OTh1C.1.

[L] T. Richter, B. Corcoran, **S.L.I. Olsson**, C. Lundström, M. Karlsson, C. Schubert, and P.A. Andrekson, "Experimental Characterization of a Phase-Sensitive Four-Mode Fiber-Optic Parametric Amplifier," in *European Conference on Optical Communication (ECOC)*, Amsterdam, The Netherlands, September 2012, paper Th.1.F.1 (Best student paper award runner-up).

[M] L. Grüner-Nielsen, D. Jakobsen, S. Herstrøm, B. Pálsdóttir, S. Dasgupta, D. Richardson, C. Lundström, **S.L.I. Olsson**, and P.A. Andrekson, "Brillouin Suppressed Highly Nonlinear Fibers," in *European Conference on Optical Communication (ECOC)*, Amsterdam, The Netherlands, September 2012, paper We.1.F.1.

[N] C. Lundström, R. Malik, L. Grüner-Nielsen, B. Corcoran, **S.L.I. Olsson**, M. Karlsson, and P.A. Andrekson, "Fiber Optic Parametric Amplifier With 10-dB Net Gain Without Pump Dithering," *IEEE Photonics Technology Letters*, vol. 25, no. 3, pp. 234-237, February 2013.

[O] C. Lundström, **S.L.I. Olsson**, B. Corcoran, M. Karlsson, and P.A. Andrekson, "Phase-Sensitive Amplifiers for Optical Links," in *Optical Fiber Communication Conference (OFC)*, Anaheim, CA, March 2013, paper OW3C.5.

[P] C. Lundström, R. Malik, A. Lorences-Riesgo, B. Corcoran, **S.L.I. Olsson**, M. Karlsson, and P.A. Andrekson, "Fiber-optic Parametric Amplifiers Without Pump Dithering," in *Workshop on Specialty Optical Fibers and their Applications*, Sigtuna, Sweden, August 2013, paper W3.12.

[Q] R. Malik, A. Kumpera, **S.L.I. Olsson**, M. Karlsson, and P.A. Andrekson, "Optical signal to noise ratio improvement through unbalanced noise beating in phase-sensitive parametric amplifiers," *Optics Express*, vol. 22, no. 9, pp. 10477–10486, April 2014.

[R] **S.L.I. Olsson**, T.A. Eriksson, C. Lundström, M. Karlsson, and P.A Andrekson, "Linear and Nonlinear Transmission of 16-QAM Over 105 km Phase-Sensitive Amplified Link," in *Optical Fiber Communication Conference (OFC)*, San Francisco, CA, March 2014, paper Th1H.3 (Corning Outstanding Student Paper Competition Honorable mention).

[S] H. Eliasson, **S.L.I. Olsson**, M. Karlsson, and P.A. Andrekson, "Comparison between Coherent Superposition in DSP and PSA for Mitigation of Nonlinearities in a Single-span Link," in *European Conference on Optical Communication (ECOC)*, Cannes, France, September 2014, paper Mo.3.5.2.

[T] A. Lorences-Riesgo, L. Liu, **S.L.I. Olsson**, R. Malik, A. Kumpera, C. Lundström, S. Radic, M. Karlsson, and P.A. Andrekson, "Quadrature demultiplexing using a degenerate vector parametric amplifier," *Optics Express*, vol. 22, no. 24, pp. 29424–29434, November 2014.

Acknowledgement

I feel very fortunate to have had the opportunity to pursue a PhD degree at the photonics laboratory at Chalmers University of Technology and I am very grateful to everyone that have made this journey possible and rewarding.

First and foremost I want to thank my supervisors Prof. Peter Andrekson and Prof. Magnus Karlsson for accepting me as a PhD student, their insightful guidance, good support, and for being excellent academic role models. A special thank goes to Dr. Bill Corcoran for his contributions to the papers in this thesis, stimulating discussions, and the close collaboration. I also want to thank Dr. Carl Lundström for his contributions to the papers and for helping me in my work.

Dr. Pontus Johannisson and Dr. Zhi Tong are acknowledged for sharing their knowledge and expertise, as well as helping me in my work in many ways. I also want to acknowledge Dr. Rohit Malik, Abel Lorences-Riesgo, Tobias Eriksson, Henrik Eliasson, Dr. Aleš Kumpera, Dr. Ekawit Tipsuwannakul, and Dr. Martin Sjödin for collaborations in the lab and fruitful discussions.

I express my gratitude to Prof. Andrew Ellis for letting me spend time at Tyndall National Institute in Cork, Ireland and to Dr. Stylianos Sygletos for sharing his knowledge and spending time with me during the visit. I also want to thank the whole photonics laboratory and visiting researches that have been in the group for creating a pleasant and inspiring work environment.

Finally I would like to thank those who are close to me for their friendship and support over the years, especially my family.

<div align="right">Samuel L. I. Olsson</div>

Göteborg
May 2015

List of acronyms

16QAM 16-ary quadrature amplitude modulation

AOM acousto-optic modulator
AQN amplified quantum noise
ASE amplified spontaneous emission

B2B back-to-back
BER bit error ratio
BPSK binary phase-shift keying

CD chromatic dispersion
CW continuous wave

DBP digital backward propagation
DFA doped fiber amplifier
DFB distributed feedback
DQPSK differential quadrature phase-shift keying
DSP digital signal processing

EDFA erbium-doped fiber amplifier

FEC forward error correction
FOPA fiber optical parametric amplifier
FWM four-wave mixing

GAWBS guided acoustic-wave Brillouin scattering

HDTV high-definition television
HNLF highly nonlinear fiber

ICT information and communication technology
IL injection locking

ML master laser

NF noise figure

NLPN nonlinear phase noise

NLSE nonlinear Schrödinger equation

NRZ non-return-to-zero

OIL optical injection locking

OOK on-off keying

OPC optical phase conjugation

OPLL optical phase-locked loop

OSNR optical signal-to-noise ratio

PC polarization controller

PDM polarization-division multiplexing

PIA phase-insensitive amplifier

PLL phase-locked loop

PM-QPSK polarization-multiplexed quadrature phase-shift keying

PMD polarization-mode dispersion

PPLN periodically poled lithium niobate

PSA phase-sensitive amplifier

QPSK quadrature phase-shift keying

RF radio frequency

RIN relative intensity noise

SBS stimulated Brillouin scattering

SE spectral efficiency

SFG sum-frequency generation

SHG second harmonic generation

SL slave laser

SNR signal-to-noise ratio

SOA semiconductor optical amplifier

SOP state of polarization

SPM self-phase modulation

SRS stimulated Raman scattering

SSMF standard single mode fiber

TWM three-wave mixing

VOA variable optical attenuator

WDM wavelength division multiplexing

XPM cross-phase modulation

ZDW zero-dispersion wavelength

Table of contents

xvi

Chapter 1

Introduction

From the beginning of humankind inventions and technical advances have driven our development and formed the world we live in. Today's society is to a large extent shaped by the information and communication technology (ICT) that emerged in the 1990's. The ICT has had a profound impact on everyday life, for instance by enabling services that make information more accessible and by providing new means of communication and media consumption. The ICT has also contributed to large-scale trends such as globalization by connecting billions of people from all around the world.

The key enabling technology for the ICT was the long-haul fiber optical communication system, making it possible to transmit information at high speeds over intercontinental distances. The long-haul fiber optical communication system was in turn realized based on a number of inventions and technical advances of the last century. The most important components were the laser [1], the low-loss optical fiber [2], and the erbium-doped fiber amplifier (EDFA) [3]. Similar to how the ICT was once enabled by technical advances, the future development in the area of ICT will to a large extent be dictated by today's advances.

This thesis concern an optical amplification technology known as phase-sensitive amplification. Phase-sensitive amplifiers (PSAs) have superior noise properties compared to conventional amplifiers and can potentially improve the performance of long-haul fiber optical communication systems. The work presented in this thesis contributes to the continued development in the area of ICT.

Chapter outline

In Section 1.1 we put this thesis work in context, motivate why the work is of importance, give a brief introduction to PSAs, and review prior work in the area. In Section 1.2 we describe the novel aspects of this work, provide a motivation for each of the appended papers, and outline the structure and content of the thesis.

1.1 Background

1.1.1 Motivation

The development of services in the area of ICT goes hand in hand with an increased demand for capacity in the fiber optical communication systems. Particularly capacity intensive services are those in the field of home entertainment, where rapid advancements in display technology and technical solutions for distribution over internet drive the demand. New standards, where current examples are ultra high-definition television (HDTV), with up to sixteen times the pixel count of standard HDTV, and 3D television, will increase the demand for capacity. Another field is business and productivity related services where, e.g., cloud computing, cloud storage, and video conferencing will contribute to an increased demand. Additionally, the number of people and devices connected to internet is expected to grow which will also add to the demand. The trends described above are reflected in a recent forecast by Cisco [4], where it is predicted that the IP traffic will grow at a compound annual growth rate of 21 percent in the period 2013-2018.

The current state-of-the-art in long-haul fiber optical communication systems is the result of four decades of development and technological advances. One of the first commercial systems, deployed in 1977, operated at 45 Mbit/s over a distance of 2.6 km [5]. Comparing this system to current state-of-the-art experiments, demonstrating data transmission at 63.5 Tbit/s over 5,380 km [6], show a capacity increase of more than six orders of magnitude, and a reach increase of more than three orders of magnitude. The remarkable increase in capacity over the last decades, as illustrated by the comparison above, has been accomplished by the development and implementation of a number of technologies [7, 8]. The most important developments have been optical fiber improvements (reduced loss), the introduction of the EDFA and implementation of wavelength division multiplexing (WDM), the introduction of coherent detection, enabling the use of advanced modulation formats and digital compensation of transmission impairments, and the use of error-correcting codes, e.g., forward error correction (FEC).

To further increase the capacity, as required to meet the growing demand, a combination of improving already existing techniques and introducing new technologies will be required. The capacity of a communication system can be expressed as the product of the spectral efficiency (SE), a measure of how efficient the spectrum is used, and the signal bandwidth. In order to increase the capacity one possible direction is to work towards improving the signal-to-noise ratio (SNR) of the transmitted signal. Improved SNR can, e.g., allow the usage of modulation formats with higher SE, which in turn can give higher capacity [9].

A long-haul fiber optical communication system, illustrated in Fig. 1.1, consists of a transmitter, transmission spans, and a receiver. The function of the transmitter is to generate a signal encoded with the data that should be transmitted. The transmission spans, containing optical fibers and in-line optical amplifiers,
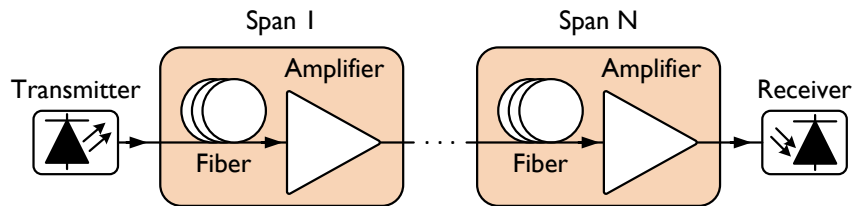
Figure 1.1: Illustration of a long-haul fiber optical communication system.

transport the signal from the origin to the destination. Despite the extremely low attenuation that can be achieved in optical fibers, with the current record being 0.1467 dB/km for light at 1550 nm [10], periodic amplification is needed to compensate for the attenuation. The receiver finally detects the transmitted signal and recovers the data. Each in-line amplifier in the transmission system will degrade the SNR by adding noise. By improving the noise properties of the amplifiers used in the system it should thus be possible to improve the SNR of the transmitted signal.

The noise added to a signal by an optical amplifier can be quantified by the amplifier noise figure (NF), defined as the ratio of the input SNR to the output SNR, assuming a shot-noise limited input signal [11]. All commercial optical amplifiers available today belong to the category of phase-insensitive amplifiers (PIAs), meaning that their gain is independent of the input signal phase. Amplifiers of this type have a quantum-limited NF of 3 dB at high gain [12], i.e., when only accounting for quantum noise and the input signal is shot-noise limited, the amplifier degrade the SNR by a factor of two.

Another category of amplifiers are the PSAs, which have a gain that depends on the phase of the input signal. The phase-dependent gain give rise to two interesting and useful properties: noiseless amplification and phase-squeezing. For high-capacity transmission systems the possibility of noiseless amplification is particularly interesting. The quantum-limited NF of PSAs is 0 dB [13], i.e., the SNR is not degraded when the input signal is shot-noise limited and only quantum noise is considered.

Due to the superior noise properties of PSAs, a transmission system based on PSAs is expected to result in less SNR degradation compared to a transmission system based on PIAs. It is therefore very interesting to investigate the properties of transmission systems based on PSAs, as well as the possibility of realizing such systems in practice. Research has been conducted in this area since the 1980's and is the main topic of this thesis.

1.1.2 Phase-sensitive amplifiers

PSAs can be realized for example using parametric gain in $\chi^{(2)}$-nonlinear materials or $\chi^{(3)}$-nonlinear materials. Parametric gain originates from nonlinear wave-mixing

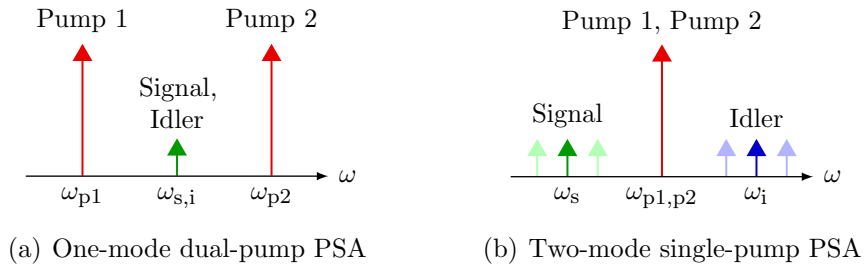(a) One-mode dual-pump PSA   (b) Two-mode single-pump PSA

Figure 1.2: Examples of PSAs implemented using FOPAs.

between several waves, through three-wave mixing (TWM) in $\chi^{(2)}$-nonlinear materials or through four-wave mixing (FWM) in $\chi^{(3)}$-nonlinear materials. Parametric gain through FWM is obtained by the amplification of two weaker waves, called signal and idler, by two stronger waves, called pumps. The process is subject to photon energy and momentum conservation which imply $\omega_{p1} + \omega_{p2} = \omega_s + \omega_i$ and $\beta_{p1} + \beta_{p2} = \beta_s + \beta_i$, where ω denotes the frequency, β denotes the propagation constant, subscript p1 denotes pump 1, subscript p2 denotes pump 2, subscript s denotes the signal, and subscript i denotes the idler.

An amplifier utilizing parametric gain in an optical fiber, a $\chi^{(3)}$-nonlinear material, is called a fiber optical parametric amplifier (FOPA). Given that the signal and pump waves are present at the input, the FOPA can operate either as a PSA or a PIA, depending on if the idler wave is present at the input or not. If the idler wave is not present at the input the FOPA will operate as a PIA and an idler wave will be generated internally at the frequency $\omega_i = \omega_{p1} + \omega_{p2} - \omega_s$, and with a momentum $\beta_i = \beta_{p1} + \beta_{p2} - \beta_s$. If on the other hand the idler wave is present at the input the FOPA will operate as a PSA.

Depending on how the frequencies of the pumps, signal, and idler waves present at the FOPA input are chosen, different amplification schemes can be realized [14]. It is common to name the schemes based on the number of distinct signal/idler frequencies. Using this practice, schemes with degenerate signal and idler waves are called one-mode, and schemes with nondegenerate signal and idler waves are called two-mode. Similarly, based on if the pump waves are degenerate or nondegenerate the schemes are called single-pump or dual-pump. Example of a one-mode PSA and a two-mode PSA are illustrated in Fig. 1.2. An important difference between one-mode and two-mode PSAs is that one-mode PSAs are inherently single-channel, i.e., they can only amplify a single signal wave, while two-mode PSAs are multi-channel compatible, as indicated in Fig. 1.2(b).

To understand the effects of the phase-sensitive gain of PSAs it is instructive to compare the output of the one-mode PSA and the two-mode PSA shown in Fig. 1.2 with the output of a PIA using phasor diagrams. Amplifying a signal, with complex amplitude A_{in}, using a PIA will produce an output signal, $A_{out,PIA}$, that have the same phase as the input signal but an amplitude that is larger by a factor

4

$$|A_{\text{out,PIA}}| = \sqrt{G_{\text{PIA}}} \cdot |A_{\text{in}}|$$
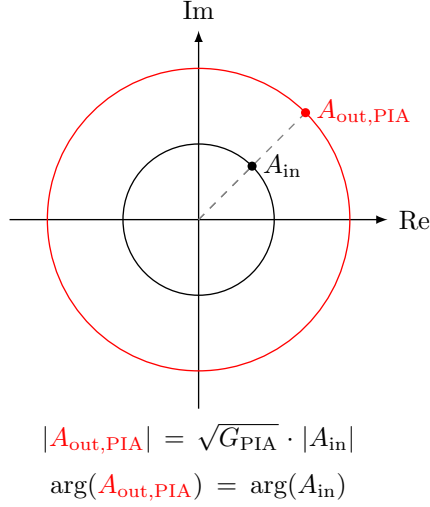
$$\arg(A_{\text{out,PIA}}) = \arg(A_{\text{in}})$$

Figure 1.3: Illustration of input (black) and output (red) signals for a PIA with gain $G_{\text{PIA}} = 4$.

of $\sqrt{G_{\text{PIA}}}$, where G_{PIA} is the PIA power gain, i.e., $G_{\text{PIA}} = |A_{\text{out,PIA}}|^2/|A_{\text{in}}|^2$. At high gain the quantum-limited NF for this process is 3 dB [12]. The amplification using a PIA, with $G_{\text{PIA}} = 4$, is illustrated in Fig. 1.3. The PIA could, e.g., be an EDFA or a FOPA operated as a PIA.

For a PSA the gain depends on the relative phase between the interacting waves [15]. In most practical systems the pumps phases can be considered to be constant while the signal and idler phases might vary with time, e.g., due to phase-modulated data encoded onto the waves. Considering the one-mode PSA illustrated in Fig. 1.2(a), given that the pumps phases are constant, the gain must depend on the signal phase since the signal and idler are the same wave. Analyzing this scheme in detail shows that one signal quadrature component will be amplified by $\sqrt{G_{\text{PSA}}}$ while the orthogonal quadrature component will be deamplified by $1/\sqrt{G_{\text{PSA}}}$ [15], where G_{PSA} is the PSA power gain, and that the quantum-limited NF for the amplified quadrature is 0 dB [13]. The deamplification in the PSA does not only apply to the signal but also to the noise accompanying the signal. This property can be used to generate so-called squeezed states [16]. In a high-gain regime the gain provided by a FOPA operated as a PSA is fourfold the gain of a FOPA operated as a PIA, i.e., $G_{\text{PSA}} = 4G_{\text{PIA}}$ [17]. The amplification using a one-mode PSA, with $G_{\text{PSA}} = 4G_{\text{PIA}} = 16$, is illustrated in Fig. 1.4. It is evident from Fig. 1.4 that the amplification of one quadrature and deamplification of the orthogonal quadrature will result in squeezing of the input signal phase. The phase-squeezing can for example be used for regeneration of binary phase-shift keying (BPSK) signals.
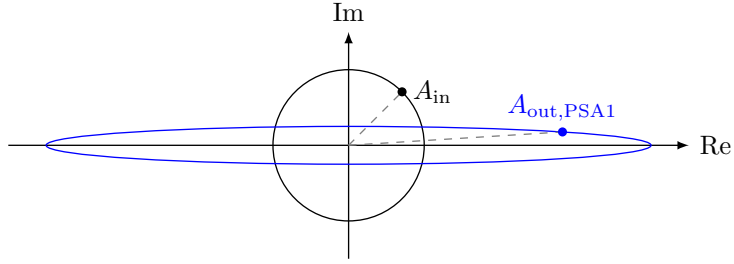
$$\text{Re}(A_{\text{out,PSA1}}) = \sqrt{G_{\text{PSA}}} \cdot \text{Re}(A_{\text{in}})$$
$$\text{Im}(A_{\text{out,PSA1}}) = 1/\sqrt{G_{\text{PSA}}} \cdot \text{Im}(A_{\text{in}})$$
$$\arg(A_{\text{out,PSA1}}) \neq \arg(A_{\text{in}})$$

Figure 1.4: Illustration of input (black) and output (blue) signals for a one-mode PSA with gain $G_{\text{PSA}} = 4G_{\text{PIA}} = 16$.
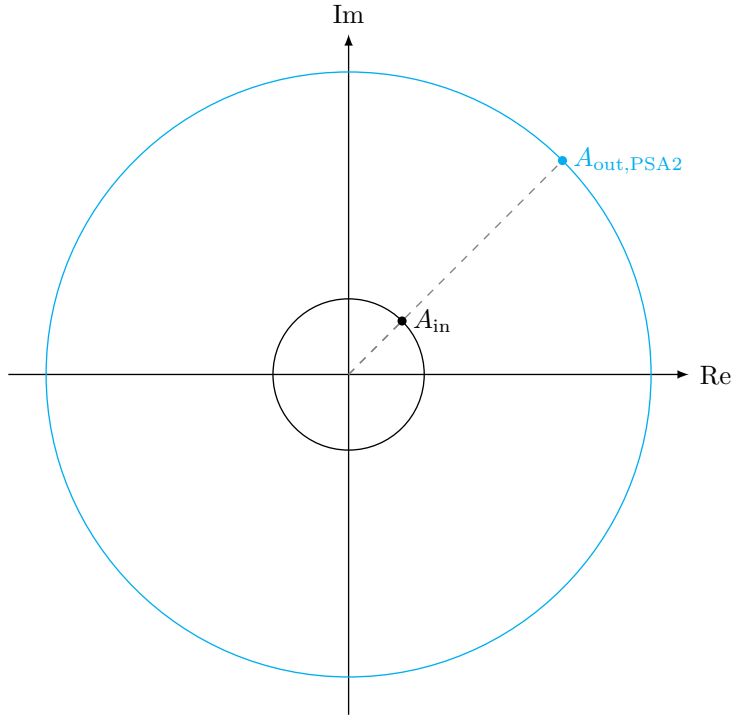
$$|A_{\text{out,PSA2}}| = \sqrt{G_{\text{PSA}}} \cdot |A_{\text{in}}|$$
$$\arg(A_{\text{out,PSA2}}) = \arg(A_{\text{in}})$$

Figure 1.5: Illustration of input (black) and output (cyan) signals for a two-mode PSA with gain $G_{\text{PSA}} = 4G_{\text{PIA}} = 16$ and idler input phase satisfying $\phi_{\text{i}} = -\phi_{\text{s}}$.

6

The two-mode single-pump PSA illustrated in Fig. 1.2(b) has a gain that depends on the phase of two separate waves, the signal and the idler, given that the pumps phases are constant. If the idler phase, ϕ_i, is kept constant also this scheme will lead to squeezing of the signal phase, ϕ_s. However, if the idler phase fulfills the condition $\phi_i = -\phi_s$, then the signal and idler phases will cancel and the PSA gain will no longer show dependence on the signal phase. As a consequence, all signal phase states can be amplified with the same gain $\sqrt{G_{PSA}}$ and with a 0 dB quantum-limited NF. This allows the two-mode PSA to operate in a modulation format independent manner, which is an important property for in-line amplifiers in transmission systems. It should be noted though that the ability of modulation format independent operation and multi-channel compatibility comes at the expense of having to transmit two data-carrying waves, the signal and the idler. The amplification by a two-mode PSA with $G_{PSA} = 4G_{PIA} = 16$ and with the idler input phase satisfying $\phi_i = -\phi_s$ is illustrated in Fig. 1.5.

A requirement for a PSAs to provide stable gain is that the interacting waves are frequency- and phase-locked. This is a major challenge when realizing PSAs in practice, especially if the interacting waves are widely separated in frequency. Other challenges when working with PSAs are polarization alignment, since PSAs are inherently polarization sensitive, and time synchronization of the interacting waves.

1.1.3 Prior work

PSAs have been an active research topic for more than four decades. Reviewing prior research shows that the applications that have attracted the most interest are generation of squeezed states [16, 18, 19], low-noise amplification [13, 20], and regeneration [21–24]. Other applications that have been explored, but not attracted the same amount of interest, are, e.g., dispersion compensation [25–27], quantum imaging [28, 29], and phase noise suppression [30, 31].

The PSAs that have been used to investigate the applications listed above have been implemented using a wide variety of material platforms. The most common material platforms have been $\chi^{(2)}$-nonlinear materials, e.g., KTP-crystals [32], and quasi-phase-matched periodically poled lithium niobate (PPLN) waveguides [33–35], and $\chi^{(3)}$-nonlinear materials, e.g., highly nonlinear fibers (HNLFs) [36,37], chalcogenide glass [38], and silicon waveguides [39]. In addition to this, semiconductor optical amplifiers (SOAs) have also been used [40].

The review presented here will primarily focus on work related to low-noise amplification, and in particular low-noise amplification for fiber optical communication systems. Moreover, the focus will be on fiber-based PSAs since they have the advantage of being easily integrated into fiber optical systems. A review of prior work on PSAs with a wider scope can be found in [14].

The possibility of constructing optical amplifiers (PSAs) that can amplify one signal quadrature without adding noise was first described in 1962 [41, 42]. How-

ever, it was not until 1982 that a precise statement of the amplifier uncertainty principle, the relation governing the noise properties of PSAs, was formulated and a more complete understanding of PSAs was reached [13]. Shortly after the capability of PSAs to achieve noiseless amplification (amplification with a 0 dB quantum-limited NF) was established [13, 43], the possible benefits of using one-mode PSAs in multi-span communication systems were theoretically investigated [44, 45]. It was shown that a 3 dB SNR improvement can be obtained in multi-span transmission systems amplified using one-mode PSAs, where the in-line amplifier gain equals the span loss, compared to a systems employing conventional PIAs [44].

The early experimental work on fiber-based PSAs was to a large extent carried out using nonlinear interferometric devices. The most commonly used device was the nonlinear Sagnac interferometer, which consists of a 3 dB coupler with a nonlinear fiber connecting the two output ports. This type of device operates using two phase-locked and frequency-degenerate waves, a signal and a strong pump. By launching the signal into one of the input ports and the pump into the other port, the signal will experience phase-sensitive gain and emerge at the signal input port.

The phase-dependent gain in the Sagnac interferometer PSA is such that one signal quadrature will be amplified by $\sqrt{G}$ while the orthogonal quadrature is deamplified by $\sqrt{1/G}$ [46]. The phase-dependence shown by the Sagnac interferometer PSA is thus identical to the phase-dependence for the one-mode PSA illustrated in Fig. 1.4, and from the phase-dependence it follows that it can provide phase-squeezing and noiseless amplification [13].

Using the nonlinear Sagnac interferometer several interesting results were demonstrated. Apart from the first demonstration of a fiber-based PSA [47], there was much work on using PSAs for low-noise in-line amplification [48–51], and regeneration of binary phase-modulated signals [52–54]. Particularly noteworthy is the first demonstration of error-free operation of an in-line PSA with 10 dB net gain [48], and the first demonstration of a NF below 3 dB using a high-gain fiber-based PSA [50]. In [48], the in-line amplifier was implemented in a back-to-back (B2B) system and the data rate was 2.4 Gbit/s. Phase-locking of the pump wave, which was generated internally, to the incoming signal was achieved using both injection locking (IL) [55], and an optical phase-locked loop (OPLL) [56]. The NF measured in [50] was 1.8 dB and it was measured at a 16 GHz offset from the pump frequency in order to avoid noise introduced by guided acoustic-wave Brillouin scattering (GAWBS).

Fiber-based nonlinear interferometric PSAs have the advantage that they are relatively easy to implement, only requiring phase-locking of two waves, which should be compared to three or four waves for FWM-based PSAs. However, the gain only grows quadratically with the pump power induced phase shift [46] (as opposed to exponentially for two-mode PSAs [57]), they are sensitive to GAWBS [58], resulting in amplitude noise at the PSA output, and any asymmetries in the coupler's splitting ratio leads to pump light leakage and signal degradation.

8

Moreover, as mentioned earlier, one-mode PSAs are not multi-channel compatible and cannot provide modulation format independent operation.

Two-mode PSAs does not suffer from any of the drawbacks of nonlinear interferometric PSAs and one-mode PSAs mentioned above. However, in general, the practical realization of two-mode PSAs is more difficult since a larger number of frequency- and phase-locked waves, often widely spaced in frequency, has to be generated. In a pioneering study on two-mode parametric interaction three phase-locked waves were generated using an acousto-optic modulator (AOM) and phase-sensitive amplification and attenuation was observed [59]. Due to a lack of schemes capable of generating phase-locked waves the experimental research on two-mode PSAs stagnated and it took almost 20 years to the first demonstration of data transmission over a transmission system amplified by a two-mode PSA [60].

The concept of using two-mode PSAs for low-noise and multi-channel amplification in fiber optical communication systems was first introduced in 2005 [61]. The first experimental demonstration of data transmission over a two-mode PSA-amplified transmission system showed error-free transmission of a 2.5 Gbit/s non-return-to-zero (NRZ) signal over a 60 km dispersion compensated link [60]. In [60], the frequency- and phase-locked pump, signal, and idler wave-triplet was generated using an optical double-sideband modulation scheme [62, 63], and the PSA was implemented using a FOPA. This scheme for generation of the frequency- and phase-locked waves has several limitations. For example, the bandwidth is limited by the bandwidth of the modulators used to generate the sidebands and the two side-bands contain the same data (idler is not a conjugate copy of the signal) which will lead to squeezing of one signal quadrature and thus not modulation format independent operation.

Frequency- and phase-locked waves can also be generated using a phase-insensitive parametric amplifier [64, 65]. By launching the signal and the pump waves into a nonlinear medium a frequency- and phase-locked idler wave, that is a conjugated copy of the signal wave, will be generated. With this scheme the bandwidth is determined by the bandwidth of the parametric amplifier, which can be very large [66]. The scheme is commonly referred to as the copier-PSA scheme and can be used to realize modulation format independent PSA-amplified transmission systems [67]. The copier-PSA scheme was later used to demonstrate phase-sensitive amplification of three WDM channels [68, 69]. However, the signals did not contain any data and the PSA was implemented in a B2B system.

The properties of PSA-amplified transmission systems based on the copier-PSA scheme was subsequently thoroughly investigated by Tong et al. It was theoretically shown that a transmission link implementation of the scheme can give up to 6 dB link NF improvement over conventional PIA-based schemes, and a 3 dB improvement over all-PSA-based schemes [67, 70]. The 6 dB link NF improvement over PIA-based schemes was also verified experimentally using a copier-loss-PSA system, where a transmission link was emulated by a lumped signal/idler loss [17, 37, 71]. The experiment showed amplification of three WDM

differential quadrature phase-shift keying (DQPSK) signals at 10 GBd using the copier-PSA configuration. Tong et al. also measured the NF of the PSA and demonstrated a record-low NF of 1.1 dB for a PSA at high gain [37].

1.2 This thesis

In this thesis we realize the first modulation format independent and multi-channel compatible single-span and multi-span transmission systems amplified by two-mode PSAs. We explore the properties of these systems and compare their performance to transmission systems based on conventional PIAs. To achieve modulation format independent and multi-channel compatible operation we use the copier-PSA scheme, implemented using FOPAs.

The first step towards realizing a PSA-amplified transmission system is taken in Paper [A]. Using the copier-PSA scheme, in which the transmission span is located between the copier and the PSA, the frequency- and phase-locked pump wave must be regenerated and amplified after the lossy transmission fiber. In Paper [A] we demonstrate and characterize a pump recovery system enabling transmission over spans with more than 40 dB loss. In Paper [B] we demonstrate the first modulation format independent and multi-channel compatible single-span PSA-amplified transmission system and show improved sensitivity compared to a conventional EDFA-amplified system, due to low-noise amplification. In Paper [C] we utilize the low-noise amplification of PSAs to demonstrate a record high sensitivity receiver.

Apart from low-noise amplification, higher SNR and improved transmission performance can also be achieved by increasing the power launched into the transmission spans. However, increasing the launch power will also increase the impact of fiber nonlinearities, which will degrade the transmitted signal [72, 73]. In Paper [D] we investigate the properties of a single-span PSA-amplified transmission system operating in the nonlinear transmission regime. We find that PSAs are capable of mitigating nonlinear distortions introduced by the fiber nonlinearities. However, the efficiency of the nonlinearity mitigation is dependent on the link dispersion map. In Paper [E] this dependence is studied both numerically and experimentally. In Paper [F] we investigate the properties of PSA-amplified transmission systems in more detail and present further demonstrations of the low-noise amplification and nonlinearity mitigation capabilities of two-mode PSA-amplified transmission systems.

In transmission systems with cascaded amplifiers, the presence of in-line amplifier noise might impact the performance. In Paper [G] we investigate, in a B2B configuration, how amplifier noise in hybrid PIA/PSA-amplified transmission systems affect the benefit gained from low-noise PSA amplification. In a multi-span PSA-amplified transmission system in-line amplifier noise will generate nonlinear phase noise (NLPN). In Paper [H] we study the impact of NLPN in PSA-amplified

transmission systems. Finally, in Paper [I] we present the first demonstration of a modulation format independent and multi-channel compatible multi-span transmission system amplified by two-mode PSAs acting as in-line amplifiers.

1.2.1   Thesis outline

This thesis is organized as follows. In Chapter 2 the topic of optical amplification is introduced and the noise limits of optical amplifiers are discussed. The amplification technology that this thesis is based on is FOPAs and in Chapter 3 this technology is described in detail. In Chapter 4 we discuss the practical implementation of PSA-amplified transmission systems, including practical implementation challenges. In Chapter 5 we conclude the thesis work and outline possible future research directions. Finally, in Chapter 6, the appended papers are summarized.

Chapter 2

Amplification and noise limits

Modern long-haul fiber optical communication systems use optical amplifiers to compensate for the loss of the transmission fiber. The noise added by these amplifiers limits the achievable capacity and transmission distance. Low-noise amplification is therefore very interesting. Particularly interesting are PSAs which have a 0 dB quantum limited NF, 3 dB lower than conventional optical amplifiers, such as the commonly used EDFA.

Chapter outline

The purpose of this chapter is to give an introduction to the topic of optical amplification in fiber optical communication systems and to provide an understanding of the fundamental noise limits of PIAs and PSAs.

In Section 2.1 we introduce the topic of optical amplification and describe the most common amplification techniques. The fundamental noise limits of optical amplifiers are governed by quantum mechanics. These quantum noise limits are discussed in Section 2.2 for PIAs and PSAs. Finally, in Section 2.3 we briefly discuss how amplifier noise impacts the performance of multi-span transmission systems.

2.1 Optical amplification

2.1.1 Introduction

Propagating a signal through an optical fiber will unavoidably lead to attenuation of the signal. The attenuation in a standard single mode fiber (SSMF) is typically 0.2 dB/km and originates from material absorption, Rayleigh scattering, and waveguide imperfections. Propagation will also lead to signal distortion due to linear and nonlinear effects occurring in the optical fiber. Linear effects, such as chromatic dispersion (CD) and polarization-mode dispersion (PMD), are

independent of the signal power. Linear effects are in general easier to mitigate than nonlinear effects, such as FWM, self-phase modulation (SPM), and cross-phase modulation (XPM), which depend on the signal power and will significantly impair the signal at high powers or long propagation distances.

A communication system relies on that the transmitted data can be accurately recovered at the receiver end. In practice this limits both the amount of acceptable signal distortion due to linear and nonlinear effects and the minimum signal power at the input of the receiver. The naive solution to satisfy the power condition would be to increase the power launched from the transmitter. However, this would increase the nonlinear distortions of the signal and is therefore not a viable path. Instead, the optical power has to be managed throughout the system in such a way that the power condition at the receiver is satisfied without introducing unacceptably large nonlinear distortions.

From the early years of long-haul fiber optical communication systems up until the mid-90's fiber attenuation was mostly managed by periodically detecting and retransmitting the signal using optoelectronic repeaters. In the mid-90's the role of optoelectronic repeaters as the leading technology for loss management was replaced by optical amplifiers, which could provide better performance. One of the most significant shortcomings of optoelectronic repeaters is that they are not practical to use in WDM systems, where information is transmitted simultaneously at several wavelengths through the same optical fiber, since one receiver-transmitter pair is needed for each wavelength channel, resulting in a complex and expensive system. Optical amplifiers, capable of simultaneous amplification of many WDM channels, quickly became the mainstream method for loss management after their introduction in 1986 [3], and lead to a significant increase in capacity by enabling WDM transmission.

2.1.2   Amplifier noise

Optical amplification comes at the price of degradation of the signal quality due to noise added by the amplifier. Without taking the receiver into account the quality of a signal can be quantified by the optical signal-to-noise ratio (OSNR), specifying the ratio between the average optical signal power and the optical noise power, with the noise power measured over a bandwidth of 0.1 nm. Both the signal and the noise at the input of an amplifier is amplified and therefore the OSNR would not degrade if the amplifier did not introduce any additional noise. However, in many cases, the amplifier adds independent internal noise to the signal, thus leading to degraded OSNR.

In multi-span transmission systems, i.e., systems with many cascaded amplifiers, the noise added by the amplifiers accumulate throughout the link and successively degrade the OSNR. For an amplified optical communication system the signal OSNR is closely related to the attainable capacity [74], with higher OSNR enabling higher capacity. The noise properties of the amplifiers are therefore very

important when designing an optical communication system.

Common for all commercially available optical amplifiers is that they are PIAs, i.e., their gain is independent of the signal phase. Moreover, they are generally operated in a linear regime, i.e., where the output signal is linearly related to the input signal. Operation in the linear regime is preferred since operation in a nonlinear regime would induce signal distortions.

The ultimate lower limit to the amount of noise added by an optical amplifier is governed by quantum mechanics. It has been shown that all PIAs operating in the linear regime with a gain $G > 1$ must add noise to the signal since a noise-free amplifier would violate Heisenberg's uncertainty principle [75, 76]. PSAs on the other hand, for which the gain is dependent on the signal phase, can in theory amplify a signal without adding any noise [13]. Instead the PSA reshapes the quantum noise to have different variances in different quadrature directions, also known as squeezing. The property of noiseless amplification make PSAs very interesting for transmission system applications.

2.1.3 System requirements

A long-haul fiber optical transmission system, illustrated in Fig. 1.1, have a typical span length of 80 km, which corresponds to a loss of about 16 dB. A basic requirement for optical amplifiers is thus that they can provide a gain of about 16 dB. Additional requirements are introduced by the technologies that are used in modern transmission systems to achieve high capacities.

One of the most important techniques to achieve high capacity is WDM. It is thus essential that the optical amplifiers in the link can provide gain over large bandwidths. Furthermore, it is important that the gain is flat over the signal bandwidth since gain differences between the channels would accumulate into large power differences after many amplifiers.

Traditionally on-off keying (OOK) has been the most commonly used modulation format in optical communication systems. However, the trend is moving towards using more advanced modulation formats with higher spectral efficiency, such as polarization-multiplexed quadrature phase-shift keying (PM-QPSK) and 16-ary quadrature amplitude modulation (16QAM) [77, 78]. This increase the requirements on the amplifier to provide gain without distorting the signal.

As for all systems, energy consumption and cost are important. It is therefore important that the amplifier has a high gain efficiency, i.e., low pump power requirement per dB of gain. Furthermore, to reduce the energy consumption and cost, a primary concern when designing a communication system is to minimize the transmission loss. In a fiber optical communication system the loss originates mainly from attenuation in the optical fiber. The loss is wavelength dependent and the range which has the lowest loss is called the conventional 'C'-band and spans 1530-1570 nm in silica fibers. It is thus important that the amplifier is capable of amplification in the C-band.

Several types of optical amplifiers, capable of amplification in the C-band, are commercially available. The most common types are doped fiber amplifiers (DFAs), with the EDFA [79], being the dominating technology. Raman amplifiers [80], SOAs [81], and FOPAs [82] are based on different gain mechanisms and have different performance and properties that will be discussed below.

2.1.4 Amplification techniques

Erbium-doped fiber amplifiers

The EDFA is the dominating technology for loss management in today's long-haul fiber optical communication systems. The EDFA was invented in 1986 [3], and quickly became an interesting technology due to its capability to amplify signals in the C-band. After its commercialization in the mid-1990's it rapidly gained its position as the leading loss management technology.

The EDFA, with a gain bandwidth of about 40 nm (5.3 THz), is mainly used for C-band operation but longer 'L'-band (1570-1610 nm) operation has been demonstrated by increasing the erbium concentration [83], and shorter 'S'-band (1490-1520 nm) operation by using a double-pass configuration [84]. DFAs operating in the S-band can also be constructed by doping with thulium instead of erbium [85].

All DFAs are optically pumped and amplification is achieved through population inversion, i.e., the majority of the ions are in an excited state, and stimulated emission. Along with stimulated emission there is also spontaneous emission. The spontaneously emitted photons will be amplified and result in amplified spontaneous emission (ASE). The ASE will then beat with the signal at detection and cause noise, which is the main noise source associated with EDFAs.

The amount of ASE noise generated in an EDFA is affected by the pump wavelength and the pumping scheme. Pumping can be done at 980 and 1480 nm, with 980 nm pumping giving better noise performance [12]. The pumping schemes commonly employed are unidirectional pumping in the forward or backward direction and bidirectional pumping.

Apart from the capability of C-band operation, the EDFA has many other valuable features. The gain mechanism in EDFAs results in a very slow gain response time, on the order of milliseconds. This feature makes it possible to operate EDFAs in gain saturation mode without inducing signal distortion and channel crosstalk in WDM systems, i.e., they can work as linear amplifiers on a bit level even if the gain is saturated on average.

From a long-haul transmission system perspective other important features are polarization insensitive and high gain, a high gain efficiency, ~ 0.1 mW pump power required per dB of gain [86], and low NF, 3.1 dB at 54 dB gain has been demonstrated [87]. Its compatibility with silica fibers and low insertion loss are also important. All these features have contributed to the popularity of the EDFA.

The gain of EDFAs is not dependent on the phase of the signal and EDFAs are

(a) Booster

(b) Preamplifier

(c) In-line amplifier
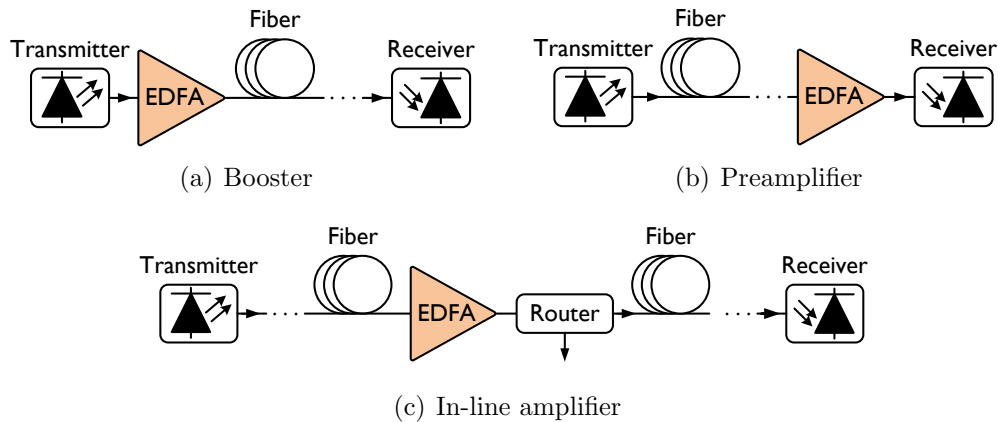
Figure 2.1: Illustration of possible amplifier placements.

therefore PIAs and have a 3 dB quantum limited NF. The actual NF is strongly dependent on the population inversion, with the lowest NF attainable at the highest population inversion. In the high gain limit the NF of an EDFA is given by $NF = 2n_{sp}$ where n_{sp} is the spontaneous emission factor, which is always greater than or equal to unity [12, p. 100]. For complete medium inversion the spontaneous emission factor equals unity and the NF take the value of 2 (3 dB). In practice the NF exceeds 3 dB and can be as large as 6-8 dB in commercial amplifiers due to other noise sources and insertion losses.

EDFAs, and amplifiers in general, have a few different common usages in fiber optical communication systems. The first usage is as a power booster placed after the optical transmitter to increase the signal level before transmission. Another usage is as a preamplifier placed before the optical receiver where the purpose is to improve the receiver sensitivity. The last common usage is as in-line amplifier in a long-haul transmission system. The in-line amplifier is used to compensate the loss from the passive fiber sections or routing losses. The three different usages are illustrated in Fig. 2.1.

Semiconductor optical amplifiers

SOAs were developed during the 1980's and can provide gain through stimulated emission in an electrically pumped semiconductor. The main advantages of SOAs are large bandwidth, low power consumption, and compactness. By varying the design SOAs can be made to operate in a range from 0.85 to 1.60 μm with gain bandwidths in the order of 50 nm (6.2 THz).

Unfortunately there are several issues with SOAs that make them problematic for use in long-haul transmission systems. A major problem is nonlinearities and crosstalk that distort the signal, especially in WDM systems, which is partly due to the picosecond gain response time [88].

17

Other concerns are coupling losses both in and out of the device due to difference in refractive index and waveguide shape compared to the silica optical fiber. The input coupling loss results in relatively high black-box NFs and the output loss reduce the achievable gain. SOAs with a 7.2 dB NF at 29 dB gain have been demonstrated [89]. Polarization dependent operation is also an issue for SOAs.

Although the SOAs have difficulties to compete with other amplification technologies for applications in long-haul fiber optical communication systems they are still interesting for signal processing applications such as wavelength converters and all-optical regeneration [81].

Raman amplifiers

Raman amplifiers utilize the phenomenon of stimulated Raman scattering (SRS), first discovered in 1962 [90, 91], for signal amplification [80, 86, 92]. Raman scattering [93], is the process when a photon is absorbed by a molecule which then emits a photon of lower frequency than the one absorbed. The energy difference between the absorbed and emitted photon is absorbed by a phonon, a vibrational mode of the molecule. The molecule can also emit a photon of higher frequency than the one absorbed but that process is much more uncommon since it requires the presence of a phonon with the correct energy. Raman scattering is a very fast process and takes place on a sub-picosecond timescale.

In Raman amplifiers, which are optical fiber based, two waves are present in the fiber, a strong pump wave that will excite the molecules and a signal wave, at a lower frequency, that will be amplified. The gain, originating from SRS, depends on the frequency separation between the pump and the signal, the medium, and the signal and pump polarization, with co-polarized waves providing highest gain. In silica-based fibers the gain bandwidth is about 40 THz (320 nm) and the peak gain occur at about 13 THz below the pump frequency. Due to the large bandwidth, Raman amplifiers are attractive for WDM systems that extend outside the C-band.

Raman amplifiers have a fairly low gain efficiency with ∼ 10 mW pump power per dB gain. However, high gain can be achieved with up to 45 dB demonstrated [94], and for pump powers above a certain threshold value the signal power builds up almost exponentially. Raman amplifiers can be implemented in polarization independent configurations by scrambling the polarization of the pump.

They can be implemented both as lumped and distributed amplifiers, i.e., the gain is distributed along the transmission fiber. In general it is attractive to use distributed amplification due to improved noise performance and reduced nonlinear distortion. Combining distributed Raman amplification with EDFAs has also been demonstrated with promising results [95, 96].

Since the amplification is taking place in the transmission fiber itself there are low insertion losses associated with the technique and low NF can be achieved. The dominant noise source for Raman amplifiers is ASE noise from spontaneous Raman scattering.

2.2 Amplifier noise limits

2.2.1 Fundamental concepts

Quantum noise and thermal noise

In contrast to the classical description of electromagnetic fields, quantum mechanics predict that the vacuum state, i.e., the state with no photons, has a non-zero ground-state energy. This energy is called zero-point energy or vacuum energy and has no analogue in the classical theory. The value of the zero-point energy for a single mode with frequency ν is $h\nu/2$, which follows from a description of the quantized electromagnetic field as composed of infinitely many uncoupled harmonic oscillators [97, p. 139–144].

A more intuitive explanation of the zero-point energy can be obtained by considering the uncertainty principle which states that there is a fundamental limit to the accuracy of a simultaneous measurement of a particle's position q and momentum p. The principle is formulated as [98, p. 43]

$$\Delta p \Delta q \geq \frac{\hbar}{2},$$ (2.1)

where Δp and Δq are the uncertainties associated with the position and momentum, respectively, and $\hbar = h/(2\pi)$ is the Planck's constant. Taking the starting point in (2.1) it can be shown that the zero-point energy is the result of zero-point fluctuations in the position and momentum of a harmonic oscillator [98, p. 81–82]. With this interpretation of the zero-point energy it is near at hand to define a minimum detectable noise power P_{QN} as

$$P_{\mathrm{QN}} = \frac{h\nu B_0}{2},$$ (2.2)

where B_0 is the bandwidth of the detector used to measure the noise. This noise power is often referred to as quantum noise [12, p. 71].

Another fundamental noise source is thermal noise. The thermal noise has a noise power given by [12, p. 71]

$$P_{\mathrm{TN}} = \frac{h\nu B_0}{\exp\left[\dfrac{h\nu}{k_{\mathrm{B}}T}\right] - 1},$$ (2.3)

where k_{B} is the Boltzmann constant and T is the temperature in Kelvin. For a system operating at a temperature > 0 K both quantum noise and thermal noise will be present. It is interesting to compare the relative contribution from these two noise sources at various frequencies. In Fig. 2.2 we have plotted the quantum noise and the thermal noise versus frequency assuming a temperature $T = 290$ K and a detector bandwidth $B_0 = 12.5$ GHz, corresponding to 0.1 nm
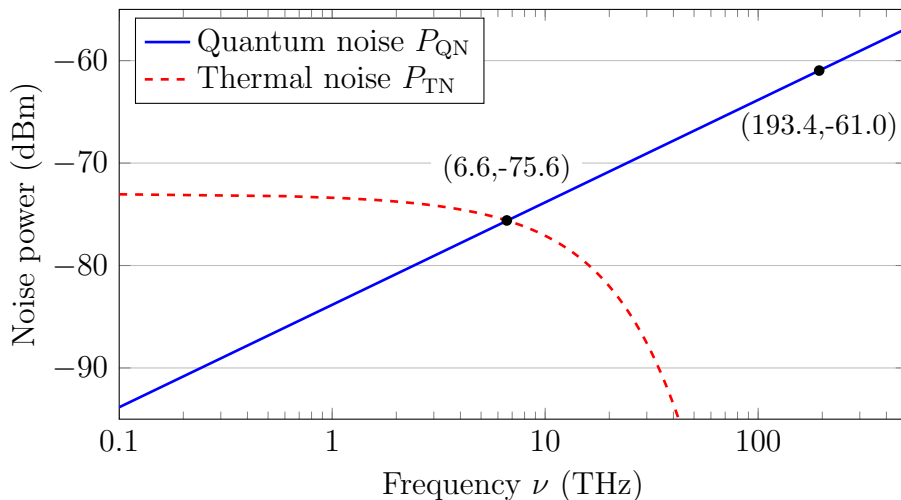
Figure 2.2: Comparison of quantum noise power P_{QN} and thermal noise power P_{TN} at a temperature $T = 290$ K and with a detector bandwidth $B_0 = 12.5$ GHz.

at a wavelength of 1550 nm. We clearly see the existence of two regimes. At low frequencies thermal noise is dominating while at high frequencies quantum noise is dominating. The intersection, where thermal noise and quantum noise is equal, occurs at a frequency of 6.6 THz (45 μm) at room temperature. This point has been indicated in Fig. 2.2. Reducing the operating temperature will shift the intersection point to lower frequencies, i.e., extend the region where quantum noise dominates. For example, at 77 K the intersection point will be at 1.8 THz (170 μm) corresponding to a noise power of -81.4 dBm, and at 4 K the intersection point will be at 0.1 THz (3 mm) corresponding to a noise power of -94.5 dBm.

The input noise for an electronic amplifier operating at radio frequencies (RFs) ($\nu < 3$ THz) and room temperature will thus be dominated by thermal noise rather than quantum noise. In this case the input signal has large excess noise beyond the quantum limit. This will lead to a negligible SNR degradation through the amplifier, considering only the addition of quantum noise in the amplifier. Amplifiers operating at RFs can therefore realize NFs arbitrarily close to 1 (0 dB) [20]. A similar situation occurs in multi-span transmission systems where the signal carries large excess noise due to previous amplification stages. At frequencies typically used in fiber optical communication systems, i.e., around 1.55 μm (193.4 THz), it is clear that, in the absence of other external noise sources, quantum noise dominates over thermal noise. We note that at $\nu = 193.4$ THz the quantum noise power over a bandwidth of 0.1 nm is -61.0 dBm. This point is indicated in Fig. 2.2.

Phasor representation of quantum states

For a qualitative understanding of the quantum noise associated with a signal, it is illustrative to use phasor representation and phasor plots. In the classical description a signal $S = A\sin(\omega t + \phi)$ can be expressed as

$$S = \mathrm{Re}\big[(X_1 + iX_2)\exp(-i\omega t)\big] = X_1\cos(\omega t) + X_2\sin(\omega t), \qquad (2.4)$$

where

$$X_1 = A\sin(\phi) \quad \text{and} \quad X_2 = A\cos(\phi) \qquad (2.5)$$

are the in-phase and quadrature components of S, respectively. Represented in this form the information is carried by slow variations in X_1 and X_2. In a phasor plot this signal would be represented by an infinitesimal point at (X_1, X_2) due to the absence of quantum noise in the classical description.

In a quantum mechanical description the information of a signal can in an analogous way be related to two operators $\hat{X}_1$ and $\hat{X}_2$ which give the amplitude of the in-phase and quadrature components, respectively. These two operators satisfy the commutation relation [13]

$$\big[\hat{X}_1, \hat{X}_2\big] = \frac{i}{2}, \qquad (2.6)$$

where the commutator is defined by $[a, b] = ab - ba$, which in turn implies the uncertainty relation [99, p. 35]

$$\big\langle (\Delta \hat{X}_1)^2\big\rangle\big\langle (\Delta \hat{X}_2)^2\big\rangle \geq \frac{1}{16}, \qquad (2.7)$$

where $\big\langle (\Delta \hat{X}_i)^2\big\rangle = \langle \hat{X}_i^2\rangle - \langle \hat{X}_i\rangle^2$ is the variance of $\hat{X}_i$, with $\langle\cdot\rangle$ denoting the expectation value and $i \in \{1, 2\}$. In the classical picture the signal power P is related to the complex amplitude $X_1 + iX_2$ by $P = |X_1 + iX_2|^2 = X_1^2 + X_2^2$. In the same manner we can express the noise power in the quantum mechanical description as $\big\langle (\Delta \hat{X}_1)^2\big\rangle + \big\langle (\Delta \hat{X}_2)^2\big\rangle$, and using (2.7) we obtain the inequality

$$\big\langle (\Delta \hat{X}_1)^2\big\rangle + \big\langle (\Delta \hat{X}_2)^2\big\rangle \geq \frac{1}{2}. \qquad (2.8)$$

The noise power in (2.8) is expressed in units of number of quanta, i.e., in energy units of $h\nu$, and we note that the minimum value of the noise power is exactly the zero-point energy $h\nu/2$.

A signal, called a state in the quantum mechanical description, with the uncertainty given by (2.8) can be illustrated in a phasor plot. The quantum state that is most similar to a classical signal is the coherent state. This state has the minimum amount of noise allowed by (2.8) and the noise is distributed equally between the in-phase and quadrature components, i.e., $\big\langle (\Delta \hat{X}_1)^2\big\rangle = \big\langle (\Delta \hat{X}_2)^2\big\rangle$, with $\big\langle (\Delta \hat{X}_i)^2\big\rangle = 1/4$. A coherent state is shown in Fig. 2.3(a). The vacuum

(a) Coherent state   (b) Vacuum state   (c) Squeezed state
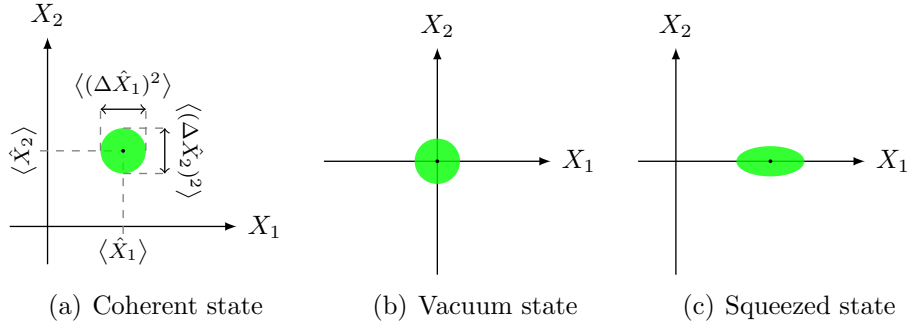
Figure 2.3: Phasor plots of various quantum mechanical states.

state, with only the zero-point fluctuations, is illustrated in Fig. 2.3(b), and a so-called squeezed state is illustrated in Fig. 2.3(c). In the squeezed state the noise is unevenly distributed between the in-phase and quadrature components, i.e., $\langle(\Delta\hat{X}_1)^2\rangle \neq \langle(\Delta\hat{X}_2)^2\rangle$.

Noise figure

When discussing noise in optical amplifiers we are in general interested in how much noise is added to the signal by the amplifier. To quantify this noise it is common to use the NF measure [11, 100]. For linear amplifiers the NF is defined as

$$\text{NF} = \frac{\text{SNR}_\text{in}}{\text{SNR}_\text{out}}, \tag{2.9}$$

where SNR_in is the SNR at the amplifier input port and SNR_out is the SNR at the amplifier output port. The SNR is defined as the ratio of the electrical signal power to the electrical noise power, measured using an ideal photodetector with quantum efficiency of unity. To ensure that the NF measure has the maximum sensitivity to noise added by the amplifier it is assumed that the input signal is only degraded by shot noise, resulting from the particle nature of light.

2.2.2   Phase-insensitive amplifiers

It was proved already in 1962 by Heffner [75], that a PIA must add noise to the signal. His argument is outlined below. The uncertainty principle (2.1) can be written as a number-phase uncertainty relation [98, p. 77]

$$\Delta n\Delta\phi \geq \frac{1}{2}, \tag{2.10}$$

where n denotes the average number of photons, related to the amplitude, and ϕ denotes the phase. The variables Δn and $\Delta\phi$ represent the uncertainties in n and ϕ, respectively, that are associated with a measurement. The crucial point in Heffner's

argument is that (2.10) has to be satisfied when performing a measurement both at the input and at the output of an amplifier. Based on this argument he showed that the minimum noise power contribution by a PIA is [75]

$$P_{\mathrm{N}} = \frac{h\nu B_0}{2}(G_{\mathrm{PIA}} - 1), \tag{2.11}$$

where B_0 is the amplifier bandwidth and G_{PIA} is the amplifier gain. With a gain $G_{\mathrm{PIA}} > 1$ the amplifier must thus add noise to the signal. If this noise was not added by the amplifier then it would be possible to gain information about the input signal, with better accuracy then stated by the uncertainty principle, by measuring the output signal. In the limit of high gain ($G_{\mathrm{PIA}} \gg 1$) (2.11) states that the noise added by the amplifier is equal to the amplification of the zero-point fluctuations present at the amplifier input.

An alternative approach for quantifying the noise added by an amplifier is to consider the in-phase and quadrature component of the signal. This approach will give both a value for the noise added by the amplifier and a lower limit for the amplifier NF. We follow the method in [13] which treat a one-mode linear amplifier. The results below should be compared to the results obtained for a two-mode parametric amplifier in Section 3.4.

In analogy with the input mode operators $\hat{X}_1$ and $\hat{X}_2$ we can introduce the output mode operators $\hat{Y}_1$ and $\hat{Y}_2$. The uncertainty in the in-phase and quadrature components, $\langle \hat{Y}_1 \rangle$ and $\langle \hat{Y}_2 \rangle$, is given by

$$\langle (\Delta \hat{Y}_{\mathrm{i}})^2 \rangle = G_{\mathrm{i}} \langle (\Delta \hat{X}_{\mathrm{i}})^2 \rangle + \langle (\Delta \hat{F}_{\mathrm{i}})^2 \rangle, \tag{2.12}$$

where G_i denotes the gain and $i \in \{1, 2\}$. The first term on the right hand side represents the amplified input noise and the second term represents the noise added by the amplifier. Based on this equation we can define the added noise number

$$A_{\mathrm{i}} = \frac{\left\langle |\Delta \hat{F}_{\mathrm{i}}|^2 \right\rangle}{G_{\mathrm{i}}} \tag{2.13}$$

which describe the added noise referred to the amplifier input in units of number of quanta.

PIAs amplify both the in-phase and quadrature components identically, since their response is insensitive to the signal phase, and therefore a single noise number A is sufficient to describe the amplifier. The noise number A satisfies the inequality [13]

$$A \geq \frac{1}{2} \left| 1 - \frac{1}{G_{\mathrm{PIA}}} \right|, \tag{2.14}$$

which is expressed in units of number of quanta. (2.14) is known as the fundamental theorem for phase-insensitive linear amplifiers [13]. The significance of this relation is the same as for (2.11), for high gain ($G_{\mathrm{PIA}} \gg 1$) the minimum noise

<div align="center">(a) PIA with $G_{\mathrm{PIA}} = 8$.   (b) One-mode PSA with $G_{\mathrm{PSA}} = 8$.</div>
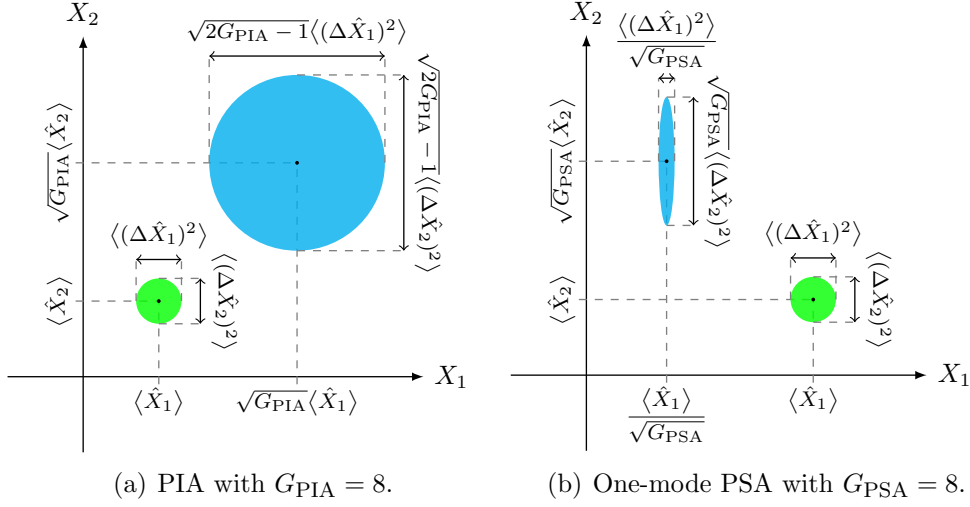
Figure 2.4: Illustrating of amplification of a coherent state using (a) a PIA and (b) a one-mode PSA. The input signal is illustrated by a green area and then output signal is illustrated by a cyan area.

contribution of the amplifier is equivalent to an additional zero-point fluctuation quantity at the input.

Using (2.14), an inequality for the PIA NF can now be derived, as [13]

$$\mathrm{NF}_{\mathrm{PIA}} \geq \left| 2 - \frac{1}{G_{\mathrm{PIA}}} \right| \tag{2.15}$$

for gains $G_{\mathrm{PIA}} \geq 1$. In the limit of high gain ($G_{\mathrm{PIA}} \gg 1$) we obtain $\mathrm{NF}_{\mathrm{PIA}} = 2$ (3 dB) which is the quantum limited NF for PIAs.

In Fig. 2.4(a) we illustrate the amplification of a coherent state by a PIA. Characteristic for phase-insensitive amplification is that noise is added, which is illustrated by the increased area, and that equal amount of noise is added to the in-phase and quadrature components, thus maintaining the circular shape of the coherent input signal.

2.2.3 Phase-sensitive amplifiers

For PIAs one noise number is enough to describe the added noise. For PSAs, where the response depends on the signal phase, two noise numbers A_1 and A_2 (and two gain numbers G_1 and G_2) are needed, since the in-phase and quadrature components are treated differently by the amplifier. The fundamental theorem for PIAs is replaced by the more general amplifier uncertainty principle [13]

$$A_1 A_2 \geq \frac{1}{16} \left| 1 - \frac{1}{\sqrt{G_1 G_2}} \right|^2 . \tag{2.16}$$

<div align="center">24</div>

(a) Type A   (b) Type B
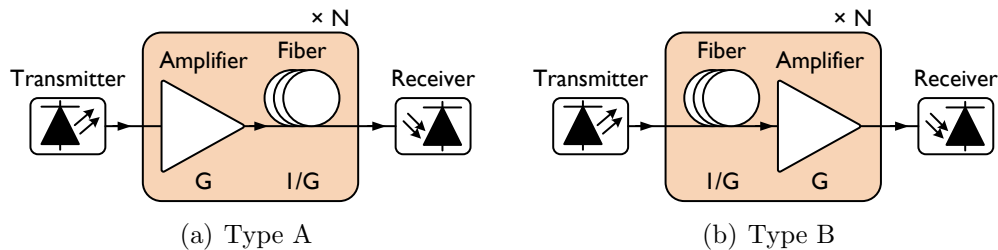
Figure 2.5: Illustration of possible in-line amplifier configurations.

We note from (2.16) that the added noise to either the in-phase or quadrate component can be reduced at the expense of the noise added to the other component. In particular, if $G_1 = 1/G_2 = G_{\text{PSA}}$, which is always the case for parametric amplifiers with signal and idler gain, the right hand side of (2.16) is zero and at least one component can be amplified without the addition of noise.

By analyzing the one-mode PSA in detail, in a similar manner to what will be done for two-mode PSAs in Section 3.4, it can be found that both the signal and the noise in the component being amplified by G_{PSA} will experience the same gain. The consequence of this is that the amplified signal component will be amplified with a 0 dB NF. The signal and the noise in the attenuated component will be attenuated in the corresponding manner and produce a squeezed output state. The amplification of a coherent state using a one-mode PSA is illustrated in Fig. 2.4(b).

2.3 Noise in multi-span links

Long-haul fiber optical communication systems typically consist of cascaded sections (spans) of loss, due to the optical fiber, and amplification, from lumped optical amplifiers. In Fig. 2.5 two generic link designs are illustrated. In a type A link, shown in Fig. 2.5(a), the loss is pre-compensated by amplification, and in a type B link, shown in Fig. 2.5(b), the loss is post-compensated by amplification. In both systems the gain in each span is assumed to be G and the loss is assumed to be $1/G$, resulting in zero net gain.

These two systems have been extensively studied for the case of PIA-amplification and one-mode PSA-amplification [12, 44]. With PIAs the link NF for the two link types are given by [70]

$$\text{NF}_{\text{A,PIA}} = 1 + 2N\left(1 - \frac{1}{G}\right) \quad \text{and} \quad \text{NF}_{\text{B,PIA}} = 1 + 2NG\left(1 - \frac{1}{G}\right), \quad (2.17)$$

and with PSAs the link NFs are given by

$$\text{NF}_{\text{A,PSA}} = 1 + N\left(1 - \frac{1}{G}\right) \quad \text{and} \quad \text{NF}_{\text{B,PSA}} = 1 + NG\left(1 - \frac{1}{G}\right), \quad (2.18)$$

where N is the number of spans. From (2.17) and (2.18) it is clear that a one-mode PSA-amplified link have a 3 dB lower link NF in the case of high gain ($G \gg 1$) and many spans. A 3 dB link NF advantage could for example translate into doubled transmission reach [101].

Chapter 3

Fiber optical parametric amplifiers

It was early discovered that FOPAs have attractive properties, e.g., high gain, large bandwidth, and capability of sub-3 dB NF amplification when operated as PSAs. However, due to absence of hardware, such as high-power amplifiers and high-quality optical fibers with high nonlinear coefficients, the number of experimental studies on FOPAs in general, and phase-sensitive FOPAs in particular, was initially limited.

Advances in hardware and experimental techniques have recently opened up new possibilities to experimentally study FOPAs. These studies have confirmed that FOPAs are very capable amplifiers and signal processing platforms. Especially exciting are the demonstrations of sub-3 dB NF amplification.

Chapter outline

The goal of this chapter is to give a detailed description of FOPAs. We start in Section 3.1 by giving an introduction to the topic. FOPAs are based on FWM, a phenomenon described in Section 3.2. In Section 3.3 we describe the gain properties of FOPAs. We introduce a transfer matrix description in Section 3.4 and use that to describe the difference between phase-insensitive and phase-sensitive FOPAs. Finally, in Section 3.5 we describe how FOPAs can be implemented in practice.

3.1 Introduction

FOPAs utilize FWM, a nonlinear phenomenon, to achieve amplification. The gain mechanism is called parametric amplification or parametric gain and describe the process when energy is transferred between several interacting waves without any energy storage in the medium.

The interaction between an electromagnetic wave and the medium it propagates through is governed by the material susceptibility χ [102, p. 15]. At high field intensities not only the linear susceptibility will be of importance but also higher order susceptibilities, which result in a nonlinear response. In materials without inversion symmetry, such as many crystals, the 2nd-order susceptibility $\chi^{(2)}$ will be the dominating higher order susceptibility and will give rise to for example second harmonic generation (SHG) and sum-frequency generation (SFG). In isotropic materials, such as silica (SiO_2) glass, all even-order susceptibilities vanishes and the 3rd-order susceptibility $\chi^{(3)}$ will dominate.

Parametric amplification can be obtained both in $\chi^{(2)}$-nonlinear materials [103–106], and $\chi^{(3)}$-nonlinear materials [107, 108]. It is in many cases preferable to work with fiber-based amplifiers due to their compatibility with fiber optical transmission systems. In optical fibers, which are made of silica glass, $\chi^{(3)}$ dominates and will give rise to FWM, which can provide parametric gain. Parametric amplifiers implemented using FWM in optical fibers are called FOPAs.

FOPAs can be operated both using pulsed and continuous wave (CW) pumps. The first FOPAs were demonstrated with pulsed pumps [107, 109, 110]. Using a pulsed pump, with high peak power, eases the requirements on the other parts of the system and high gain can be obtained over short lengths of fiber with only modest nonlinear coefficients. However, for most communication related applications a CW pump is required.

In order to demonstrate FOPAs with CW pumps, fibers with high nonlinear coefficients and low zero-dispersion wavelength (ZDW) variations are required. Furthermore, a high-power pump source is needed. These requirements slowed the development of FOPAs for a long time and it was not until the mid-1990's that progress started to gain pace and CW pumped FOPAs were demonstrated [111]. Particularly noteworthy was the first demonstration of a CW pumped FOPA with significant black-box signal gain [112].

The gain mechanism in FOPAs is fundamentally different from the mechanism that provide gain in EDFAs, which also lead to fundamentally different amplifier properties. The operating range and bandwidth of FOPAs is mainly determined by the nonlinear fiber design. FOPAs have been demonstrated with gain over a large range of frequencies and with bandwidths as large as 155 nm using a dual-pump configuration [113], and 270 nm using a single-pump configuration [66]. Gain values of 70 dB have been demonstrated [114], and the gain efficiency is comparable to that of Raman amplifiers with ~ 10 mW pump power per dB gain. A NF of 3.7 dB has been demonstrated for phase-insensitive FOPAs [115], and 1.1 dB at 26.5 dB gain for phase-sensitive FOPAs [37]. It is estimated that Raman coupled noise will limit the NF of phase-sensitive FOPAs to at best 0.5 dB [116].

A basic property of parametric amplifiers is the ultra-fast gain mechanism with a femtosecond response time. This should be compared to the millisecond response time in EDFAs. While this prevent FOPAs from operating in saturation in many applications it opens up for nonlinear signal processing applications. Some

demonstrations of nonlinear signal processing using parametric effects in fibers are sampling [117], demultiplexing [118], amplitude regeneration [119], and format conversion [120].

Another property that is fundamentally connected to the gain mechanism is the polarization dependence of the gain. This is a major drawback for transmission system applications. However, at the expense of efficiency and complexity, it is possible to obtain polarization-insensitive operation for phase-insensitive FOPAs using two orthogonally polarized pumps [121–123].

3.2 Four-wave mixing

FWM, also named four-photon mixing, originates from the $\chi^{(3)}$ nonlinearity and involves the interaction of four waves. An intuitive understanding of the process can be obtained by considering the refractive index modulation that is induced by a high-intensity wave through the Kerr-effect.

If two waves at frequencies ω_1 and ω_2 co-propagate through a fiber then they will beat at a frequency $\omega_2 - \omega_1$ and through this intensity beating modulate the refractive index with the same frequency. If a third wave is added, with frequency ω_3, then it will become phase modulated with the frequency $\omega_2 - \omega_1$ and develop sidebands at $\omega_3 \pm (\omega_2 - \omega_1)$ due to the modulated refractive index. Similarly will ω_3 beat with ω_1 and phase modulate ω_2 such that ω_2 generate sidebands at $\omega_2 \pm (\omega_3 - \omega_1)$. Considering all possible combinations, new frequency components will be generated at $\omega_{jkl} = \omega_j + \omega_k - \omega_l$ with $j, k, l \in \{1, 2, 3\}$ [124]. Some of these components will overlap, either with each other or with the original waves. Components that overlap with the original waves provide gain. There will be nine newly generated frequency components and these will have varying power, the stronger ones are usually referred to as idlers and the weaker ones are usually neglected.

For the specific case of one degenerate strong wave (pump) and one weaker wave (signal) one significant new frequency component will be generated (idler) and gain will be provided to the signal. This is the case we study in this thesis, called single-pump two-mode scheme. The FWM process is highly polarization dependent and in the discussion below we will assume that all waves have the same state of polarization over the entire interaction length.

In a quantum mechanical picture FWM can be understood as the annihilation of two photons and the creation of two photons, with frequencies such that momentum and energy is conserved. In the case of degenerate FWM, where two waves have the same frequency ω_1, the process must satisfy $2\omega_1 = \omega_2 + \omega_3$ and $\Delta\beta = \beta_2 + \beta_3 - 2\beta_1 = 0$.

To get a more complete description of FWM we consider the field amplitude of the electromagnetic wave of three co-polarized waves propagating in a SSMF. One degenerate pump wave, denoted by index p, one signal wave, denoted by index

s, and an idler wave, denoted by index i. The sum of the electrical fields can be written as [102]

$$E(x, y, z) = \frac{f(x,y)}{2} \sum_{k \in \{p,s,i\}} \left\{ A_k(z) \exp\left[i(\beta_k z - \omega_k t)\right] \right\} + \text{c.c.}, \qquad (3.1)$$

where c.c. denotes the complex conjugate which is usually omitted in the calculations, and $f(x,y)$ is the transverse mode profile, common for all waves. Each of the three waves is represented by the slowly varying complex field amplitude $A(z)$, the propagation constant β, and the frequency ω. By inserting (3.1) into the nonlinear Schrödinger equation (NLSE) the following coupled equations can be derived [102]

$$\frac{dA_{\text{p}}}{dz} = i\gamma \left\{ \left[|A_{\text{p}}|^2 + 2\left(|A_{\text{s}}|^2 + |A_{\text{i}}|^2 \right) \right] A_{\text{p}} + 2 A_{\text{s}} A_{\text{i}} A_{\text{p}}^* \exp\left(i\Delta\beta z\right) \right\}, \qquad (3.2)$$

$$\frac{dA_{\text{s}}}{dz} = i\gamma \left\{ \left[|A_{\text{s}}|^2 + 2\left(|A_{\text{p}}|^2 + |A_{\text{i}}|^2 \right) \right] A_{\text{s}} + A_{\text{i}}^* A_{\text{p}}^2 \exp\left(-i\Delta\beta z\right) \right\}, \qquad (3.3)$$

$$\frac{dA_{\text{i}}}{dz} = i\gamma \left\{ \left[|A_{\text{i}}|^2 + 2\left(|A_{\text{p}}|^2 + |A_{\text{s}}|^2 \right) \right] A_{\text{i}} + A_{\text{s}}^* A_{\text{p}}^2 \exp\left(-i\Delta\beta z\right) \right\}, \qquad (3.4)$$

where

$$\Delta\beta = 2\beta_{\text{p}} - \beta_{\text{s}} - \beta_{\text{i}} \qquad (3.5)$$

is the propagation constant mismatch and γ is the nonlinear coefficient. In order to arrive at this set of equations we have neglected fiber attenuation, higher-order dispersion, any wavelength dependence of γ, and the Raman effect.

We note that the first two terms on the right hand side of (3.2)-(3.4) give rise to nonlinear phase-shifts, the first term corresponds to SPM and the second to XPM. The last term governs a power transfer between the waves and is due to FWM. It is clear that the FWM term depends on $\Delta\beta$, which is determined by the relative phase of the waves. We also note that XPM and SPM do not need phase-matching since they only depend on the intensity.

By defining $A_{\text{j}} = \sqrt{P_{\text{j}}} \exp(i\phi_{\text{j}})$ for $j \in \{p, s, i\}$, where P_{j} is the power and ϕ_{j} is the phase of wave j, (3.2)-(3.5) can be written as [82]

$$\frac{dP_{\text{p}}}{dz} = -4\gamma (P_{\text{p}}^2 P_{\text{s}} P_{\text{i}})^{1/2} \sin(\theta), \qquad (3.6)$$

$$\frac{dP_{\text{s}}}{dz} = \frac{dP_{\text{i}}}{dz} = 2\gamma (P_{\text{p}}^2 P_{\text{s}} P_{\text{i}})^{1/2} \sin(\theta), \qquad (3.7)$$

and

$$\frac{d\theta}{dz} = \Delta\beta + \gamma(2P_{\text{p}} - P_{\text{s}} - P_{\text{i}}) + \left(\sqrt{\frac{P_{\text{p}}^2 P_{\text{s}}}{P_{\text{i}}}} + \sqrt{\frac{P_{\text{p}}^2 P_{\text{i}}}{P_{\text{s}}}} - 4\sqrt{P_{\text{s}} P_{\text{i}}} \right) \cos(\theta), \quad (3.8)$$

where $\theta = 2\phi_\mathrm{p} - \phi_\mathrm{s} - \phi_\mathrm{i}$. It is clear from (3.6) and (3.7) that the FWM efficiency is maximized for $\theta = \pi/2$. This condition is referred to as the process being phase-matched. If $\theta = \pi/2$ then the last term in (3.8) will be zero and in order for the process to stay phase-matched we need

$$\kappa \equiv \Delta\beta + 2\gamma P_\mathrm{p} = 0, \tag{3.9}$$

assuming that the pump power is much larger than signal and idler powers.

Before we move on to discuss the phase-matching condition in more detail we note from (3.6) and (3.7) that the direction in which the energy is transferred, from the pump to the signal and idler or from the signal and idler to the pump, depends on the relative phase θ. For the parametric gain process to be efficient it is thus important that the relative phase is kept constant throughout the interaction length.

3.2.1   Phase-matching

Phase-matching refers to keeping the relative phase θ of the interacting waves constant during propagation, and is essential in order to obtain high FWM efficiency. The interacting waves will acquire a phase-shift during propagation due to linear and nonlinear effects. This is illustrated by (3.9), where the first term on the right hand side represents the linear phase-shift, which is induced by the difference in propagation constant between the waves, and the second term represents the nonlinear phase-shift which is due to SPM and XPM. In practice phase-matching means making sure the linear and nonlinear phase-shifts cancel out, also referred to as nonlinear phase-matching, and the relative phase θ kept constant.

We see from (3.9) that in order for phase-matching to be feasible $\Delta\beta$ must be negative. In the single (degenerate) pump case with the pump frequency ω_p close to the fiber zero dispersion frequency ω_0 the phase-matching condition can be written as [82]

$$\kappa = \beta_3(\omega_\mathrm{p} - \omega_0)(\omega_\mathrm{s} - \omega_\mathrm{p})^2 + 2\gamma P_\mathrm{p} = 0, \tag{3.10}$$

where β_3 is the third derivative of the propagation constant at ω_0. From (3.10) we see that phase-matching is only possible if the pump is in the anomalous dispersion regime, which is important to consider when designing a FOPA. From (3.10) we can also see that there are only two signal frequencies that give $\kappa = 0$. There will thus be two gain maxima, symmetrically located around the pump. Furthermore, we note that the gain bandwidth will increase with decreased dispersion slope, due to a reduced dependence on the frequency selection of the waves.

In the case when no idler wave is present at the input, an idler will be generated in the FOPA and take a phase such that the relative phase θ is $\pi/2$. In that case the gain is independent of the signal phase at the input and the amplifier is said to be phase-insensitive. On the other hand, when the idler is present at the input, the gain will be depend on the signal phase and the amplifier is phase-sensitive.
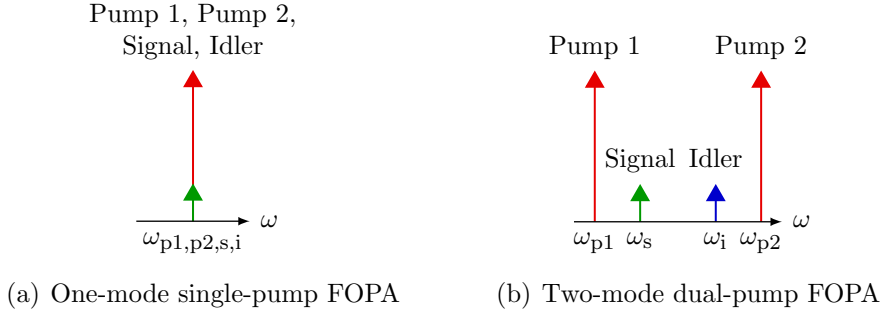
(a) One-mode single-pump FOPA (b) Two-mode dual-pump FOPA

Figure 3.1: Illustration of possible FOPA schemes (complementing Fig. 1.2).

3.3 Parametric amplification

Based on the previous section we can think of parametric amplification in $\chi^{(3)}$-nonlinear material as phase-matched FWM where two pump waves (degenerate or nondegenerate) transfer energy to a weak signal wave. Depending of how the wavelengths are selected different amplification schemes can be obtained. In addition to the one-mode dual-pump FOPA and the two-mode single-pump FOPA illustrated in Fig. 1.2 it is also possible to implement FOPAs according to the configurations illustrated in Fig. 3.1.

One-mode FOPAs are inherently phase-sensitive. The two-mode FOPAs will be phase-sensitive if an idler wave at the correct frequency is present at the input. If the idler wave is not present then it will be generated internally, at the wavelength given by energy conservation, and the process is phase-insensitive.

For the purpose of amplification we are interested in the amplifier gain. An expression for the gain can be derived from (3.2)-(3.4). We assume that the pump waves are much stronger than the signal and idler waves during the whole process, i.e., there is no pump depletion. In this case one might set $dA_p/dz = 0$ and the signal gain G is given by [82]

$$G = \left\{ 1 + \left[\frac{\gamma P_p}{g} \sinh(gL_{\text{eff}}) \right] \right\}^2 , \tag{3.11}$$

where g is the parametric gain coefficient given by

$$g = \left[(\gamma P_p)^2 - \left(\frac{\kappa}{2} \right)^2 \right], \tag{3.12}$$

and L_{eff} is the effective length defined by $L_{\text{eff}} = \left[1 - \exp(-\alpha L) \right]/\alpha$, with α denoting the fiber loss coefficient and L the fiber length.

We remind ourselves that κ describes the phase-matching and in the case of perfect nonlinear phase-matching, i.e., when $\kappa = 0$, and $\gamma P_p L_{\text{eff}} \gg 1$, the

expression for the signal gain simplifies to [82]

$$G \approx \frac{1}{4} \exp(2\gamma P_\mathrm{p} L_\mathrm{eff}). \tag{3.13}$$

We note from (3.13) that in this case the signal will grow exponentially with respect to pump power, this is called the exponential gain regime.

Another interesting regime is when there is no relative phase-shift due to dispersion, i.e., when the signal and pump are at the same wavelength, and consequently $\kappa = -2\gamma P_\mathrm{p}$. In this case the signal gain simplifies to [82]

$$G \approx (2\gamma P_\mathrm{p} L_\mathrm{eff})^2 \tag{3.14}$$

and we note the quadratic dependence on the pump power. This regime is called the quadratic gain regime.

It is important to realize that FWM will also take place between the pumps and the zero-point fluctuations that are always present at all frequencies. This will give rise to amplified quantum noise (AQN), also called parametric ASE. This is the fundamental noise source in FOPAs.

3.4 Transfer matrix description

Using a transfer matrix to describe a system is common in a number of fields. The method is particularly convenient when analyzing cascaded systems, in which case a transfer matrix for the combined system is obtained simply by multiplying the transfer matrices of the individual sub-systems. A general system with two input ports and two output ports can be described by

$$\begin{bmatrix} B_1 \\ B_2 \end{bmatrix} = \underbrace{\begin{bmatrix} s_{11} & s_{12} \\ s_{21} & s_{22} \end{bmatrix}}_{\mathbf{S}} \begin{bmatrix} A_1 \\ A_2 \end{bmatrix}, \tag{3.15}$$

where A_1 and A_2 are the input modes, B_1 and B_2 are the output modes, and $\mathbf{S}$ is the transfer matrix.

In optics the modes can be represented by the complex amplitude, which contains information about both the amplitude and the phase. Transfer matrices can be used to describe, e.g., beam splitters and combiners, optical couplers, parametric processes, and loss elements.

A general two-mode parametric process with signal and idler gain can, when the pump waves are treated as constant fields (no pump depletion), be described by [125]

$$\begin{bmatrix} B_\mathrm{s} \\ B_\mathrm{i}^* \end{bmatrix} = \begin{bmatrix} \mu & \nu \\ \nu^* & \mu^* \end{bmatrix} \begin{bmatrix} A_\mathrm{s} \\ A_\mathrm{i}^* \end{bmatrix}, \tag{3.16}$$

where index s and i denote the signal and idler waves respectively, superscript $*$ represents the complex conjugate, and μ and ν are complex transfer coefficients.

The exact form of μ and ν can be found in [61], but are not important for the analysis presented here. We will be contented by knowing that they depend on the pump power, the phase-matching, the nonlinear interaction strength, and the polarization state. However, it is important that μ and ν satisfy the relation [125]

$$|\mu|^2 - |\nu|^2 = 1, \tag{3.17}$$

which in practice means that the signal and idler waves experience gain and are amplified. The two-mode parametric process described by (3.16) could for example be a FOPA.

To gain insight about the parametric process we evaluate (3.16) and get the transfer function

$$\begin{cases} B_{\rm s} = \mu A_{\rm s} + \nu A_{\rm i}^* \\ \\ B_{\rm i} = \nu A_{\rm s}^* + \mu A_{\rm i}. \end{cases} \tag{3.18}$$

Due to the coupled propagation of the signal and idler waves it is not easy to interpret (3.18). However, the two coupled propagation equations (3.18) can be written as two independent modes by carrying out the variable substitution

$$\begin{cases} A_+ = \dfrac{A_{\rm s} + A_{\rm i}}{\sqrt{2}} \\ \\ A_- = \dfrac{A_{\rm s} - A_{\rm i}}{\sqrt{2}}, \end{cases} \tag{3.19}$$

which gives us, see A.1,

$$\begin{cases} B_+ = \mu A_+ + \nu A_+^* \\ \\ B_- = \mu A_- - \nu A_-^*, \end{cases} \tag{3.20}$$

where B_+ and B_- are defined analogous to A_+ and A_-. We take one more step and rewrite this set of equations, see A.2, and obtain

$$\begin{cases} B_+ = \exp(i\theta_{\rm r}^+)\Big[\big(|\mu| + |\nu|\big)\mathrm{Re}(A_{\rm r,+}) + i\big(|\mu| - |\nu|\big)\mathrm{Im}(A_{\rm r,+})\Big] \\ \\ B_- = \exp(i\theta_{\rm r}^+)\Big[\big(|\mu| - |\nu|\big)\mathrm{Re}(A_{\rm r,-}) + i\big(|\mu| + |\nu|\big)\mathrm{Im}(A_{\rm r,-})\Big], \end{cases} \tag{3.21}$$

where

$$A_{\rm r,+} = A_+ \exp(i\theta_{\rm r}^-) \quad \text{and} \quad A_{\rm r,-} = A_- \exp(i\theta_{\rm r}^-) \tag{3.22}$$

and

$$\theta_{\rm r}^+ = \frac{\theta_\mu + \theta_\nu}{2} \quad \text{and} \quad \theta_{\rm r}^- = \frac{\theta_\mu - \theta_\nu}{2}. \tag{3.23}$$

The angles θ_μ and θ_ν are defined by $\mu = |\mu| \exp(i\theta_\mu)$ and $\nu = |\nu| \exp(i\theta_\nu)$, respectively. From (3.21) we see that one quadrature component of each mode, either

the real part or the imaginary part, will be amplified by $G = (|\mu| + |\nu|)^2$ while the other quadrature component will be attenuated by $1/G = (|\mu| - |\nu|)^2$. This is an important conclusion since it tells us that a two-mode parametric amplifier can phase-sensitively amplify two independent quadrature components simultaneously. The relation $(|\mu| + |\nu|)^2 = 1/(|\mu| - |\nu|)^2$ can be shown using $|\mu|^2 - |\nu|^2 = 1$.

Up until this point we have not considered the quantum noise in our model of the two-mode parametric process. In the transfer matrix description quantum noise can easily be included by adding a noise term n to the input modes

$$\begin{bmatrix} B_{\mathrm{s}} \\ B_{\mathrm{i}}^* \end{bmatrix} = \begin{bmatrix} \mu & \nu \\ \nu^* & \mu^* \end{bmatrix} \begin{bmatrix} A_{\mathrm{s}} + n_{\mathrm{s}} \\ A_{\mathrm{i}}^* + n_{\mathrm{i}}^* \end{bmatrix}, \tag{3.24}$$

where n_{s} and n_{i} is the quantum noise associated with the signal and idler waves, respectively. The noise is taken as additive Gaussian noise that satisfies $\langle n_m \rangle = 0$, $\langle n_m n_l \rangle = 0$, and $\langle |n_m|^2 \rangle = \hbar \omega_m / 2$ with $m, l \in \{\mathrm{s, i}\}$ [125]. The model given by (3.24), with the assumption of Gaussian noise at the input, is a so-called semiclassical model.

By evaluating (3.24) we get the transfer function

$$\begin{cases} B_{\mathrm{s}} = \mu A_{\mathrm{s}} + \nu A_{\mathrm{i}}^* + \mu n_{\mathrm{s}} + \nu n_{\mathrm{i}}^* \\[2mm] B_{\mathrm{i}} = \nu A_{\mathrm{s}}^* + \mu A_{\mathrm{i}} + \nu n_{\mathrm{s}}^* + \mu n_{\mathrm{i}}. \end{cases} \tag{3.25}$$

Given that the noise, n_{s} and n_{i}, are uncorrelated vacuum fluctuations the noise amplification will be $|\mu|^2 + |\nu|^2$, independent of the signal and idler modes. As we will see below, the gain when the parametric amplifier is operated as a PIA is $G_{\mathrm{PIA}} = |\mu|^2$ and thus the noise amplification can be written as $|\mu|^2 + |\nu|^2 = 2|\mu|^2 - 1 = 2G_{\mathrm{PIA}} - 1$. From (3.25) we see that the noise at the output of the parametric amplifier will be correlated. This will be of importance when studying the so-called copier-PSA scheme, used to realize PSA-amplified links, in which two parametric amplifiers are cascaded.

The model given by (3.24) is a semiclassical description of a quantum mechanical system. However, it has been proved that the results given by the semiclassical model are of comparable accuracy with those from a complete quantum mechanical model, given that the photon-number is large [67, 126].

In the following sections we will analyze three modes of operation. First, we will consider the case when no idler wave is present at the input, which results in phase-insensitive operation. Second, we will consider the case when an idler wave, that is a direct copy of the signal wave, is present at the input. This will result in phase-sensitive operation and signal phase-squeezing. Third, we consider the case when an idler wave, that is a conjugated copy of the signal wave, is present at the input. This will result in in phase-sensitive operation without signal phase-squeezing. In all cases we assume the input to be a coherent state with uncorrelated vacuum noise on the signal and idler waves.

3.4.1 Phase-insensitive operation

When no idler wave is present at the input, i.e., $A_\mathrm{i} = 0$, the general input-output relation (3.16) takes the form

$$\begin{bmatrix} B_\mathrm{s} \\ B_\mathrm{i}^* \end{bmatrix} = \begin{bmatrix} \mu & \nu \\ \nu^* & \mu^* \end{bmatrix} \begin{bmatrix} A_\mathrm{s} \\ 0 \end{bmatrix}. \tag{3.26}$$

By evaluating (3.26) we obtain the transfer function

$$\begin{cases} B_\mathrm{s} = \mu A_\mathrm{s} \\[2mm] B_\mathrm{i} = \nu A_\mathrm{s}^* \end{cases} \tag{3.27}$$

and we see that the output signal will be the input signal amplified by $G_\mathrm{PIA} = |\mu|^2$ and the output idler will be a phase-conjugated copy of the signal amplified by $|\nu|^2 = G_\mathrm{PIA} - 1$, given that θ_μ and θ_ν are both zero.

Based on the previous calculation of the noise gain we can now calculate the NF for PIA-amplification

$$\mathrm{NF}_\mathrm{PIA} = \frac{2G_\mathrm{PIA} - 1}{G_\mathrm{PIA}} = 2 - \frac{1}{G_\mathrm{PIA}}, \tag{3.28}$$

which in the limit of high gain ($G_\mathrm{PIA} \gg 1$) take the value 2 (3 dB). The input and output modes of a PIA, with $\theta_\mu = \theta_\nu = 0$ and $G_\mathrm{PIA} = 8$, are illustrated in Fig. 3.2(a).

3.4.2 Phase-sensitive operation

Phase-sensitive operation with $A_\mathrm{i} = A_\mathrm{s}$

When the idler wave is a direct copy of the signal, i.e., $A_\mathrm{i} = A_\mathrm{s}$, the general input-output relation (3.16) takes the form

$$\begin{bmatrix} B_\mathrm{s} \\ B_\mathrm{i}^* \end{bmatrix} = \begin{bmatrix} \mu & \nu \\ \nu^* & \mu^* \end{bmatrix} \begin{bmatrix} A_\mathrm{s} \\ A_\mathrm{s}^* \end{bmatrix} \tag{3.29}$$

and by evaluating this relation we get the transfer function

$$\begin{cases} B_\mathrm{s} = \mu A_\mathrm{s} + \nu A_\mathrm{s}^* \\[2mm] B_\mathrm{i} = \mu A_\mathrm{s} + \nu A_\mathrm{s}^*. \end{cases} \tag{3.30}$$

We can immediately see from (3.30) that the output signal and idler will be identical. Evaluating (3.22) we find that

$$A_\mathrm{r,+} = \sqrt{2} A_\mathrm{s} \exp(i\theta_\mathrm{r}^-) \quad \text{and} \quad A_\mathrm{r,-} = 0. \tag{3.31}$$

Since one of the modes is zero we can conclude that only one signal quadrature component, either the in-phase component or the quadrature component, will be amplified by $G_{\mathrm{PSA}} = (|\mu| + |\nu|)^2 = (\sqrt{G_{\mathrm{PIA}}} + \sqrt{G_{\mathrm{PIA}} - 1})^2$ while the other quadrature component will be attenuated by $1/G_{\mathrm{PSA}}$. We note that in the limit of high gain, i.e., $|\mu| \approx |\nu|$, $G_{\mathrm{PSA}} = 4G_{\mathrm{PIA}}$, or in other words the PSA gain is 6 dB higher than the PIA gain. This gain advantage is explained by the coherent addition of the signal and idler fields.

In the same way as we calculated the signal NF for the PIA we can calculate the signal NF for the PSA. However, since one signal quadrature component will be amplified and the other quadrature component attenuated we will obtain two NFs. For the amplified component we get

$$\mathrm{NF}_{\mathrm{PSA,amp}} = \frac{2G_{\mathrm{PIA}} - 1}{\left(\sqrt{G_{\mathrm{PIA}}} + \sqrt{G_{\mathrm{PIA}} - 1}\right)^2} \longrightarrow \frac{1}{2}, \tag{3.32}$$

and for the attenuated component we get

$$\mathrm{NF}_{\mathrm{PSA,att}} = \frac{2G_{\mathrm{PIA}} - 1}{\left(\sqrt{G_{\mathrm{PIA}}} - \sqrt{G_{\mathrm{PIA}} - 1}\right)^2} \longrightarrow \infty, \tag{3.33}$$

where the limits are taken for $G_{\mathrm{PIA}} \to \infty$. The negative NF of -3 dB (1/2) for the amplified component might seem confusing but find its explanation in the strong nonlinear coupling between signal and idler modes at high gain. In (3.32) only the signal input power is considered but due to the coupling also the idler power should be taken into account which increase the input SNR by 3 dB and thus result in a NF of 0 dB. In Fig. 3.2(b) we illustrate the input and output modes of a two-mode PSA with $A_{\mathrm{i}} = A_{\mathrm{s}}$ for the case when $\theta_\mu = \theta_\nu = 0$ and $G_{\mathrm{PSA}} = G_{\mathrm{PSA}}(G_{\mathrm{PIA}} = 8)$.

We note from Fig. 3.2(b) that signal (and idler) phase is squeezed while the noise does not experience any squeezing. This is explained by the coherent addition of the signal and idler waves and the incoherent addition of the uncorrelated vacuum noise accompanying the waves. This should be compared to the one-mode PSA, illustrated in Fig. 1.4, which demonstrate squeezing of both the signal phase and the noise.

Phase-sensitive operation with $A_{\mathrm{i}} = A_{\mathrm{s}}^*$

When the idler wave is a phase-conjugated copy of the signal wave, i.e., $A_{\mathrm{i}} = A_{\mathrm{s}}^*$, the general input-output relation (3.16) takes the form

$$\begin{bmatrix} B_{\mathrm{s}} \\ B_{\mathrm{i}}^* \end{bmatrix} = \begin{bmatrix} \mu & \nu \\ \nu^* & \mu^* \end{bmatrix} \begin{bmatrix} A_{\mathrm{s}} \\ A_{\mathrm{s}} \end{bmatrix} \tag{3.34}$$

and by evaluating this relation we get the transfer function

$$\begin{cases} B_{\mathrm{s}} = \mu A_{\mathrm{s}} + \nu A_{\mathrm{s}} \\ \\ B_{\mathrm{i}} = \mu A_{\mathrm{s}}^* + \nu A_{\mathrm{s}}^*. \end{cases} \tag{3.35}$$

(a) PIA ($A_i = 0$)

(b) Two-mode PSA with $A_i = A_s$

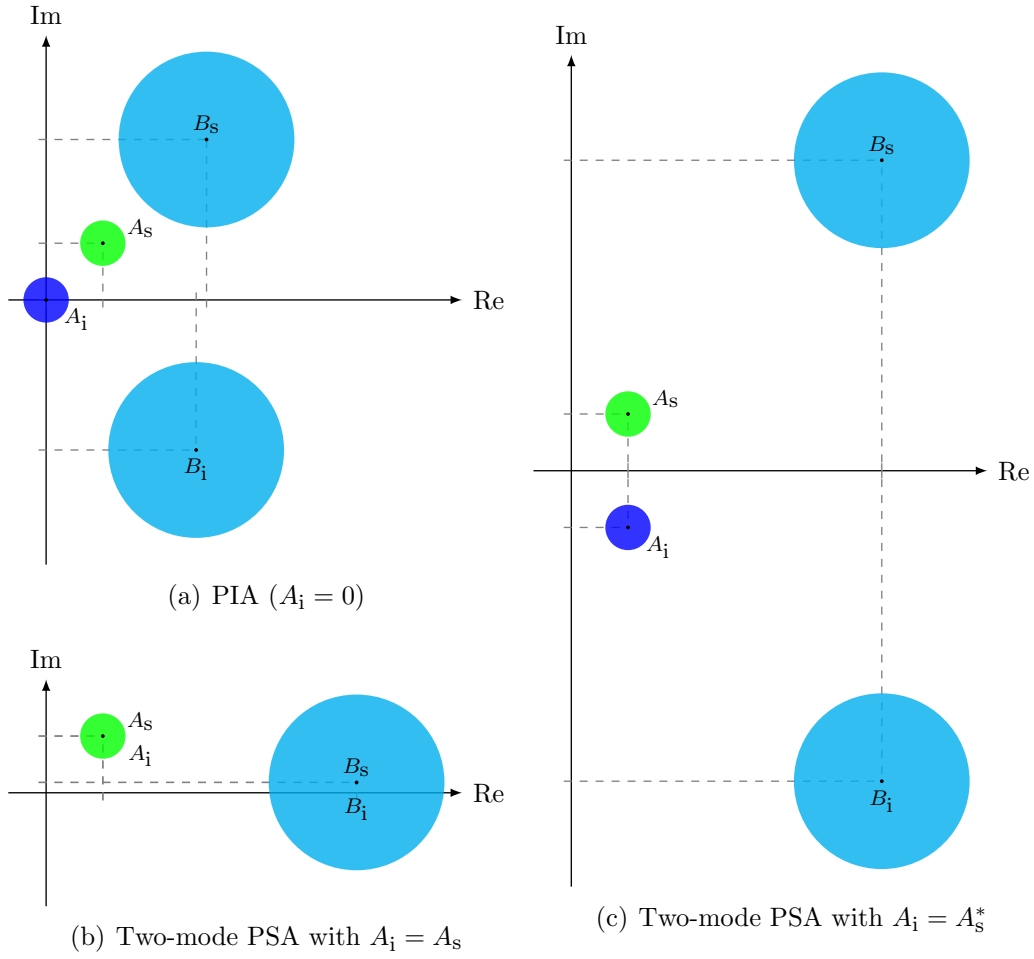(c) Two-mode PSA with $A_i = A_s^*$

Figure 3.2: Illustration of signal input (green), idler input (blue), and signal output (cyan) modes for parametric amplification with the angles $\theta_\mu = \theta_\nu = 0$ and $G_{PIA} = 8$. The input modes are assumed to be coherent states. In all cases the noise gain is $2G_{PIA} - 1$ while the signal and idler gain is different.

In this case (3.22) gives us

$$A_{\mathrm{r},+} = \sqrt{2}\mathrm{Re}(A_{\mathrm{s}})\exp(i\theta_{\mathrm{r}}^-) \quad \text{and} \quad A_{\mathrm{r},-} = i\sqrt{2}\mathrm{Im}(A_{\mathrm{s}})\exp(i\theta_{\mathrm{r}}^-), \qquad (3.36)$$

which tells us that both signal components will be amplified with a gain of $G_{\mathrm{PSA}} = (|\mu| + |\nu|)^2$. In this case the NF for both signal quadrature components is given by $\mathrm{NF}_{\mathrm{PSA,amp}}$ and takes the value -3 dB at high gain, or, when also considering the idler power at the input, 0 dB. The input and output modes of a two-mode PSA with $A_{\mathrm{i}} = A_{\mathrm{s}}^*$ for the case when $\theta_\mu = \theta_\nu = 0$ and $G_{\mathrm{PSA}} = G_{\mathrm{PSA}}(G_{\mathrm{PIA}} = 8)$ are illustrated in Fig. 3.2(c).

3.5 Implementation

The most important component of a FOPA is the optical fiber where FWM takes place. For high efficiency operation the fiber should have high nonlinear coefficient, ZDW in or close to the C-band, and low dispersion slope. Today so-called HNLFs are often used to realize FOPAs. Silica-based HNLFs can have a nonlinear coefficient of about 20 $(\mathrm{W}\ \mathrm{km})^{-1}$ and attenuation of about 1 dB/km [127]. The nonlinear coefficient should be compared to the nonlinear coefficient in ordinary SSMF which is about 1.5 $(\mathrm{W}\ \mathrm{km})^{-1}$. Although fibers with high nonlinear coefficient are available, high pump powers and long fiber sections are still needed to obtain high gain. Fibers used for FOPAs are usually in the range of 100-1000 m long and booster EDFAs are used to reach CW pump powers in the range of 0.5-10 W.

The amount of pump power that is launched into the HNLF, and thus also the FOPA gain, is limited by stimulated Brillouin scattering (SBS). SBS is similar to SRS in that pump power is absorbed by the material and then emitted as a frequency-shifted wave. In silica fibers the wave is down-shifted around 10 GHz and has a bandwidth of tens of MHz. The generated wave propagates in the backward direction, relative to the pump, and above a certain threshold power all additional pump power will be transferred to the down-shifted wave, thus limiting the pump power.

Several methods for reducing SBS have been proposed. The most common method is to broaden the pump spectrum using a phase modulator [128]. Another technique is to concatenate several pieces of HNLF with isolators in between, in order to block and prevent the SBS from building up [129]. There are also techniques that rely on frequency-shifting the backscattered wave along the fiber, either using a temperature gradient [130], or fiber stretching [131], and techniques that rely on doping the fiber, for example with Al or Ge [132].

The fundamental noise source in FOPAs is AQN, which leads to the 3 dB quantum limited NF for phase-insensitive FOPAs. In a real system there are excess noise sources present which will result in a NF that is larger than 3 dB. The excess noise sources include Raman phonon seeded excess noise [116], pump
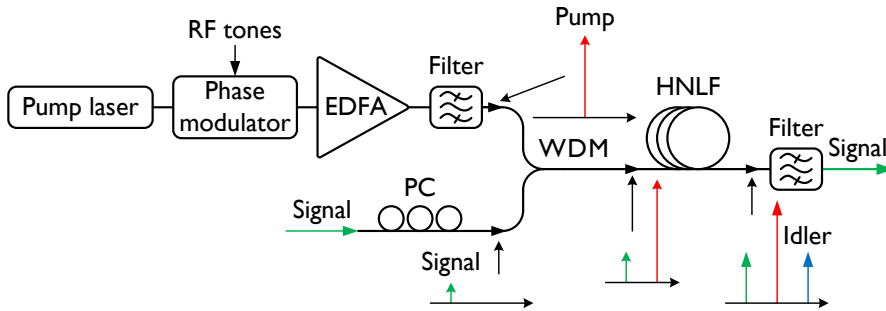
Figure 3.3: Typical implementation of a phase-insensitive FOPA with phase-modulated pump for SBS suppression.

transferred noise [133, 134], and residual pump noise [135]. In a well designed FOPA these can often be kept small.

A typical setup for a phase-insensitive FOPA using a CW pump is illustrated in Fig. 3.3. The pump wave originates from a laser and is then phase-modulated to reduce the SBS in the HNLF. After phase modulation the pump is boosted with an EDFA and filtered to remove ASE using a band-pass filter. The pump is then combined with the signal using a WDM coupler, in order minimize the coupling loss. Since the FWM process is polarization dependent the signal polarization has to be tuned using a polarization controller (PC) for highest gain. After the HNLF the signal wave is filtered out. The spectra in Fig. 3.3 illustrate the waves present at the various stages. Phase-sensitive FOPAs can be implemented using the so-called copier-PSA scheme which will be discussed in Chapter 4.

Chapter 4

Phase-sensitive amplified transmission

Fiber optical transmission systems amplified using two-mode PSAs, with the input idler wave being a conjugated copy of the signal wave, can benefit both from the low-noise amplification and the nonlinearity mitigation provided by the PSA. Moreover, they are multi-channel compatible and modulation format independent, which makes them interesting to consider for high-capacity transmission. The price paid for these benefits is increased complexity and reduced SE.

Chapter outline

In Section 4.1 we describe how a multi-channel compatible and modulation format independent PSA-amplified transmission system can be realized in practice using the so-called copier-PSA scheme. We discuss the properties of the copier-PSA scheme and the practical problems that have to be solved to implement a PSA-amplified transmission system. In Section 4.2 we discuss how the need to transmit two data-carrying waves impact the capacity. Finally, In Section 4.3 we discuss the mitigation of nonlinear transmission distortions.

4.1 Design and implementation

4.1.1 The copier-PSA scheme

A multi-channel compatible and modulation format independent PSA-amplified transmission system can be realized using the so-called copier-PSA scheme. A single-span implementation of the copier-PSA scheme consists of two cascaded FOPAs, one at each end of the transmission fiber. The purpose of the first FOPA, the copier, is to generate a set of three frequency- and phase-locked waves, with the idler being a conjugated copy of the signal, and the purpose of the second FOPA,
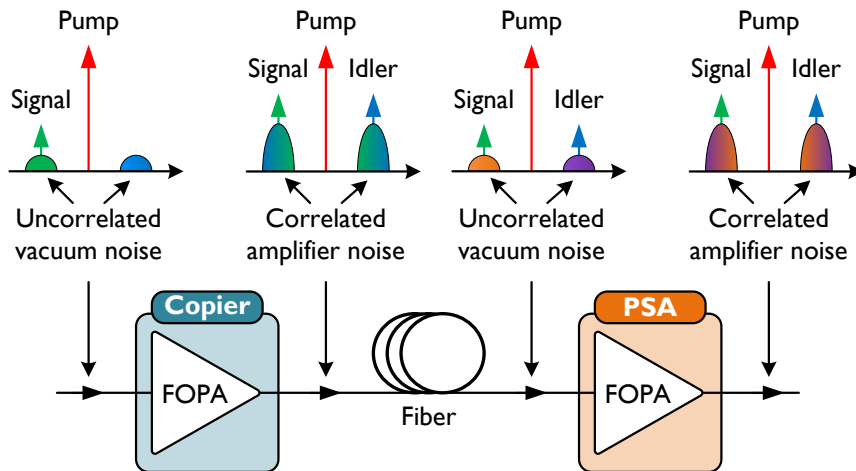
Figure 4.1: Illustration of the copier-PSA scheme.

the PSA, is to provide low-noise phase-sensitive amplification. In a single-span copier-PSA-based PSA-amplified transmission link the PSA will thus operate as a preamplifier, cf. Fig. 2.1(b).

The copier-PSA scheme is illustrated in Fig. 4.1 and can be described in more detail as follows: the signal is launched into the copier together with a high-power pump, whereby a conjugate copy of the signal is generated at the idler wavelength through FWM. At the input of the PSA three frequency- and phase-locked waves will be present which will result in phase-sensitive operation. Since the idler is a conjugated copy of the signal the PSA gain will be independent of the modulated data phase, and modulation format independent operation is obtained.

For the PSA to provide full advantage of low-noise amplification it is crucial that the noise accompanying the signal and idler waves at the PSA input is uncorrelated vacuum noise, illustrated by the spectra in Fig. 4.1. At the copier input uncorrelated vacuum noise is present at the signal and idler wavelengths if the waves are shot-noise limited. In the copier this noise will be amplified and added incoherently resulting in correlated amplifier noise at the signal and idler wavelengths at the copier output. The noise thus has to be decorrelated before entering the PSA. This can be achieved by attenuating the waves, since attenuation will both reduce the correlated amplifier noise and introduce new uncorrelated vacuum noise [67, 126]. Attenuation of the waves can for example be accomplished by propagation through an optical fiber. With fully uncorrelated vacuum noise accompanying the signal and idler waves at the PSA input, an ideal PSA will provide 6 dB higher SNR at the receiver than what a PIA, e.g., a FOPA with only signal and pump waves present at the input, will provide.

If the correlated amplifier noise is not sufficiently attenuated before the PSA the advantage will be reduced. This scenario has been investigated in Paper [H]. In Paper [G] we investigate a related scenario, the impact of uncorrelated amplifier

noise present at the PSA input.

A multi-span, multi-channel compatible and modulation format independent PSA-amplified transmission system can also be realized using the copier-PSA scheme. In such a system the copier is followed by several sections of transmission fiber and PSAs which will operate as in-line amplifiers, cf. Fig. 2.1(c).

Transfer matrix description

The copier-PSA scheme can be analyzed using transfer matrices, similar to how we analyzed a two-mode FOPA in Section 3.4. In this section we will use the transfer matrix description to better understand the decorrelation of the amplifier noise generated by the copier. The transfer matrix equation for a single-span implementation of the copier-PSA system takes the form [17]

$$
\begin{bmatrix} B_{\text{s}} \\ B_{\text{i}}^* \end{bmatrix} = \mathbf{G}_{\text{PSA}} \hat{\mathbf{T}} \mathbf{G}_{\text{copier}} \begin{bmatrix} A_{\text{s}} + n_{\text{s}} \\ n_{\text{i}}^* \end{bmatrix},
\tag{4.1}
$$

where A denotes the input modes, B denotes the output modes, n represents the input quantum noise, subscript s denotes the signal wave, subscript i denotes the idler wave, and superscript $*$ denotes the conjugation operation. $\mathbf{G}_{\text{copier}}$ denotes the copier transfer matrix, $\mathbf{G}_{\text{PSA}}$ denotes the PSA transfer matrix, and $\hat{\mathbf{T}}$ represents an attenuation operator that satisfies [136]

$$
\hat{\mathbf{T}}\mathbf{X} = \begin{bmatrix} \sqrt{T_{\text{s}}} & 0 \\ 0 & \sqrt{T_{\text{i}}} \end{bmatrix} \mathbf{X} + \begin{bmatrix} \sqrt{1 - T_{\text{s}}}n_{\text{s}}' \\ \sqrt{1 - T_{\text{i}}}n_{\text{i}}'^* \end{bmatrix},
\tag{4.2}
$$

where $\mathbf{X}$ is a vector containing two modes, T represents the transmittance of the lossy section, and n' represents quantum noise introduced by the loss process. The quantum noise terms n_{s}' and n_{i}' are uncorrelated with n_{s} and n_{i} but have the same mean value and variance.

If we let $\mathbf{X} = [A_{\text{s,c-out}} + N_{\text{s,c-out}}, A_{\text{i,c-out}} + N_{\text{i,c-out}}]^{\text{T}}$ represent the signal and idler modes at the output of the copier, with signal A and amplifier noise N, then, by evaluating (4.2), the modes after the lossy section can be expressed as

$$
\hat{\mathbf{T}}\mathbf{X} = \begin{bmatrix} \sqrt{T_{\text{s}}}(A_{\text{s,c-out}} + N_{\text{s,c-out}}) + \sqrt{1 - T_{\text{s}}}n_{\text{s}}' \\ \sqrt{T_{\text{i}}}(A_{\text{i,c-out}} + N_{\text{i,c-out}}) + \sqrt{1 - T_{\text{i}}}n_{\text{i}}' \end{bmatrix}.
\tag{4.3}
$$

From (4.3) we see that the loss will attenuate the amplifier noise N, created by the copier, while uncorrelated quantum noise n' is introduced. The attenuation operator can be thought of as a 4-port beam-splitter that couples quantum noise to the signal and idler waves [67]. With enough loss the noise will be dominated by uncorrelated vacuum noise and the full 6 dB SNR advantage can be obtained.

Link noise figure

The properties of both single-span and multi-span two-mode PSA-amplified transmission systems, based on the copier-PSA scheme, have previously been investigated theoretically [37,67,70]. It has been shown that the link NF of a single-span system based on the copier-PSA scheme is given by [37,67]

$$\text{NF}_{\text{copier-PSA}} \approx 1 + \frac{G}{2} \qquad (4.4)$$

when the link net gain is zero, i.e., the gain of the copier and the PSA is balanced by the loss of the transmission span, and the loss between the copier and the PSA is large compared to unity. The corresponding link NF for a system based on a PIA-PIA scheme, i.e., two cascaded PIAs with a lossy transmission span in between, is given by [37,67]

$$\text{NF}_{\text{PIA-PIA}} \approx 1 + 2G. \qquad (4.5)$$

The gain G that appears in (4.4) and (4.5) is the gain of the second amplifier, the amplifier after the lossy section. We see that at large gains ($G \gg 1$) the copier-PSA system gives a 6 dB link NF advantage over the PIA-PIA system.

In a multi-span transmission system based on the copier-PSA scheme, with in-line amplifier gain equal to the span loss, the link NFs are given by [70]

$$\text{NF}_{\text{A,copier-PSA}} = \frac{5}{2} + \frac{N}{2} \quad \text{and} \quad \text{NF}_{\text{B,copier-PSA}} = \frac{3G}{2} + \frac{NG}{2}, \qquad (4.6)$$

for the type A and type B configurations discussed in Section 2.3, respectively. In this case G represents the in-line amplifier gain. Comparing (4.6) to (2.17) and (2.18) we see that in the limit of many spans ($N \gg 1$) and high gain ($G \gg 1$) the systems based on the copier-PSA scheme give a 6 dB link NF benefit compared to the all-PIA-based schemes and a 3 dB link NF benefit compared to the all-PSA-based schemes. The explanation to why the copier-PSA schemes give a 6 dB link NF improvement over the all-PSA-based schemes lies in the generation of the idler wave in the copier, which is considered to be an internal mode of the system. If the idler power was accounted for as input signal then the improvement would be reduced to 3 dB.

4.1.2 Implementation challenges

PSAs rely on coherent interaction between the input waves and are therefore highly sensitive to the properties of these waves. For efficient operation it is essential that the waves are synchronized in time, aligned in polarization, and that their relative phase is stable and such that the PSA gain is maximized. Furthermore, to avoid noise transfer from the high-power pump wave to the signal and idlers waves it is crucial that the pump OSNR is high (> 65 dB) [133].
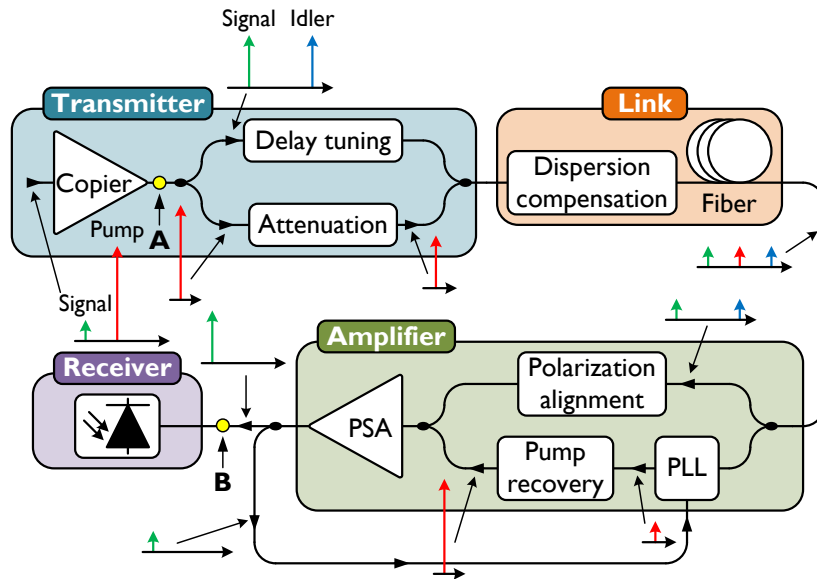
Figure 4.2: Illustration of a single-span PSA-amplified transmission system implemented using the copier-PSA scheme.

In the copier-PSA scheme the waves fulfill the condition for efficient PSA operation immediately after the copier. However, in a transmission system implementation of the copier-PSA scheme the transmission fiber is placed between the copier and the PSA and will therefore alter the waves. For efficient PSA operation the impact of the transmission fiber on the timing, polarization, and relative phase of the waves thus has to be compensated for. Moreover, the pump wave, attenuated by the transmission fiber, must be restored to high power and high OSNR to operate as pump in the PSA without noise transfer.

A single-span PSA-amplified transmission system, implemented using the copier-PSA scheme, is shown in Fig. 4.2. As illustrated in the figure, several stages for wave conditioning are required. A dispersion compensation stage is needed to compensate for the chromatic dispersion of the transmission fiber and a polarization alignment stage has to be included to align the polarization of the signal and idler waves with the pump wave before the PSA. The transmission of the pump wave requires that the pump is first attenuated, to avoid SBS during transmission, and then recovered before the PSA. The pump wave handling in turn requires that the pump wave is separated from the signal and idler waves, as illustrated in the figure.

Splitting the signal and idler waves from the pump wave and propagating them through different fibers will cause the relative phase of the waves to drift due to temperature variations and acoustic vibrations. To obtain stable PSA gain this phase drift has to be compensated for. This can be done using a phase-locked loop

(PLL) that use a small fraction of the signal wave at the PSA output as feedback. Furthermore, the optical path length undertaken by the signal and idler waves and the pump wave has to be matched, at least to within the coherence length of the pump wave, which is done using a delay tuning stage.

The strict requirements on the waves at the PSA input makes two-mode PSA-amplified transmission systems challenging to implement. Among the conditioning stages shown in Fig. 4.2, those that requires the most attention are the pump recovery and the PLL. Due to the low pump power at the end of the transmission span and high OSNR requirement, pump recovery cannot be achieved using only conventional EDFA-amplification. One way to accomplish the task is to use optical injection locking (OIL). An injection-locked laser has the capability to transfer the phase information, up to a certain bandwidth, of an injected wave to an output, higher power, wave while suppressing the amplitude information, i.e., noise. Pump recovery is the topic of Paper [A], and the enabling technique, i.e., IL, will be described in more detail in the next section. The first demonstration of a multi-channel compatible and modulation format independent single-span PSA-amplified transmission system is presented in Paper [B].

In a multi-span PSA-amplified transmission system the section between point A and point B, indicated in Fig. 4.2, is repeated for each span. Wave conditioning is thus needed for each transmission span. A possible complication in a multi-span system is phase noise accumulation on the pump wave which might successively degrade the performance of the PSA-stages. Paper [I] presents the first demonstration of a multi-channel compatible and modulation format independent multi-span PSA-amplified transmission system.

Injection locking

The concept of IL describe the phenomenon when the signal from an oscillator, e.g., a mechanical oscillator, is injected into another oscillator causing the second oscillator to lock in frequency and phase to the first one. An early documented observation of this phenomenon was done by Christiaan Huygens in a letter to his father, Constantyn Huygens, in 1665 [137]. In the letter Huygens described his observation of how the pendulums of two clocks hanging on a wall, initially swinging unsynchronized, with time became synchronized, i.e., locked in frequency and phase. He also noted that the time for reaching the synchronized state depended on the distance between the clocks. Later he concluded that the cause of synchronization was mechanical vibrations, originating from the clocks, mediated by the wall which they were hanging on.

IL can also be observed in electrical systems. An early study of IL in electronic circuits was done by Adler in 1946 when he analyzed IL of an electrical oscillator with an external frequency source [138]. In this study he derived one of the fundamental properties of IL, for locking to occur the frequency difference between the impressed signal and the free-running oscillator cannot be too large.
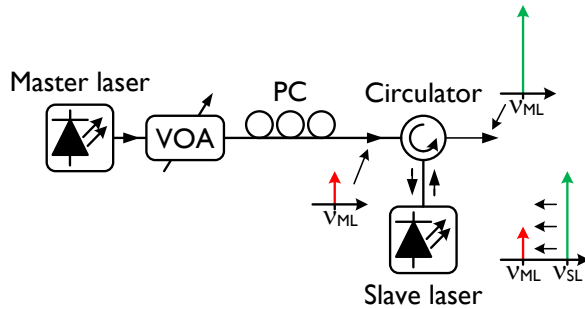
46

Figure 4.3: Illustration of setup for IL of laser.

Adler's theory was later extended by Pantell in 1965 to include optical system, i.e., IL of lasers [139], and one year later, Stover and Steier demonstrated the first injection-locked laser using two red He-Ne lasers [140].

In the case of OIL light from one laser, termed master laser (ML), is coupled into another laser, termed slave laser (SL), which cause the frequency and phase of the SL to lock to that of the ML. OIL of semiconductor distributed feedback (DFB) lasers was first demonstrated in 1991 [141], and has since found many applications. IL can for example significantly enhance the performance of directly modulated DFB lasers. Noticeable results have been published on single-mode performance and enhanced side-mode suppression [142], suppressed nonlinear distortion [143], reduced frequency chirp [144], reduced relative intensity noise (RIN) and linewidth [145], and enhanced resonance frequency and modulation bandwidth [146].

A typical setup for realizing IL of a semiconductor laser is illustrated in Fig. 4.3. This scheme for IL, in which only one of the laser facets is used for coupling, is called reflection style. The ML must be isolated from the SL and this is done by coupling the ML light into the SL via a circulator. Important parameters for the locking process are the power, tuned using a variable optical attenuator (VOA), and the state of polarization (SOP), tuned using a PC, of the light injected into the SL, the free-running output power of the SL and the free-running wavelengths of the SL and ML. For efficient locking the ML SOP has to be matched to the mode of the SL. The importance and impact of the other parameters will be discussed below.

The dependence on the power injected into the SL and the free-running output power of the SL is usually described by the external injection ratio, defined as the ratio between the two powers. It can also be described by the internal injection ratio, defined by instead using the injected power internal to the SL cavity and the internal power of the free-running SL. For practical reasons the external injection ratio is most common in experimental studies.

The frequency difference between the ML, ν_{ML}, and the free-running SL, ν_{SL}, is also an important parameter for the locking process. Locking of the SL to the ML will only be possible within a certain range of the frequency difference

$\Delta\nu = \nu_{\mathrm{ML}} - \nu_{\mathrm{SL}}$. The range within which the locking occur is called the locking bandwidth and is determined by, among other aspects, the external (or internal) injection ratio. Higher injected power (larger injection ratio) leads to wider locking bandwidth. At an injection ratio of 30 dB, the locking bandwidth is typically a few hundreds of MHz.

Several models have been developed to describe the locking dynamics of OIL. The gain competition model was introduced in [147] and describe the competition between ASE and injected light. Another way to understand the dynamics of the OIL process is through the phasor diagram model [147]. This model describes how the steady-state is reached. The third approach is to use the rate-equations which provides an expression for the locking bandwidth [148].

4.2 Fundamental capacity considerations

The benefits from low-noise amplification and nonlinearity mitigation in transmission systems amplified by two-mode PSAs comes at the cost of halved SE since also the idler waves, occupying the same bandwidth as the signal waves, have to be transmitted. The net effect of this trade-off in terms of capacity and reach is not obvious and it is therefore interesting to investigate this in more detail. It is also interesting to compare two-mode PSA-amplified transmission systems to PIA-amplified transmission systems that occupy the same bandwidth and transmit the same total power.

Due to low-noise amplification, two-mode PSA-amplified transmission systems can, in theory, provide 6 dB higher SNR at the receiver than PIA-amplified transmission systems, independent of parameters such as modulation format, symbol rate, etc. [17]. The benefit from nonlinearity mitigation on the other hand will depend on a number of parameters, such as the modulation format used, and can therefore not be quantified with a common single number. For simplicity we will here assume linear transmission and only consider the performance gain from low-noise amplification.

The ultimate (Shannon) capacity (bit/s) for a transmission system can be expressed as a function of the signal bandwidth B (Hz) and the SNR [9]

$$C = B \cdot \log_2(1 + \mathrm{SNR}), \tag{4.7}$$

where the factor $\log_2(1 + \mathrm{SNR})$ represents the SE (bit/s/Hz). The expression for the SE tells us that, in the regime of high SNR (SNR $\gg$ 1), the 6 dB (four times) SNR advantage obtained using two-mode PSAs can be traded for an increase in SE by 2 bit/s/Hz [149]. The 6 dB SNR advantage could alternatively be traded for a fourfold increase in transmission reach by increasing the number of spans [101].

We will compare two-mode PSA-amplified transmission systems to PIA-amplified transmission systems by considering two cases: 1) only the bandwidth and power of the signal waves are accounted for, i.e., the idler waves are neglected,

Table 4.1: Summary of parameters used in case 1.

System	Number of waves	Bandwidth per wave	Power per wave
PIA	N	B	P
PSA	$2N$	B	P

and 2) the bandwidth and power of both the signal waves and the idler waves is accounted for. In case 1 the idler waves are considered to be internal modes of the transmission system while in case 2 the idlers are not considered to be internal modes.

It can be argued that the bandwidth occupied by the idlers in a PSA-amplified transmission system does not have to be accounted for since FOPAs can have much larger gain bandwidth than for example EDFAs. However, the same FOPAs that are used to implement a PSA-amplified transmission system can in principle be used to implement a PIA-amplified transmission system where the bandwidth occupied by the idlers is used to transmit signals with independent data. Case 2, where the bandwidth of both the signal and the idler waves are accounted for, therefore represents a more fair comparison between PIA- and PSA-amplified transmission systems.

Case 1: Signal accounted for and idler neglected

When neglecting the bandwidth and power of the idler waves the same signal bandwidth and signal launch power P (W) can be used in both the PIA- and the PSA-amplified transmission systems. The parameters for comparing the two systems according to case 1 are summarized in Table 4.1.

We will first consider the scenario in which the SNR advantage for the PSA-amplified transmission system is traded for increased SE. With $\mathrm{SNR_{PIA}}$ denoting the SNR in the PIA-amplified transmission system, the SE in the PSA-amplified transmission system will be $\mathrm{SE_{PSA}} = \log_2(1 + 4 \cdot \mathrm{SNR_{PIA}})$. By calculating the capacity using (4.7) we get $C_{\mathrm{PIA}} = B \cdot \log_2(1 + \mathrm{SNR_{PIA}})$ and $C_{\mathrm{PSA}} = B \cdot \log_2(1 + 4 \cdot \mathrm{SNR_{PIA}})$ for the PIA- and PSA-amplified transmission systems, respectively. The ratio of the capacities can thus be expressed as

$$\frac{C_{\mathrm{PSA}}}{C_{\mathrm{PIA}}} = \frac{\log_2(1 + 4 \cdot \mathrm{SNR_{PIA}})}{\log_2(1 + \mathrm{SNR_{PIA}})}. \tag{4.8}$$

This ratio is plotted in Fig. 4.4 and we see that the PSA-amplified transmission system provides the largest capacity advantage, an increase by four times, in the limit of low $\mathrm{SNR_{PIA}}$. As $\mathrm{SNR_{PIA}}$ grows larger the advantage is reduced. In the regime of high $\mathrm{SNR_{PIA}}$ ($\mathrm{SNR_{PIA}} \gg 1$) the ratio can be written as

$$\frac{C_{\mathrm{PSA}}}{C_{\mathrm{PIA}}} = 1 + \frac{2}{\log_2(1 + \mathrm{SNR_{PIA}})} = 1 + \frac{2}{\mathrm{SE_{PIA}}}, \tag{4.9}$$
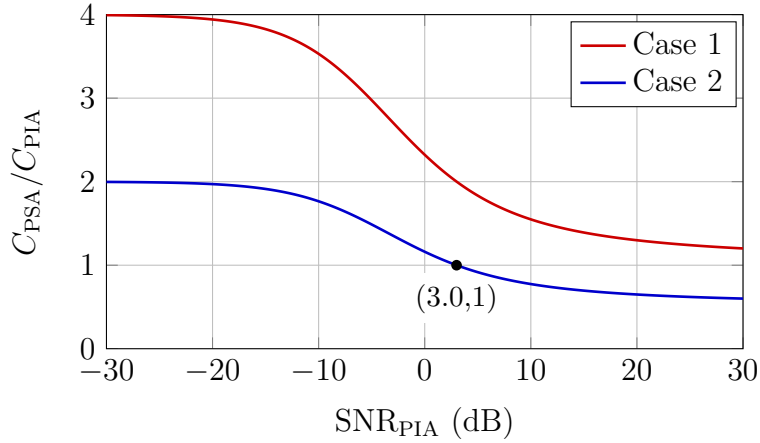
Figure 4.4: Comparison of two-mode PSA-amplified transmission systems to PIA-amplified transmission systems in terms of capacity. Transmission is assumed to be linear and benefits from nonlinearity mitigation are not considered.

Table 4.2: Summary of parameters used in case 2.

System	Number of waves	Bandwidth per wave	Power per wave
PIA	N	B	P
PSA	$2N$	$B/2$	$P/2$

where SE_{PIA} is the SE in the PIA-amplified system.

In the scenario described above the transmission distance was the same in both systems and the SNR advantage was traded for increased SE. Alternatively the SNR advantage can be traded for increased reach. In that scenario we have $C_{\text{PSA}}/C_{\text{PIA}} = 1$, independent of SNR_{PIA}, and a fourfold reach increase.

By neglecting the idler waves, i.e., considering the idler waves to be internal modes of the transmission system, the PSA-amplified transmission system can always provide an advantage in terms of capacity and/or reach.

Case 2: Both signal and idler accounted for

We now consider the case in which both the signal waves and the idler waves are accounted for. In this case both the bandwidth and the launch power of the signal and idler waves has to be reduced by a factor of two (3 dB) compared to the signal waves in the PIA-amplified transmission system. The parameters for comparing the two systems according to case 2 are summarized in Table 4.2.

Both changing the launch power and reducing the bandwidth in the PSA-amplified transmission system will impact the SNR of the transmitted signal. The SNR can be expressed as $\text{SNR} = P/(N_0 B)$, where N_0 is the noise power spectral

density. Reducing the signal power by 3 dB will thus reduce the SNR by 3 dB. However, reducing the bandwidth by a factor of two will reduce the noise by 3 dB and improve the SNR by 3 dB. The net effect will therefore be that the SNR is unchanged and the SNR advantage for the PSA-amplified transmission system is still 6 dB.

For the comparison we will again first consider the scenario in which the SNR advantage is traded for increased SE. In this case the SE of the PSA-amplified transmission system will be $SE_{PSA} = \log_2(1 + 4 \cdot SNR_{PIA})/2$ and the ratio between the capacities

$$\frac{C_{PSA}}{C_{PIA}} = \frac{\log_2(1 + 4 \cdot SNR_{PIA})}{2 \cdot \log_2(1 + SNR_{PIA})}. \tag{4.10}$$

The ratio is plotted in Fig. 4.4. As can be seen from the figure, $C_{PSA} < C_{PIA}$ for $SNR_{PIA} > 3$ dB. This means that the PSA-amplified transmission system only can provide a capacity advantage when $SNR_{PIA} < 3$ dB. In the limit of low SNR_{PIA} the capacity advantage is twofold. In the regime of high SNR_{PIA} ($SNR_{PIA} \gg 1$) the ratio can be written as

$$\frac{C_{PSA}}{C_{PIA}} = \frac{1}{2} + \frac{1}{\log_2(1 + SNR_{PIA})} = \frac{1}{2} + \frac{1}{SE_{PIA}}. \tag{4.11}$$

Instead of trading the SNR advantage for improved SE it could be traded for a fourfold increase in reach. In this case $C_{PSA}/C_{PIA} = 1/2$ and the reach increase thus comes at the cost of halved capacity.

The conclusion that can be drawn from the discussion above is that, when only accounting for the gain from low-noise amplification, it is less beneficial to use PSAs in transmission systems operating at high SNR. Examples of systems that requires high SNR are systems where high-order multi-level modulation formats are used.

4.3 Nonlinearity mitigation

The achievable reach and capacity is not only limited by amplifier noise but also by fiber nonlinearities [72,73,150,151]. The fiber nonlinearities can be classified as intra-channel and inter-channel effects [72]. Intra-channel effects describe nonlinear interactions that only involve the fields present within the frequency band of the channel of interest. Intra-channel effects can be divided into nonlinear signal-signal interaction, which results in SPM, and nonlinear signal-noise interaction, resulting in NLPN. The nonlinear signal-noise interaction is sometimes referred to as the Gordon-Mollenauer effect [152]. Inter-channel effects describe the nonlinear interactions involving at least one field outside the frequency band of the channel of interest. Inter-channel effects are thus only present in WDM systems, where they give rise to XPM and FWM through nonlinear signal-signal interaction and NLPN through nonlinear signal-noise interaction.

Several techniques have been proposed for mitigation of nonlinear transmission distortions. Mid-link optical phase conjugation (OPC) [153–155], utilizes an

optical [156], or electrical [157], device to perform a phase-conjugation of the signal in the middle of the transmission system whereby nonlinear distortions introduced in the first half of the system will be reversed in the second half. It is also possible to perform multiple phase-conjugations along the link which has been demonstrated to give improved performance compared to conventional mid-link OPC [158]. Other methods for nonlinearity mitigation are digital backward propagation (DBP) [159,160], which relies solely on digital signal processing (DSP), and optoelectronic methods based on performing an intensity dependent phase rotation that compensates for the phase rotation introduced by fiber nonlinearities [161].

In addition to the techniques listed above it is also possible to mitigate nonlinearities by co-propagating a signal, with complex amplitude $\mathbf{E}_1$, with its conjugate, with complex amplitude $\mathbf{E}_2 = \mathbf{E}_1^*$, in an orthogonal dimension and subsequently coherently add the signal with the conjugate of the conjugated wave [162], i.e., perform the summation $\mathbf{E}_1 + \mathbf{E}_2^*$. Using perturbation theory it has been shown that the nonlinear distortions $\delta\mathbf{E}$ experienced by the signal and its conjugate during transmission are anti-correlated to first order, i.e., $\delta\mathbf{E}_2 = -(\delta\mathbf{E}_1)^*$, if the two waves experience the same anti-symmetric dispersion map and the same symmetric power map [162]. When performing the coherent addition of the signal the conjugate of the conjugate the nonlinear distortions on the two waves will be cancelled [162]. Nonlinearity mitigation in both single-channel and multi-channel systems based on this method have been demonstrated with the coherent addition performed in DSP after detecting the waves, propagated on orthogonal polarization states [163], different frequencies [164–166], and different time slots [167].

Two-mode PSA-amplified transmission systems are inherently compatible with the technique described above since the idler wave is a conjugated copy of the signal wave and the PSA performs a coherent addition of the signal and the conjugate of the idler. In a transmission system with lumped amplification, such as the PSA-amplified transmission systems studied in this thesis, the power map is not symmetric and it is therefore not clear what dispersion map will provide the most efficient nonlinearity mitigation. Moreover, the signal and idler waves are transmitted at different wavelengths and will thus experience slightly different dispersion and attenuation. This will also impact the optimal dispersion map. The dispersion map dependence of the nonlinearity mitigation efficiency in PSA-amplified transmission systems was investigated experimentally and numerically in Papers [E, F].

Mitigation of nonlinear transmission distortions in two-mode PSA-amplified transmission systems has been demonstrated in both single-span, Papers [D-F, H] and [166], and multi-span systems, Paper [I]. In Paper [E] we demonstrate mitigation of SPM induced distortions on a 10 GBd quadrature phase-shift keying (QPSK) transmitted over a 105 km single-span link. The nonlinearity mitigation in Paper [E] resulted in an increased launch power tolerances of 3 dB compared to a PIA-amplified system. A similar investigation was done in Paper [F], where we demonstrate an increased launch power tolerances of 6 dB when transmitting a

10 GBd 16QAM signal. It is interesting to note that the launch power tolerance is larger for 16QAM than for QPSK, suggesting that the benefit from using two-mode PSAs increases with modulation format complexity.

In multi-span transmission systems amplifier noise will accumulate with the number of in-line amplifiers. Due to the accumulation of amplifier noise a significant amount of NLPN can be generated through nonlinear signal-noise interaction. In PSA-amplified transmission systems the amplifier noise will be correlated at the signal and idler waves which will result in correlated NLPN, which can be mitigated by the in-line PSAs. The mitigation of NLPN in PSA-amplified transmission systems was studied in Paper [H].

4.3.1 Illustration of nonlinearity mitigation

We conclude this section by illustrating the nonlinearity mitigation capability of two-mode PSA-amplified transmission systems using a simple model in which the signal and idler waves acquire a nonlinear phase shift $\phi \propto P$ due to fiber nonlinearities. We consider the mitigation of a NLPN-like distortion by modeling the signal and idler waves accompanied by amplifier noise that is either correlated or uncorrelated between the signal and idler waves. In a copier-PSA-based two-mode PSA-amplified transmission system the amplifier noise on the signal and idler waves will be correlated. However, it is instructive to also study the case of uncorrelated amplifier noise.

At the copier output the signal and idler modes can be represented by the vector $[A_s + N_s, A_i + N_i]^T$, where A_s represents the signal, A_i represents the idler, N_s represents the amplifier noise at the signal, and N_i represents the amplifier noise at the idler. The idler is a conjugated copy of the signal, e.g., $A_i = A_s^*$ and in the case of correlated amplifier noise $N_i = N_s^*$. The modes at the copier output are illustrated in Fig. 4.5(a).

Using the simple model introduced above, propagation through the transmission fiber will introduce a phase shift $\exp(\phi)$, resulting in signal and idler modes $[(A_s + N_s) \exp(\phi), (A_i + N_i) \exp(\phi)]^T$, see Fig. 4.5(b). The combined operation performed by the PLL and the PSA, see Fig. 4.2, can be illustrated in three steps. The PLL will align the relative phase between the signal, idler, and pump waves such that the PSA gain is maximized. This can be illustrated by rotating the idler such that $|A_s + A_i^*|^2$ is maximized. The modes after idler rotation are illustrated in Fig. 4.5(c). Finally, the idler is conjugated, as illustrated in Fig. 4.5(d), and added to the signal. Fig. 4.5(a)-(d) illustrates the case of correlated amplifier noise on the signal and idler waves but can also represent the case of uncorrelated amplifier noise since the qualitative appearance is identical.

The difference between correlated and uncorrelated amplifier noise appears first at the PSA output, illustrated in Fig. 4.5(e) and (f). As can be seen from the figures, in both cases the coherent addition performed by the PSA redistributes the noise. However, significant reduction of NLPN can only be seen in the case

Copier out	Fiber out	PLL rotated	Conjugated

(a)	(b)	(c)	(d)

PSA out

Correlated amplifier noise	Uncorrelated amplifier noise

(e)	(f)

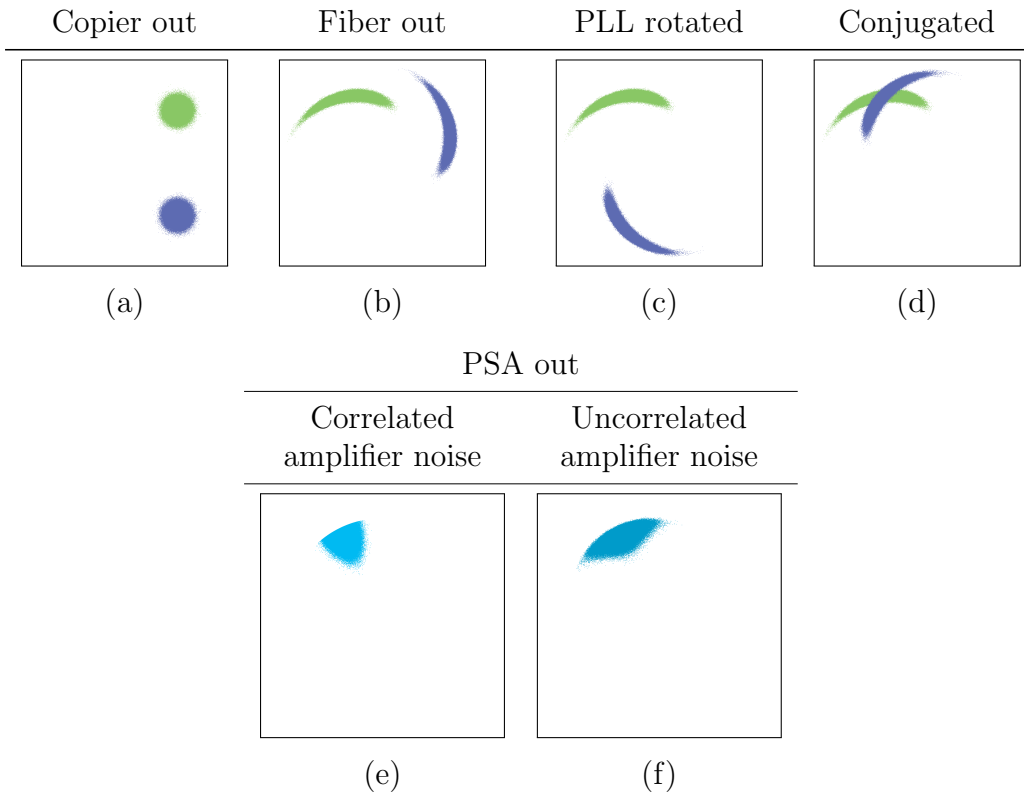Figure 4.5: Step-by-step illustration of NLPN mitigation using a two-mode PSA-amplified transmission system with signal A_{s} (green), idler A_{i} (blue), and output (cyan).

of correlated amplifier noise. All states in Fig. 4.5 are normalized. This simple example of NLPN mitigation schematically illustrates the principle for nonlinearity mitigation in two-mode PSA-amplified transmission systems.

Chapter 5

Conclusions and outlook

In the appended papers we have demonstrated the first multi-channel compatible and modulation format independent PSA-amplified transmission systems in single-span, Paper [B], and multi-span, Paper [I], configurations. We have shown that the theoretically predicted 6 dB SNR improvement for copier-PSA-based two-mode PSA-amplified transmission systems over PIA-amplified transmission systems can be obtained in practice, and provide either improved sensitivity or increased transmission reach. Moreover, we have demonstrated that two-mode PSA-amplified transmission systems are capable of mitigating nonlinear transmission distortions, Papers [E, F, H, I], and thereby provide further benefits, in addition to low-noise amplification, over conventional PIA-amplified transmission systems. These results have significantly advanced the state-of-the-art in PSA-amplified transmission.

The analysis in Section 4.2 indicates that two-mode PSAs are less beneficial in transmission systems operating at high SNR. However, the analysis in Section 4.2 does not consider the benefits from nonlinearity mitigation. The results in Paper [E] and Paper [F] suggest that the benefit from nonlinearity mitigation increase with modulation format complexity, i.e., is larger for systems operating at high SNR. For a more complete understanding of the net benefit provided by two-mode PSAs, considering both low-noise amplification and nonlinearity mitigation, the nonlinearity mitigation capability should be studied in more detail. Further studies on multi-span two-mode PSA-amplified transmission, where NLPN is present, are particularly interesting.

In this thesis we have studied single-channel transmission of single-polarization signals. A natural extension of this work would be to demonstrate multi-channel transmission. The copier-PSA scheme is multi-channel compatible, which has also been experimentally demonstrated in a B2B configuration [71], and multi-channel transmission is therefore in principle possible. However, channel-wise tuning of phase, polarization, delay, and dispersion is required, which is practically challenging. Moreover, nonlinear crosstalk between the channels in the PSA might cause significant signal degradation [168, 169]. In addition to multi-channel transmission, amplification of polarization-division multiplexing (PDM) signals should

also be demonstrated. Promising work has been carried out towards realizing polarization-insensitive PSAs capable of amplifying PDM signals [170, 171], but no transmission system implementation has been demonstrated this far.

FOPAs and PSA may also be interesting candidates for amplification in future optical communication systems utilizing space-division multiplexing [150, 172, 173], to increase the capacity or in communication systems where long reach is of more value than high SE.

Chapter 6

Summary of papers

This thesis is based on nine appended papers, all related to PSA-based transmission. In this chapter the papers are put in context and the main results are summarized, along with a description of my contribution.

There are a number of challenges associated with realizing transmission systems amplified by two-mode PSAs implemented in a modulation format independent and multi-channel compatible scheme. Paper [A] concerns one of the main challenges which is to recover the pump wave after a lossy transmission span. Using the system for pump recovery developed in Paper [A], a single-span PSA-amplified transmission system, operating in the linear transmission regime, is demonstrated in Paper [B]. In Paper [C] we demonstrate a record high sensitivity receiver using a PSA implemented as a preamplifier.

Paper [D] investigates the properties of PSA-amplified transmission systems operating in the nonlinear transmission regime. The capability of PSA-amplified transmission systems to mitigate nonlinear transmission distortions is dependent on the dispersion map and this is the topic of Paper [E]. Paper [F] provides a theoretical description of the properties of two-mode PSA-amplified transmission systems, as well as extensions of the work presented in Papers [B,D-E].

In transmission systems with cascaded amplifiers, in-line amplifier noise will affect the performance. Papers [G-H] deal with the impact of in-line amplifier noise in PSA-amplified transmission systems. Finally, in Paper [I] we demonstrate a multi-span PSA-amplified transmission system.

Paper A

S.L.I. Olsson, B. Corcoran, C. Lundström, E. Tipsuwannakul, S. Sygletos, A.D. Ellis, Z. Tong, M. Karlsson, and P.A. Andrekson, "Injection locking-based pump recovery for phase-sensitive amplified links," *Optics Express*, vol. 21, no. 12, pp. 14512–14529, June 2013.

In this paper we demonstrate a hybrid IL/EDFA-based pump recovery system, enabling PSA-amplified transmission systems with more than 40 dB span loss. We perform bit error ratio (BER) measurements with 10 GBd DQPSK data and show penalty-free recovery of a pump wave, phase modulated with two sinusoidal RF-tones at 0.1 GHz and 0.3 GHz, with 64 dB amplification, from -30 dBm to 34 dBm. We carry out a detailed experimental investigation and show that the operating power limit for the pump recovery system is governed by the noise transfer characteristics and the phase modulation transfer characteristics of the injection-locked laser. We quantify and explain the penalties occurring when operating outside the power limit.

My contribution: I designed and built the pump recovery system. I planned the investigation and built the measurement setups used to characterize the system. I carried out the measurements, analyzed the data, and wrote the paper.

Paper B

B. Corcoran, **S.L.I. Olsson**, C. Lundström, M. Karlsson, and P. Andrekson, "Phase-sensitive Optical Pre-Amplifier Implemented in an 80km DQPSK Link," in *Optical Fiber Communication Conference (OFC)*, Los Angeles, CA, March 2012, postdeadline paper PDP5A.4.

In this postdeadline paper we present the first demonstration of a modulation format independent and multi-channel compatible PSA-amplified transmission system including a significant length of transmission fiber. With an 80 km dispersion compensated transmission span we measure 1.3 dB higher sensitivity, at a BER of 10^{-3}, for a PSA-amplified system compared to a conventional EDFA-amplified system occupying the same bandwidth.

My contribution: I and B. Corcoran jointly planned the experiment, built the setup, and carried out the measurements. I contributed in writing the paper.

Paper C

R. Malik, **S.L.I. Olsson**, P. Andrekson, C. Lundström, and M. Karlsson, "Record-high sensitivity receiver using phase sensitive fiber optical parametric amplification," in *Optical Fiber Communication Conference (OFC)*, San Francisco, CA, March 2014, paper Th2A.54.

In this paper we demonstrate record high sensitivity for NRZ-OOK modulation at 10 GBd using a PSA as preamplifier. At a BER of 10^{-9} we obtain a sensitivity of -41.5 dBm, corresponding to 55 photons per bit, and at a BER of 10^{-3} we obtain a sensitivity of -47.8 dBm, corresponding to 13 photons per bit. These sensitivities

are improvements by 1.4 dB and 1.8 dB, respectively, compared to previous records.

My contribution: I took part in planning the experiment and building the setup. I performed most of the measurements, with assistance from R. Malik.

Paper D

S.L.I. Olsson, B. Corcoran, C. Lundström, M. Sjödin, M. Karlsson, and P.A. Andrekson, "Phase-Sensitive Amplified Optical Link Operating in the Nonlinear Transmission Regime," in *European Conference on Optical Communication (ECOC)*, Amsterdam, The Netherlands, September 2012, paper Th.2.F.1 (Best student paper award winner).

In this paper we present the first characterization of a PSA-amplified transmission system operating in the nonlinear transmission regime. When transmitting a 10 GBd DQPSK signal over an 80 km pre-compensated transmission span we observe less nonlinear penalty in a PSA-amplified system compared to an EDFA-amplified system.

My contribution: I planned the experiment, built the setup, and carried out most of the measurements. I contributed in writing the paper. I presented the paper at the conference.

Paper E

B. Corcoran, **S.L.I. Olsson**, C. Lundström, M. Karlsson, and P.A. Andrekson, "Mitigation of Nonlinear Impairments on QPSK Data in Phase-Sensitive Amplified Links," in *European Conference on Optical Communication (ECOC)*, London, England, September 2013, paper We.3.A.1.

In this paper we investigate the mitigation of nonlinear transmission impairments using PSAs both numerically and experimentally. In particular we investigate the impact of the dispersion map on the efficiency of the nonlinearity mitigation and show that dispersion map optimization is essential for efficient mitigation. Transmitting 10 GBd DQPSK data over a 105 km span with optimized dispersion map we experimentally demonstrate a 3 dB reduction in nonlinear penalty using a PSA-amplified system compared to using a PIA-amplified system.

My contribution: I took part in planning the experiment and assisted during some of the measurements. I presented the paper at the conference.

Paper F

In this invited paper we investigate the properties of PSA-amplified transmission systems. Using an analytical description based on a transfer matrix approach we explain the principles enabling improved sensitivity and nonlinearity mitigation in PSA-amplified systems.

We demonstrate improved sensitivity and mitigation of SPM- and NLPN-induced distortions in a system transmitting 16QAM using numerical simulations and conclude that NLPN mitigation only is possible if the noise on the signal and idler waves is correlated at the input of the transmission span. We also present a detailed numerical investigation of the dispersion map dependence and show that the optimal dispersion map for efficient nonlinearity mitigation roughly corresponds to pre-compensation of an amount equal to the effective length.

Finally we present an experimental demonstration of 10 GBd 16QAM transmission over a 105 km PSA-amplified transmission system. The combined effect of improved sensitivity and nonlinearity mitigation allow for more than 12 dB larger span loss in a PSA-amplified system compared to a conventional PIA-amplified system.

My contribution: I wrote the paper, with input from B. Corcoran on the section about dispersion map dependence. I performed the numerical simulations related to 16QAM transmission and the experimental demonstration.

Paper G

In this paper we investigate the impact of having uncorrelated amplifier noise on the signal and idler waves at the input of a PSA, which could occur in a hybrid PSA-amplified transmission system. We show, both theoretically and experimentally, that a PSA improve the output OSNR by 3 to 6 dB, depending on the amount of uncorrelated amplifier noise present at its input.

My contribution: I took part in planning the experiment and contributed in the paper writing.

Paper H

S.L.I. Olsson, M. Karlsson, and P.A. Andrekson, "Nonlinear phase noise mitigation in phase-sensitive amplified transmission systems," *Optics Express*, vol. 23, no. 9, pp. 11724–11740, May 2015.

In this paper we investigate the impact of in-line amplifier noise in PSA-amplified transmission systems both experimentally and numerically. We present the first experimental demonstration of NLPN mitigation in a modulation format independent PSA-amplified transmission system. We also present a record high sensitivity receiver, enabled by low-noise PSA-amplification, requiring only 4.1 photons per bit to obtain a BER of 10^{-3} with 10 GBd QPSK data.

My contribution: I performed the numerical simulations, the experimental demonstration, and wrote the paper.

Paper I

S.L.I. Olsson, C. Lundström, M. Karlsson, and P.A. Andrekson, "Long-Haul (3465 km) Transmission of a 10 GBd QPSK Signal with Low Noise Phase-Sensitive In-Line Amplification," in *European Conference on Optical Communication (ECOC)*, Cannes, France, September 2014, postdeadline paper PD.2.2.

In this postdeadline paper we present the first demonstration of low-noise in-line PSAs in a long-haul circulating loop setup. With a 10 GBd QPSK signal a maximum transmission distance of 3465 km was achieved using in-line PSAs, which is a threefold reach improvement compared to the maximum reach of 1050 km that was obtained using in-line EDFAs at optimal launch power. The reach improvement using in-line PSAs is attributed to low-noise amplification and nonlinearity mitigation.

My contribution: I planned the experiment, built the setup, carried out the measurements, and analyzed the data. I wrote the paper with assistance from C. Lundström. I presented the paper at the conference.

References

[1] T. H. Maiman, "Stimulated optical radiation in ruby," *Nature*, vol. 187, no. 4736, pp. 493–494, August 1960.

[2] K. C. Kao and G. A. Hockham, "Dielectric-fibre surface waveguides for optical frequencies," *Proceedings of the Institution of Electrical Engineers*, vol. 113, no. 7, pp. 1151–1158, July 1966.

[3] S. B. Poole, D. N. Payne, R. J. Mears, M. E. Fermann, and R. I. Laming, "Fabrication and characterization of low-loss optical fibers containing rare-earth ions," *Journal of Lightwave Technology*, vol. LT-4, no. 7, pp. 870–876, July 1986.

[4] Cisco, "Cisco visual networking index: forecast and methodology, 2013-2018," Tech. Rep., June 2014, Accessed: March 2015. [Online]. Available: http://www.cisco.com/c/en/us/solutions/collateral/service-provider/ip-ngn-ip-next-generation-network/white_paper_c11-481360.pdf

[5] T. C. Cannon, D. L. Pope, and D. D. Sell, "Installation and performance of the Chicago lightwave transmission system," *IEEE Transactions on Communications*, vol. COM-26, no. 7, pp. 1056–1060, July 1978.

[6] J. X. Cai, H. G. Batshon, M. Mazurczyk, H. Zhang, Y. Sun, O. V. Sinkin, D. G. Foursa, and A. Pilipetskii, "64QAM based coded modulation transmission over transoceanic distance with > 60 Tb/s capacity," in *Optical Fiber Communication Conference (OFC)*, March 2015, paper Th5C.8.

[7] A. H. Gnauck, R. W. Tkach, A. R. Chraplyvy, and T. Li, "High-capacity optical transmission systems," *Journal of Lightwave Technology*, vol. 26, no. 9, pp. 1032–1045, May 2008.

[8] P. J. Winzer, "High-spectral-efficiency optical modulation formats," *Journal of Lightwave Technology*, vol. 30, no. 24, pp. 3824–3835, December 2012.

[9] C. E. Shannon, "Communication in the presence of noise," *Proceedings of the IRE*, vol. 37, no. 1, pp. 10–21, September 1949.

[10] S. Makovejs, C. C. Roberts, F. Palacios, H. B. Matthews, D. A. Lewis, D. T. Smith, P. G. Diehl, J. J. Johnson, J. D. Patterson, C. R. Towery, and S. Y. Ten, "Record-low (0.1460 dB/km) attenuation ultra-large A_{eff} optical fiber for submarine applications," in *Optical Fiber Communication Conference (OFC)*, March 2015, paper Th5A.2.

[11] D. M. Baney, P. Gallion, and R. S. Tucker, "Theory and measurement techniques for the noise figure of optical amplifiers," *Optical Fiber Technology*, vol. 6, no. 2, pp. 122–154, April 2000.

[12] E. Desurvire, *Erbium-doped fiber amplifiers.* John Wiley & Sons, 1994.

[13] C. M. Caves, "Quantum limits on noise in linear amplifiers," *Physical Review D*, vol. 26, no. 8, pp. 1817–1839, October 1982.

[14] Z. Tong and S. Radic, "Low-noise optical amplification and signal processing in parametric devices," *Advances in Optics and Photonics*, vol. 5, no. 3, pp. 318–384, August 2013.

[15] C. J. McKinstrie and S. Radic, "Phase-sensitive amplification in a fiber," *Optics Express*, vol. 12, no. 20, pp. 4973–4979, September 2004.

[16] D. F. Walls, "Squeezed states of light," *Nature*, vol. 306, no. 10, pp. 141–146, November 1983.

[17] Z. Tong, C. Lundström, P. A. Andrekson, M. Karlsson, and A. Bogris, "Ultralow noise, broadband phase-sensitive optical amplifiers, and their applications," *IEEE Journal of Selected Topics in Quantum Electronics*, vol. 18, no. 2, pp. 1016–1032, March/April 2012.

[18] R. E. Slusher and B. Yurke, "Squeezed light for coherent communications," *Journal of Lightwave Technology*, vol. 8, no. 3, pp. 466–477, March 1990.

[19] M. C. Teich and B. E. A. Saleh, "Squeezed states of light," *Quantum Optics*, vol. 1, no. 2, pp. 153–191, December 1989.

[20] Y. Yamamoto and K. Inoue, "Noise in amplifiers," *Journal of Lightwave Technology*, vol. 21, no. 11, pp. 2895–2915, November 2003.

[21] K. Croussore and G. Li, "Phase and amplitude regeneration of differential phase-shift keyed signals using phase-sensitive amplification," *IEEE Journal of Selected Topics in Quantum Electronics*, vol. 14, no. 3, pp. 648–658, May/June 2008.

[22] R. Slavík, A. Borgis, F. Parmigiani, J. Kakande, M. Westlund, M. Sköld, L. Grüner-Nielsen, R. Phelan, D. Syvridis, P. Petropoulos, and D. J. Richardson, "Coherent all-optical phase and amplitude regenerator of binary phase-encoded signals," *IEEE Journal of Selected Topics in Quantum Electronics*, vol. 18, no. 2, pp. 859–869, March/April 2012.

[23] J. Kakande, C. Lundström, P. A. Andrekson, Z. Tong, M. Karlsson, P. Petropoulos, F. Parmigiani, and D. J. Richardson, "Multilevel quantization of optical phase in a novel coherent parametric mixer architecture," *Nature Photonics*, vol. 5, no. 12, pp. 748–752, October 2011.

[24] T. Umeki, M. Asobe, H. Takara, Y. Miyamoto, and H. Takenouchi, "Multispan transmission using phase and amplitude regeneration in PPLN-based PSA," *Optics Express*, vol. 21, no. 15, pp. 18 170–18 177, July 2013.

[25] R.-D. Li, P. Kumar, and W. L. Kath, "Dispersion compensation with phase-sensitive optical amplifiers," *Journal of Lightwave Technology*, vol. 12, no. 3, pp. 541–549, March 1994.

[26] J. N. Kutz, C. V. Hile, and W. L. Kath, "Pulse propagation in nonlinear optical fiber lines that employ phase-sensitive parametric amplifiers," *Journal of the Optical Society of America B*, vol. 11, no. 10, pp. 2112–2123, October 1994.

[27] M. Asobe, T. Umeki, K. Enbutsu, O. Tadanaga, and H. Takenouchi, "Phase squeezing and dispersion tolerance of phase sensitive amplifier using periodically poled LiNbO$_3$ waveguide," *Journal of the Optical Society of America B*, vol. 31, no. 12, pp. 3164–3169, December 2014.

[28] M. I. Kolobov, "The spatial behavior of nonclassical light," *Reviews of Modern Physics*, vol. 71, no. 5, pp. 1539–1589, October 1999.

[29] E. Lantz and F. Devaux, "Parametric amplification of images: From time gating to noiseless amplification," *IEEE Journal of Selected Topics in Quantum Electronics*, vol. 14, no. 3, pp. 635–647, May/June 2008.

[30] H. P. Yuen, "Reduction of quantum fluctuation and suppression of the Gordon-Haus effect with phase-sensitive linear amplifiers," *Optics Letters*, vol. 17, no. 1, pp. 73–75, January 1992.

[31] Y. Mu and C. M. Savage, "Parametric amplifiers in phase-noise-limited optical communications," *Journal of the Optical Society of America B*, vol. 9, no. 1, pp. 65–70, January 1992.

[32] J. A. Levenson, I. Abram, T. Rivera, and P. Fayolle, "Quantum optical cloning amplifier," *Physical Review Letters*, vol. 70, no. 3, pp. 267–270, January 1993.

[33] K. J. Lee, F. Parmigiani, S. Liu, J. Kakande, P. Petropoulos, K. Gallo, and D. Richardson, "Phase sensitive amplification based on quadratic cascading in a periodically poled lithium niobate waveguide," *Optics Express*, vol. 17, no. 22, pp. 20 393–20 400, October 2009.

[34] T. Umeki, M. Asobe, and H. Takenouchi, "In-line phase sensitive amplifier based on PPLN waveguides," *Optics Express*, vol. 21, no. 10, pp. 12 077–12 084, May 2013.

[35] B. J. Puttnam, D. Mazroa, S. Shinada, and N. Wada, "Phase-squeezing properties of non-degenerate PSAs using PPLN waveguides," *Optics Express*, vol. 19, no. 26, pp. B131–B139, November 2011.

[36] R. Slavík, F. Parmigiani, J. Kakande, C. Lundström, M. Sjödin, P. A. Andrekson, R. Weerasuriya, S. Sygletos, A. D. Ellis, L. Grüner-Nielsen, D. Jakobsen, S. Herstrøm, R. Phelan, J. O′Gorman, A. Bogris, D. Syvridis, S. Dasgupta, P. Petropoulos, and D. J. Richardson, "All-optical phase and amplitude regenerator for next-generation telecommunications systems," *Nature Photonics*, vol. 4, pp. 690–695, October 2010.

[37] Z. Tong, C. Lundström, P. A. Andrekson, C. J. McKinstrie, M. Karlsson, D. J. Blessing, E. Tipsuwannakul, B. J. Puttnam, H. Toda, and L. Grüner-Nielsen, "Towards ultrasensitive optical links enabled by low-noise phase-

sensitive amplifiers," *Nature Photonics*, vol. 5, no. 7, pp. 430–436, June 2011.

[38] R. Neo, J. Schröder, Y. Paquot, D.-Y. Choi, S. Madden, B. Luther-Davies, and B. J. Eggleton, "Phase-sensitive amplification of light in a $\chi^{(3)}$ photonic chip using a dispersion engineered chalcogenide ridge waveguide," *Optics Express*, vol. 21, no. 7, pp. 7926–7933, March 2013.

[39] F. D. Ros, D. Vukovic, A. Gajda, K. Dalgaard, L. Zimmermann, B. Tillack, M. Galili, K. Petermann, and C. Peucheret, "Phase regeneration of DPSK signals in a silicon waveguide with reverse-biased p-i-n junction," *Optics Express*, vol. 22, no. 5, pp. 5029–5036, February 2014.

[40] S. Sygletos, M. J. Power, F. C. G. Gunning, R. P. Webb, R. J. Manning, and A. D. Ellis, "Simultaneous dual channel phase regeneration in SOAs," in *European Conference and Exhibition on Optical Communication (ECOC)*, September 2012, paper Tu.1.A.2.

[41] H. A. Haus and C. H. Townes, "Comments on "Noise in photoelectric mixing"," *Proceedings of the IRE*, vol. 50, no. 6, pp. 1544–1545, June 1962.

[42] B. M. Oliver, "Reply to H. A. Haus and C. H. Townes, 'Comments on "Noise in photoelectric mixing"'," *Proceedings of the IRE*, vol. 50, no. 6, pp. 1545–1546, June 1962.

[43] H. P. Yuen, "Amplification of quantum states and noiseless photon amplifiers," *Physical Letters A*, vol. 113A, no. 8, pp. 405–407, January 1986.

[44] R. Loudon, "Theory of noise accumulation in linear optical-amplifier chains," *IEEE Journal of Quantum Electronics*, vol. QE-21, no. 7, pp. 766–773, July 1985.

[45] H. P. Yuen, "Design of transparent optical networks by using novel quantum amplifiers and sources," *Optics Letters*, vol. 12, no. 10, pp. 789–791, October 1987.

[46] W. Imajuku and A. Takada, "Gain characteristics of coherent optical amplifiers using a MachZehnder interferometer with Kerr media," *IEEE Journal of Quantum Electronics*, vol. 35, no. 11, pp. 1657–1665, November 1999.

[47] M. E. Marhic, C. H. Hsia, and J. M. Jeong, "Optical amplification in a nonlinear fibre interferometer," *Optics Letters*, vol. 27, no. 3, pp. 210–211, January 1991.

[48] W. Imajuku and A. Takada, "Error-free operation of in-line phase-sensitive amplifier," *Electronics Letters*, vol. 34, no. 17, pp. 1673–1674, August 1998.

[49] ——, "In-line optical phase-sensitive amplifier with pump light source controlled by optical phase-lock loop," *Journal of Lightwave Technology*, vol. 17, no. 4, pp. 637–646, April 1999.

[50] W. Imajuku, A. Takada, and Y. Yamabayashi, "Low-noise amplification under the 3 dB noise figure in high-gain phase-sensitive fibre amplifier," *Electronics Letters*, vol. 35, no. 22, pp. 1954–1955, October 1999.

66

[51] ——, "Inline coherent optical amplifier with noise figure lower than 3 dB quantum limit," *Electronics Letters*, vol. 36, no. 1, pp. 63–64, January 2000.

[52] K. Croussore, C. Kim, and G. Li, "All-optical regeneration of differential phase-shift keying signals based on phase-sensitive amplification," *Optics Letters*, vol. 29, no. 20, pp. 2357–2359, October 2004.

[53] K. Croussore, I. Kim, Y. Han, C. Kim, G. Li, and S. Radic, "Demonstration of phase-regeneration of DPSK signals based on phase-sensitive amplification," *Optics Express*, vol. 13, no. 11, pp. 3945–3950, May 2005.

[54] K. Croussore, I. Kim, C. Kim, Y. Han, and G. Li, "Phase-and-amplitude regeneration of differential phase-shift keyed signals using a phase-sensitive amplifier," *Optics Express*, vol. 14, no. 6, pp. 2085–2094, March 2006.

[55] A. Takada and W. Imajuku, "In-line optical phase-sensitive amplifier employing pump laser injection-locked to input signal light," *Electronics Letters*, vol. 34, no. 3, pp. 274–276, February 1998.

[56] W. Imajuku and A. Takada, "In-line phase-sensitive amplifier with optical-PLL-controlled internal pump light source," *Electronics Letters*, vol. 33, no. 25, pp. 2155–2156, December 1997.

[57] J. Kakande, C. Lundström, P. A. Andrekson, Z. Tong, M. Karlsson, P. Petropoulos, F. Parmigiani, and D. J. Richardson, "Detailed characterization of a fiber-optic parametric amplifier in phase-sensitive and phase-insensitive operation," *Optics Express*, vol. 18, no. 5, pp. 4130–4137, March 2010.

[58] R. M. Shelby, M. D. Levenson, and P. W. Bayer, "Guided acoustic-wave Brillouin scattering," *Physical Review B*, vol. 31, no. 8, pp. 5244–5252, April 1985.

[59] I. Bar-Joseph, A. A. Friesem, R. G. Waarts, and H. H. Yaffe, "Parametric interaction of a modulated wave in a single-mode fiber," *Optics Letters*, vol. 11, no. 8, pp. 534–536, August 1986.

[60] R. Tang, P. Devgan, V. S. Grigoryan, and P. Kumar, "Inline frequency-nondegenerate phase-sensitive fibre parametric amplifier for fibre-optic communication," *Electronics Letters*, vol. 41, no. 19, pp. 1072–1074, September 2005.

[61] M. Vasilyev, "Distributed phase-sensitive amplification," *Optics Express*, vol. 13, no. 19, pp. 7563–7571, September 2005.

[62] R. Tang, P. Devgan, J. Lasri, V. Grigoryan, and P. Kumar, "Experimental investigation of a frequency-nondegenerate phase-sensitive optical parametric amplifier," in *Optical Fiber Communication Conference (OFC)*, March 2005, paper OWN6.

[63] R. Tang, P. Devgan, P. L. Voss, V. S. Grigoryan, and P. Kumar, "In-line frequency-nondegenerate phase-sensitive fiber-optical parametric amplifier," *IEEE Photonics Technology Letters*, vol. 17, no. 9, pp. 1845–1847, September 2005.

[64] R. Tang, J. Lasri, P. S. Devgan, V. Grigoryan, P. Kumar, and M. Vasilyev, "Gain characteristics of a frequency nondegenerate phase-sensitive fiber-optic parametric amplifier with phase self-stabilized input," *Optics Express*, vol. 13, no. 26, pp. 10 483–10 493, December 2005.

[65] P. Kumar, J. Lasri, P. Devgan, and R. Tang, "Fiber nonlinearity based devices for advanced fiber-optic communication and signal processing," in *Annual Meeting of the IEEE Lasers and Electro-Optics Society*, 2003, paper MK1.

[66] M. Jamshidifar, A. Vedadi, and M. E. Marhic, "Continuous-wave one-pump fiber optical parametric amplifier with 270 nm gain bandwidth," in *European Conference and Exhibition on Optical Communication (ECOC)*, September 2009, paper 1.1.4.

[67] C. J. McKinstrie, M. Karlsson, and Z. Tong, "Field-quadrature and photon-number correlations produced by parametric processes," *Optics Express*, vol. 18, no. 19, pp. 19 792–19 823, September 2010.

[68] R. Tang, P. S. Devgan, V. S. Grigoryan, P. Kumar, and M. Vasilyev, "In-line phase-sensitive amplification of multichannel CW signals based on frequency nondegenerate four-wave-mixing in fiber," *Optics Express*, vol. 16, no. 12, pp. 9046–9053, June 2008.

[69] R. Tang, M. Shin, P. Devgan, V. S. Grigoryan, M. Vasilyev, and P. Kumar, "Toward in-line phase-sensitive fiber-parametric amplification of multichannel signals," in *Conference on Lasers and Electro-Optics (CLEO)*, 2006, paper JThC81.

[70] Z. Tong, C. J. McKinstrie, C. Lundström, M. Karlsson, and P. A. Andrekson, "Noise performance of optical fiber transmission links that use non-degenerate cascaded phase-sensitive amplifiers," *Optics Express*, vol. 18, no. 15, pp. 15 426–15 439, July 2010.

[71] Z. Tong, C. Lundström, E. Tipsuwannakul, M. Karlsson, and P. A. Andrekson, "Phase-sensitive amplified DWDM DQPSK signals using free-running lasers with 6-dB link SNR improvement over EDFA-based systems," in *European Conference and Exhibition on Optical Communication (ECOC)*, September 2010, paper PDP1.3.

[72] R.-J. Essiambre, G. Kramer, P. J. Winzer, G. J. Foschini, and B. Goebel, "Capacity limits of optical fiber networks," *Journal of Lightwave Technology*, vol. 28, no. 4, pp. 662–701, February 2010.

[73] A. D. Ellis, J. Zhao, and D. Cotter, "Approaching the non-linear Shannon limit," *Journal of Lightwave Technology*, vol. 28, no. 4, pp. 423–433, February 2010.

[74] E. Lach and W. Idler, "Modulation formats for 100G and beyond," *Optical Fiber Technology*, vol. 17, no. 5, pp. 377–386, August 2011.

[75] H. Heffner, "The fundamental noise limit of linear amplifiers," *Proceedings of the IRE*, vol. 50, no. 7, pp. 1604–1608, July 1962.

[76] H. A. Haus and J. A. Mullen, "Quantum noise in linear amplifiers," *Physical Review*, vol. 128, no. 5, pp. 2407–2413, December 1962.

[77] E. Ip, A. P. T. Lau, D. J. F. Barros, and J. M. Kahn, "Coherent detection in optical fiber systems," *Optics Express*, vol. 16, no. 2, pp. 753–791, January 2008.

[78] G. Li, "Recent advances in coherent optical communication," *Advances in Optics and Photonics*, vol. 1, no. 2, pp. 279–307, February 2009.

[79] R. J. Mears, L. Reekie, I. M. Jauncey, and D. N. Payne, "Low-noise erbium-doped fibre amplifier operating at 1.54μm," *Electronics Letters*, vol. 23, no. 19, pp. 1026–1028, September 1987.

[80] M. N. Islam, "Raman amplifiers for telecommunications," *IEEE Journal of Selected Topics in Quantum Electronics*, vol. 8, no. 3, pp. 493–494, May/June 2002.

[81] M. J. Connelly, *Semiconductor optical amplifiers.* Kluwer, 2004.

[82] J. Hansryd, P. A. Andrekson, M. Westlund, J. Li, and P.-O. Hedekvist, "Fiber-based optical parametric amplifiers and their applications," *IEEE Journal of Selected Topics in Quantum Electronics*, vol. 8, no. 3, pp. 506–520, May/June 2002.

[83] F. A. Flood, "L-band erbium-doped fiber amplifiers," in *Optical Fiber Communication Conference (OFC)*, March 2000, paper WG1.

[84] J. B. Rosolem and A. A. Juriollo, "S band EDFA using standard erbium doped fiber, 1450 nm pumping and single stage ASE filtering," in *Optical Fiber Communication Conference (OFC)*, March 2008, paper OTuN3.

[85] S. Aozasa, H. Masuda, H. Ono, T. Sakamoto, T. Kanamori, Y. Ohishi, and M. Shimizu, "1480-1510 nm-band Tm doped fiber amplifier (TDFA) with a high power conversion efficiency of 42 %," in *Optical Fiber Communication Conference (OFC)*, March 2001, paper PD1.

[86] J. Bromage, "Raman amplification for fiber communications systems," *Journal of Lightwave Technology*, vol. 22, no. 1, pp. 79–93, January 2004.

[87] R. I. Laming, M. N. Zervas, and D. N. Payne, "Erbium-doped fiber amplifier with 54 dB gain and 3.1 dB noise figure," *IEEE Photonics Technology Letters*, vol. 4, no. 12, pp. 1345–1347, December 1992.

[88] X. Li and G. Li, "Electrical postcompensation of SOA impairments for fiber-optic transmission," *IEEE Photonics Technology Letters*, vol. 21, no. 9, pp. 581–583, May 2009.

[89] A. E. Kelly, I. F. Lealman, L. J. Rivers, S. D. Perrin, and M. Silver, "Low noise figure (7.2 dB) and high gain (29 dB) semiconductor optical amplifier with a single layer AR coating," *Electronics Letters*, vol. 33, no. 6, pp. 536–538, March 1997.

[90] E. J. Woodbury and W. K. Ng, "Ruby laser operating in the near IR," *Proceedings of the IRE*, vol. 50, no. 11, p. 2367, November 1962.

[91] G. Eckhardt, R. W. Hellwarth, F. J. McClung, S. E. Schwarz, D. Weiner, and E. J. Woodbury, "Stimulated Raman scattering from organic liquids," *Physical Review Letters*, vol. 9, no. 11, pp. 455–457, December 1962.

[92] R. H. Stolen and E. P. Ippen, "Raman gain in glass optical waveguides," *Applied Physics Letters*, vol. 22, no. 276, pp. 276–278, March 1973.

[93] C. V. Raman and K. S. Krishnan, "A new type of secondary radiation," *Nature*, vol. 121, no. 3048, pp. 501–502, March 1928.

[94] E. Desurvire, M. Papuchon, J. P. Pocholle, and J. Raffy, "High-gain optical amplification of laser diode signal by Raman scattering in single-mode fibres," *Electronics Letters*, vol. 19, no. 19, pp. 751–753, September 1983.

[95] H. Masuda, S. Kawai, and K. I. Suzuki, "Optical SNR enhanced amplification in long-distance recirculating-loop WDM transmission experiment using 1580 nm band hybrid amplifier," *Electronics Letters*, vol. 35, no. 5, pp. 411–412, March 1999.

[96] E. Pincemin, T. Guillossou, N. Evanno, S. Lobanov, and S. Ten, "Record transmission distances over ultra low loss G.652 fibre with NRZ-OOK or NRZ-DPSK 40 Gbps WDM systems," in *Optical Fiber Communication Conference (OFC)*, March 2009, paper OThC2.

[97] R. Loudon, *The quantum theory of light*. Oxford University Press, 2000.

[98] D. Marcuse, *Principles of quantum electronics*. Academic press, 1980.

[99] J. J. Sakurai, *Modern quantum mechanics*. Addison Wesley Longman, 1994.

[100] H. T. Friis, "Noise figures of radio receivers," *Proceedings of the IRE*, vol. 32, no. 7, pp. 419–422, July 1944.

[101] G. P. Agrawal, *Fiber-optic communication systems*, 4th ed. John Wiley & Sons, 2010.

[102] ——, *Nonlinear fiber optics*, 5th ed. Academic press, 2012.

[103] J. A. Armstrong, N. Bloembergen, J. Ducuing, and P. S. Pershan, "Interactions between light waves in a nonlinear dielectric," *Physical Review*, vol. 127, no. 6, pp. 1918–1939, September 1962.

[104] N. M. Kroll, "Parametric amplification in spatially extended media and application to the design of tuneable oscillators at optical frequencies," *Proceedings of the IEEE*, vol. 51, no. 1, pp. 110–114, January 1963.

[105] S.-K. Choi, R.-D. Li, C. Kim, and P. Kumar, "Traveling-wave optical parametric amplifier: investigation of its phase-sensitive and phase-insensitive gain response," *Journal of the Optical Society of America B*, vol. 14, no. 7, pp. 1564–1575, July 1997.

[106] D. J. Lovering, J. A. Levenson, P. Vidakovic, J. Webjörn, and P. S. J. Russell, "Noiseless optical amplification in quasi-phase-matched bulk lithium niobate," *Optics Letters*, vol. 21, no. 18, pp. 1439–1441, September 1996.

[107] R. H. Stolen, "Phase-matched-stimulated four-photon mixing in silica-fiber waveguides," *IEEE Journal of Quantum Electronics*, vol. QE-11, no. 3, pp. 100–103, March 1975.

[108] R. H. Stolen and J. E. Bjorkholm, "Parametric amplification and frequency conversion in optical fibers," *IEEE Journal of Quantum Electronics*, vol. QE-18, no. 7, pp. 1062–1072, July 1982.

[109] C. Lin, W. A. Reed, A. D. Pearson, and H. T. Shang, "Phase matching in the minimum-chromatic-dispersion region of single-mode fibers for stimulated four-photon mixing," *Optics Letters*, vol. 6, no. 10, pp. 493–495, October 1981.

[110] K. Washio, K. Inoue, and S. Kishida, "Efficient large-frequency-shifted three-wave mixing in low dispersion wavelength region in single-mode optical fibre," *Electronics Letters*, vol. 16, no. 17, pp. 658–660, August 1980.

[111] F. Yang, M. Marhic, and L. Kazovsky, "CW fibre optical parametric amplifier with net gain and wavelength conversion efficiency > 1," *Electronics Letters*, vol. 32, no. 25, pp. 2336–2338, December 1996.

[112] J. Hansryd and P. A. Andrekson, "Broad-band continuous-wave-pumped fiber optical parametric amplifier with 49-dB gain and wavelength-conversion efficiency," *IEEE Photonics Technology Letters*, vol. 13, no. 3, pp. 194–196, March 2001.

[113] J. M. C. Boggio, S. Moro, E. Myslivets, J. R. Windmiller, N. Alic, and S. Radic, "155-nm continuous-wave two-pump parametric amplification," *IEEE Photonics Technology Letters*, vol. 21, no. 10, pp. 612–614, May 2009.

[114] T. Torounidis, P. A. Andrekson, and B.-E. Olsson, "Fiber-optical parametric amplifier with 70-dB gain," *IEEE Photonics Technology Letters*, vol. 18, no. 10, pp. 1194–1196, May 2006.

[115] P. L. Voss, R. Tang, and P. Kumar, "Measurement of the photon statistics and the noise figure of a fiber-optic parametric amplifier," *Optics Letters*, vol. 28, no. 7, pp. 549–551, April 2003.

[116] P. L. Voss, K. G. Köprülü, and P. Kumar, "Raman-noise-induced quantum limits for $\chi^{(3)}$ nondegenerate phase-sensitive amplification and quadrature squeezing," *Journal of the Optical Society of America B*, vol. 23, no. 4, pp. 598–610, April 2006.

[117] P. A. Andrekson, "Picosecond optical sampling using four-wave mixing in fibre," *Electronics Letters*, vol. 27, no. 16, pp. 1440–1441, August 1991.

[118] P. A. Andrekson, N. A. Olsson, J. R. Simpson, T. Tanbun-ek, R. A. Logan, and M. Haner, "16 Gbit/s all-optical demultiplexing using four-wave mixing," *Electronics Letters*, vol. 27, no. 11, pp. 922–924, May 1991.

[119] K. Inoue, "Optical level equalisation based on gain saturation in fibre optical parametric amplifier," *Electronics Letters*, vol. 36, no. 12, pp. 1016–1017, June 2000.

[120] G.-W. Lu and T. Miyazaki, "Optical phase erasure based on FWM in HNLF enabling format conversion from 320-Gb/s RZDQPSK to 160-Gb/s RZ-DPSK," *Optics Express*, vol. 17, no. 16, pp. 13 346–13 353, August 2009.

[121] R. Jopson and R. Tench, "Polarisation-independent phase conjugation of lightwave signals," *Electronics Letters*, vol. 29, no. 25, pp. 2216–2217, December 1993.

[122] K. Inoue, "Polarization independent wavelength conversion using fiber four-wave mixing with two orthogonal pump lights of different frequencies," *Journal of Lightwave Technology*, vol. 12, no. 11, pp. 1916–1920, November 1994.

[123] K. K. Y. Wong, M. E. Marhic, K. Uesaka, and L. G. Kazovsky, "Polarization-independent two-pump fiber optical parametric amplifier," *IEEE Photonics Technology Letters*, vol. 14, no. 7, pp. 911–913, July 2002.

[124] M. Oskar van Deventer, *Fundamentals of bidirectional transmission over a single optical fibre.* Kluwer Academic, 1996.

[125] C. J. McKinstrie, S. Radic, and M. G. Raymer, "Quantum noise properties of parametric amplifiers driven by two pump waves," *Optics Express*, vol. 12, no. 21, pp. 5037–5066, October 2004.

[126] Z. Tong, A. Bogris, C. Lundström, C. J. McKinstrie, M. Vasilyev, M. Karlsson, and P. A. Andrekson, "Modeling and measurement of the noise figure of a cascaded non-degenerate phase-sensitive parametric amplifier," *Optics Express*, vol. 18, no. 14, pp. 14 820–14 835, July 2010.

[127] M. Hirano, T. Nakanishi, T. Okuno, and M. Onishi, "Silica-based highly nonlinear fibers and their application," *IEEE Journal of Selected Topics in Quantum Electronics*, vol. 15, no. 1, pp. 103–113, January/February 2009.

[128] S. K. Korotky, P. B. Hansen, L. Eskildsen, and J. J. Veselka, "Efficient phase modulation scheme for suppressing stimulated brillouin scattering," in *International Conference Integrated Optics and Optical Fiber Communications (IOOC)*, 1995, paper WD2.

[129] C. Lundström, R. Malik, L. Grüner-Nielsen, B. Corcoran, S. L. I. Olsson, M. Karlsson, and P. A. Andrekson, "Fiber optic parametric amplifier with 10-dB net gain without pump dithering," *IEEE Photonics Technology Letters*, vol. 25, no. 3, pp. 234–237, February 2013.

[130] J. Hansryd, F. Dross, M. Westlund, P. A. Andrekson, and S. N. Knudsen, "Increase of the SBS threshold in a short highly nonlinear fiber by applying a temperature distribution," *Journal of Lightwave Technology*, vol. 19, no. 11, pp. 1691–1697, November 2001.

[131] J. M. C. Boggio, S. Moro, E. Myslivets, J. R. Windmiller, N. Alic, and S. Radic, "Experimental and numerical investigation of the SBS-threshold increase in an optical fiber by applying strain distributions," *Journal of Lightwave Technology*, vol. 23, no. 11, pp. 3808–3814, November 2005.

[132] T. Nakanishi, M. Tanaka, T. Hasegawa, M. Hirano, T. Okuno, and M. Onishi, "Al2O3-SiO2 core highly nonlinear dispersion-shifted fiber with Bril-

louin gain suppression improved by 6.1dB," in *European Conference and Exhibition on Optical Communication (ECOC)*, September 2006, paper Th4.2.2.

[133] A. Durécu-Legrand, C. Simonneau, D. Bayart, A. Mussot, T. Sylvestre, E. Lantz, and H. Maillotte, "Impact of pump OSNR on noise figure for fiber-optical parametric amplifiers," *IEEE Photonics Technology Letters*, vol. 17, no. 6, pp. 1178–1180, June 2005.

[134] P. Kylemark, P. O. Hedekvist, H. Sunnerud, M. Karlsson, and P. A. Andrekson, "Noise characteristics of fiber optical parametric amplifiers," *Journal of Lightwave Technology*, vol. 22, no. 2, pp. 409–416, February 2004.

[135] J. L. Blows and S. E. French, "Low-noise-figure optical parametric amplifier with a continuous-wave frequency-modulated pump," *Optics Letters*, vol. 27, no. 7, pp. 491–493, April 2002.

[136] A. Mecozzi and P. Tombesi, "Parametric amplification and signal-to-noise ratio in optical transmission lines," *Optics Communications*, vol. 75, no. 3,4, pp. 256–262, March 1990.

[137] A. Pikovsky, M. Rosenblum, and J. Kurths, *Synchronization: a universal concept in nonlinear sciences*, ser. Cambridge Nonlinear Science Series. Cambridge University Press, 2003, vol. 12.

[138] R. Adler, "A study of locking phenomena in oscillators," *Proceedings of the IRE*, vol. 34, pp. 351–357, June 1946.

[139] R. H. Pantell, "The laser oscillator with an external signal," *Proceedings of the IEEE*, vol. 53, no. 5, pp. 474–477, May 1965.

[140] H. L. Stover and W. H. Steier, "Locking of laser oscillators by light injection," *Applied Physics Letters*, vol. 8, no. 4, pp. 91–93, February 1966.

[141] R. Hui, A. D'Ottavi, A. Mecozzi, and P. Spano, "Injection locking in distributed feedback semiconductor lasers," *IEEE Journal of Quantum Electronics*, vol. 27, no. 6, pp. 1688–1695, June 1991.

[142] K. Iwashita and K. Nakagawa, "Suppression of mode partition noise by laser diode light injection," *IEEE Journal of Quantum Electronics*, vol. QE-18, no. 10, pp. 1669–1674, October 1982.

[143] X. J. Meng, T. Chau, D. T. K. Tong, and M. C. Wu, "Suppression of second harmonic distortion in directly modulated distributed feedback lasers by external light injection," *Electronics Letters*, vol. 34, no. 21, pp. 2040–2041, October 1998.

[144] C. Lin and F. Mengel, "Reduction of frequency chirping and dynamic linewidth in high-speed directly modulated semiconductor lasers by injection locking," *Electronics Letters*, vol. 20, no. 25/26, pp. 1073–1075, December 1984.

[145] N. Schunk and K. Petermann, "Noise analysis of injection-locked semiconductor injection lasers," *IEEE Journal of Quantum Electronics*, vol. QE-22, no. 5, pp. 642–650, May 1986.

[146] E. K. Lau, L. J. Wong, X. Zhao, Y.-K. Chen, C. J. Chang-Hasnain, and M. C. Wu, "Bandwidth enhancement by master modulation of optical injection-locked lasers," *Journal of Lightwave Technology*, vol. 26, no. 15, pp. 2584–2593, August 2008.

[147] C. H. Henry, N. A. Olsson, and N. K. Dutta, "Locking range and stability of injection locked 1.54 μm InGaAsP semiconductor lasers," *IEEE Journal of Quantum Electronics*, vol. QE-21, no. 8, pp. 1152–1156, August 1985.

[148] R. Lang, "Injection locking properties of a semiconductor laser," *IEEE Journal of Quantum Electronics*, vol. QE-18, no. 6, pp. 976–983, June 1982.

[149] C. J. McKinstrie, M. Karlsson, and Z. Tong, "Higher-capacity communication links based on two-mode phase-sensitive amplifiers," *Optics Express*, vol. 19, no. 13, pp. 11 977–11 991, June 2011.

[150] R.-J. Essiambre and R. W. Tkach, "Capacity trends and limits of optical communicationnnetworks," *Proceedings of the IEEE*, vol. 100, no. 5, pp. 1035–1055, May 2012.

[151] E. Agrell, "Nonlinear fiber capacity," in *European Conference and Exhibition on Optical Communication (ECOC)*, September 2013, paper We.4.D.3.

[152] J. P. Gordon and L. F. Mollenauer, "Phase noise in photonic communications systems using linear amplifiers," *Optics Letters*, vol. 15, no. 23, pp. 1351–1353, December 1990.

[153] R. A. Fisher, B. R. Suydam, and D. Yevick, "Optical phase conjugation for time-domain undoing of dispersive self-phase-modulation effects," *Optics Letters*, vol. 8, no. 12, pp. 611–613, December 1983.

[154] S. L. Jansen, D. van den Borne, P. M. Krummrich, S. Spälter, G.-D. Khoe, and H. de Waardt, "Long-haul DWDM transmission systems employing optical phase conjugation," *IEEE Journal of Selected Topics in Quantum Electronics*, vol. 12, no. 4, pp. 505–520, July/August 2006.

[155] P. Minzioni, "Nonlinearity compensation in a fiber-optic link by optical phase conjugation," *Fiber and Integrated Optics*, vol. 28, no. 3, pp. 179–209, May 2009.

[156] S. L. Jansen, D. van den Borne, B. Spinnler, S. Calabrò, H. Suche, P. M. Krummrich, W. Sohler, G.-D. Khoe, and H. de Waardt, "Optical phase conjugation for ultra long-haul phase-shift-keyed transmission," *Journal of Lightwave Technology*, vol. 24, no. 1, pp. 54–64, January 2006.

[157] E. F. Mateo, X. Zhou, and G. Li, "Electronic phase conjugation for nonlinearity compensation in fiber communication systems," in *Optical Fiber Communication Conference (OFC)*, March 2011, paper JWA25.

[158] H. Hu, R. M. Jopson, A. H. Gnauck, M. Dinu, S. Chandrasekhar, X. Liu, C. Xie, M. Montoliu, S. Randel, and C. J. McKinstrie, "Fiber nonlinearity compensation of an 8-channel WDM PDM-QPSK signal using multiple phase conjugations," in *Optical Fiber Communication Conference (OFC)*, March 2014, paper M3C.2.

[159] E. Ip and J. M. Kahn, "Compensation of dispersion and nonlinear impairments using digital backpropagation," *Journal of Lightwave Technology*, vol. 26, no. 20, pp. 3416–3425, October 2008.

[160] N. Alic, E. Myslivets, E. Temprana, B. P.-P. Kuo, and S. Radic, "Nonlinearity cancellation in fiber optic links based on frequency referenced carriers," *Journal of Lightwave Technology*, vol. 32, no. 15, pp. 2690–2698, August 2014.

[161] B. Foo, B. Corcoran, and A. Lowery, "Optoelectronic method for inline compensation of XPM in long-haul optical links," *Optics Express*, vol. 23, no. 2, pp. 859–872, January 2015.

[162] X. Liu, S. Chandrasekhar, P. J. Winzer, R. W. Tkach, and A. R. Chraplyvy, "Fiber-nonlinearity-tolerant superchannel transmission via nonlinear noise squeezing and generalized phase-conjugated twin waves," *Journal of Lightwave Technology*, vol. 32, no. 4, pp. 766–775, February 2014.

[163] X. Liu, A. R. Chraplyvy, P. J. Winzer, R. W. Tkach, and S. Chandrasekhar, "Phase-conjugated twin waves for communication beyond the Kerr nonlinearity limit," *Nature Photonics*, vol. 7, pp. 560–568, May 2013.

[164] Y. Tian, Y.-K. Huang, S. Zhang, P. R. Prucnal, , and T. Wang, "Demonstration of digital phase-sensitive boosting to extend signal reach for long-haul WDM systems using optical phase-conjugated copy," *Optics Express*, vol. 21, no. 4, pp. 5099–5106, February 2013.

[165] X. Liu, H. Hu, S. Chandrasekhar, R. M. Jopson, A. H. Gnauck, M. Dinu, C. Xie, and P. J. Winzer, "Generation of 1.024-Tb/s Nyquist-WDM phase-conjugated twin vector waves by a polarization-insensitive optical parametric amplifier for fiber-nonlinearity-tolerant transmission," *Optics Express*, vol. 22, no. 6, pp. 6478–6485, March 2014.

[166] H. Eliasson, S. L. Olsson, M. Karlsson, and P. A. Andrekson, "Comparison between coherent superposition in DSP and PSA for mitigation of nonlinearities in a single-span link," in *European Conference and Exhibition on Optical Communication (ECOC)*, September 2014, paper Mo.3.5.2.

[167] H. Eliasson, P. Johannisson, M. Karlsson, and P. A. Andrekson, "Mitigation of nonlinearities using conjugate data repetition," *Optics Express*, vol. 23, no. 3, pp. 2392–2402, February 2015.

[168] I. Sackey, R. Elschner, M. Nlle, T. Richter, L. Molle, C. Meuer, M. Jazayerifar, S. Warm, K. Petermann, and C. Schubert, "Characterization of a fiber-optical parametric amplifier in a 5 × 28-GBd 16-QAM DWDM system," in *Optical Fiber Communication Conference (OFC)*, March 2014, paper W3E.3.

[169] T. Torounidis, H. Sunnerud, P. O. Hedekvist, and P. A. Andrekson, "Amplification of WDM signals in fiber-based optical parametric amplifiers," *IEEE Photonics Technology Letters*, vol. 15, no. 8, pp. 1061–1063, August 2003.

[170] A. Lorences-Riesgo, T. A. Eriksson, C. Lundström, M. Karlsson, and P. A. Andrekson, "Phase-sensitive amplification of 28 GBaud DP-QPSK signal,"

in *Optical Fiber Communication Conference (OFC)*, March 2015, paper W4C.4.

[171] T. Umeki, T. Kazama, O. Tadanaga, K. Enbutsu, M. Asobe, Y. Miyamoto, and H. Takenouchi, "PDM signal amplification using PPLN-based polarization-independent phase-sensitive amplifier," *Journal of Lightwave Technology*, vol. 33, no. 7, pp. 1326–1332, April 2015.

[172] D. J. Richardson, J. M. Fini, and L. E. Nelson, "Space-division multiplexing in optical fibres," *Nature*, vol. 7, no. 5, pp. 354–362, May 2013.

[173] P. J. Winzer, "Making spatial multiplexing a reality," *Nature*, vol. 8, no. 5, pp. 345–348, May 2014.

Appendix A

Derivations

A.1 Derivation of $B_+(A_+)$ and $B_-(A_-)$

We take our starting point in (3.19)

$$
\begin{cases}
A_+ = \dfrac{A_{\mathrm{s}} + A_{\mathrm{i}}}{\sqrt{2}} \\[2mm]
A_- = \dfrac{A_{\mathrm{s}} - A_{\mathrm{i}}}{\sqrt{2}}
\end{cases}
\tag{A.1}
$$

$$\Rightarrow$$

$$
\begin{cases}
A_{\mathrm{s}} = \dfrac{A_+ + A_-}{\sqrt{2}} \\[2mm]
A_{\mathrm{i}} = \dfrac{A_+ - A_-}{\sqrt{2}}.
\end{cases}
\tag{A.2}
$$

We can now define B_+ and B_- and show (3.20) using (3.18) and (A.2). We obtain:

$$
\begin{aligned}
B_+ &= \frac{B_{\mathrm{s}} + B_{\mathrm{i}}}{\sqrt{2}} = \frac{\mu A_{\mathrm{s}} + \nu A_{\mathrm{i}}^* + \nu A_{\mathrm{s}}^* + \mu A_{\mathrm{i}}}{\sqrt{2}} \\[2mm]
&= \frac{\mu(A_+ + A_-) + \nu(A_+ - A_-)^* + \nu(A_+ + A_-)^* + \mu(A_+ - A_-)}{2} \\[2mm]
&= \mu A_+ + \nu A_+^*
\end{aligned}
\tag{A.3}
$$

and

$$
\begin{aligned}
B_- &= \frac{B_{\mathrm{s}} - B_{\mathrm{i}}}{\sqrt{2}} = \frac{\mu A_{\mathrm{s}} + \nu A_{\mathrm{i}}^* - (\nu A_{\mathrm{s}}^* + \mu A_{\mathrm{i}})}{\sqrt{2}} \\[2mm]
&= \frac{\mu(A_+ + A_-) + \nu(A_+ - A_-)^* - \left[\nu(A_+ + A_-)^* + \mu(A_+ - A_-)\right]}{2} \\[2mm]
&= \mu A_- - \nu A_-^*.
\end{aligned}
\tag{A.4}
$$

A.2 Derivation of $B_+(A_{\mathrm{r},+})$ and $B_-(A_{\mathrm{r},-})$

The expressions for B_+ and B_- in (3.21) can be obtained as follows:

$$
\begin{aligned}
B_+ &= \mu A_+ + \nu A_+^* = |\mu| \exp(i\theta_\mu) A_+ + |\nu| \exp(i\theta_\nu) A_+^* = \left[\theta_{\mathrm{r}}^+ = \frac{\theta_\mu + \theta_\nu}{2} \right] = \\
&= \exp(i\theta_{\mathrm{r}}^+) \left[|\mu| \exp\left(i\frac{2\theta_\mu - \theta_\mu - \theta_\nu}{2} \right) A_+ + |\nu| \exp\left(i\frac{2\theta_\nu - \theta_\mu - \theta_\nu}{2} \right) A_+^* \right] \\
&= \left[\theta_{\mathrm{r}}^- = \frac{\theta_\mu - \theta_\nu}{2} \right] = \exp(i\theta_{\mathrm{r}}^+) \left[|\mu| \exp(i\theta_{\mathrm{r}}^-) A_+ + |\nu| \exp(-i\theta_{\mathrm{r}}^-) A_+^* \right] = \\
&= \left[A_{\mathrm{r},+} = A_+ n \exp(i\theta_{\mathrm{r}}^-) \right] = \exp(i\theta_{\mathrm{r}}^+) \left(|\mu| A_{\mathrm{r},+} + |\nu| A_{\mathrm{r},+}^* \right) = \\
&= \exp(i\theta_{\mathrm{r}}^+) \left\{ |\mu| \left[\mathrm{Re}(A_{\mathrm{r},+}) + i\mathrm{Im}(A_{\mathrm{r},+}) \right] + |\nu| \left[\mathrm{Re}(A_{\mathrm{r},+}) - i\mathrm{Im}(A_{\mathrm{r},+}) \right] \right\} \\
&= \exp(i\theta_{\mathrm{r}}^+) \left[(|\mu| + |\nu|)\mathrm{Re}(A_{\mathrm{r},+}) + i(|\mu| - |\nu|)\mathrm{Im}(A_{\mathrm{r},+}) \right]
\end{aligned}
$$

$$(\text{A.5})$$

and

$$
\begin{aligned}
B_- &= \mu A_- - \nu A_-^* = |\mu| \exp(i\theta_\mu) A_- - |\nu| \exp(i\theta_\nu) A_-^* = \left[\theta_{\mathrm{r}}^+ = \frac{\theta_\mu + \theta_\nu}{2} \right] = \\
&= \exp(i\theta_{\mathrm{r}}^+) \left[|\mu| \exp\left(i\frac{2\theta_\mu - \theta_\mu - \theta_\nu}{2} \right) A_- - |\nu| \exp\left(i\frac{2\theta_\nu - \theta_\mu - \theta_\nu}{2} \right) A_-^* \right] \\
&= \left[\theta_{\mathrm{r}}^- = \frac{\theta_\mu - \theta_\nu}{2} \right] = \exp(i\theta_{\mathrm{r}}^+) \left[|\mu| \exp(i\theta_{\mathrm{r}}^-) A_- - |\nu| \exp(-i\theta_{\mathrm{r}}^-) A_-^* \right] = \\
&= \left[A_{\mathrm{r},-} = A_- \exp(i\theta_{\mathrm{r}}^-) \right] = \exp(i\theta_{\mathrm{r}}^+) \left(|\mu| A_{\mathrm{r},-} - |\nu| A_{\mathrm{r},-}^* \right) = \\
&= \exp(i\theta_{\mathrm{r}}^+) \left\{ |\mu| \left[\mathrm{Re}(A_{\mathrm{r},-}) + i\mathrm{Im}(A_{\mathrm{r},-}) \right] - |\nu| \left[\mathrm{Re}(A_{\mathrm{r},-}) - i\mathrm{Im}(A_{\mathrm{r},-}) \right] \right\} \\
&= \exp(i\theta_{\mathrm{r}}^+) \left[(|\mu| - |\nu|)\mathrm{Re}(A_{\mathrm{r},-}) + i(|\mu| + |\nu|)\mathrm{Im}(A_{\mathrm{r},-}) \right].
\end{aligned}
$$

$$(\text{A.6})$$